ELECTRONIC STRUCTURE AND PHYSICAL PROPERTIES OF SMALL MOLECULES

by

Alan Sutton

A thesis submitted to

THE UNIVERSITY OF LEICESTER

for the degree of

Ph.D.

in the Faculty of Science

1971

ACKNOWLEDGEMENTS

Thanks are extended to Professors E.A. Stewardson and J.E. Enderby of the Physics Department of Leicester University where this work was undertaken. An S.R.C. Award is gratefully acknowledged. Special thanks are due to Dr R.B. Hake for the use of certain computer routines and to Miss J.M. Coleman for the tedious work involved in the preparation of this thesis.

Finally I would like to express my gratitude to Dr K.E. Banyard for his encouragement and guidance during the course of this work.

A. Sutton

ABSTRACT

Parts I and II of this thesis have certain common features. Thus both parts are concerned with molecules of the form XH_n (including XH_n^+). Also a theoretical technique appropriate for dealing with molecular systems of the type mentioned - the single-centre method - features in Part I and Part II.

The united-atom approximation (UA) - an early single-centre approach - is used in Part I in calculations on AlH_4^-, NeH^+ and AH^+. Properties evaluated include electronic energy, force constant, diamagnetic susceptibility and X-ray scattering factor. The performance of the UA technique is discussed in relation to previous applications of the method to ten and eighteen electron systems.

In Part II an analysis of Hartree-Fock-Roothaan (HFR) calculations on CH_4 and HF is presented. Single-centre calculations are included and are related to polycentre calculations by means of one-electron expectation values, electron density expansions and density contour maps. The expectation values calculated include multipole moments, $\langle r^n \rangle$ and X-ray scattering factors. Where possible comparisons with experimental results are made.

CONTENTS

PART I

UNITED-ATOM STUDIES OF AlH_4^-, NeH^+ AND AH^+

CHAPTER 1 - THE UNITED-ATOM APPROXIMATION 1

Details of the UA Approximation 2

The Wave Function and Energy 3

CHAPTER 2 - PHYSICAL PROPERTIES OF AlH_4^- 6

The Co-ordinate System 6

Physical Properties for AlH_4^-

A. X-Ray Scattering Factor 9

B. Diamagnetic Susceptibility 13

C. Force Constant 15

D. Discussion of Results for AlH_4^- 18

CHAPTER 3 - THE RARE GAS HYDRIDE IONS NeH^+ AND AH^+ 22

Co-ordinate System 22

Discussion of Results 25

A. General Remarks 25

B. Forces on the Nuclei in a Molecule 26

C. Force Calculation Using UA Wave Function 29

D. Proton Force Results 30

PART II

ONE ELECTRON EXPECTATION VALUES AND ELECTRON DENSITIES FROM HFR WAVE FUNCTIONS FOR HF AND CH_4

CHAPTER 4 - WAVE FUNCTIONS FOR HF AND CH_4 35

Introduction 35

HFR Wave Functions and Energies for HF and CH_4 37

PCE Bases 38

OCE Bases 43

Comments 47

CHAPTER 5 - ELECTRON DENSITY EXPANSIONS AND EXPECTATION VALUES ... 49

The Electron Density Expansions 49

The Tetrahedral Harmonics 51

Expectation Values 62

Multipole Moments 65

The Bond Moment for CH_4 74

X-Ray Scattering Factor 74

Numerical Techniques 79

Determination of $R_1(r)$ for OCE Functions 80

The PCE Bases 83

CHAPTER 6 - DISCUSSION OF RESULTS 87

The PCE Results 87

The OCE Results 95

The OCE Electron Density Expansions 97

The Electron Densities 104

Concluding Remarks 113

APPENDIX - MOLECULAR INTEGRALS 119

REFERENCES

PART I

UNITED-ATOM STUDIES OF AlH_4^-, NeH^+ AND AH^+

CHAPTER I

THE UNITED-ATOM APPROXIMATION

In its application to problems in quantum chemistry the single-centre method may be further simplified by representing each molecular orbital by a single analytic atomic orbital. This approach, which will be designated united-atom (UA), has been extensively used on hydrides of the neon and argon-like series[1-7]. Early calculations concentrated on the ten electron hydrides. Gasper[1] applied the UA approximation to OH^-, H_2O and H_3O^+ while Bishop et al[2] studied NH_3, H_2O and HF. Banyard and Hake[5,6] published a series of papers on the argon-like series and were able to evaluate the performance of the approximation by comparison with experiment and with the results of other theoretical investigations.

The results of applications of the UA method, taking into account its inherent crudity, showed pleasing agreement with experiments in evaluations of molecular geometry, total electronic energy and other physical properties[5]. Comparisons with more extensive calculations[6] on XH_n systems (X representing the heavy nucleus in the hydride molecule) further strengthened the case for the UA method as a simple approach capable of yielding reasonable results for many properties of interest.

In this work the range of UA calculations is extended to include the systems NeH^+, AH^+ and AlH_4^-. Although experimental data

on these systems is meagre, the UA results may be compared with those of other theoretical studies.

Details of the UA Approximation

A full account of the UA method has been given elsewhere[8]. The essential features of the method are reproduced here.

Molecular Orbitals

Each molecular orbital is approximated by a single atomic orbital of the form

$$\psi(r, \theta, \phi) = N^{r} r^{l} e^{-\mu r} P(r) S_{lm}(\theta, \phi) \qquad (1.1)$$

where $S_{lm}(\theta, \phi)$ denotes a real spherical harmonic and P(r) is a polynomial in r. Explicit forms for the radial normalization factor, N^{r}, appear below. These functions were originally used by Fock and Petrashen[9]. The atomic orbitals appearing in the total wave function will be those appropriate to the united-atom of the molecule, i.e. the atom formed by coalescing all nuclei. Thus the electron configuration may be described as neon or argon-like when considering ten or eighteen electron systems respectively.

A set of orthonormal UA molecular orbitals is obtained by choosing the coefficients which appear in the polynomials P(r). The resulting radial factors for the 1s, 2s, 2p, 3s and 3p orbitals

may be written:

$$
\begin{aligned}
R(1s) &= N_{1s}\, e^{-\alpha r} \\
R(2s) &= N_{2s}\left[1 - \tfrac{1}{3}(\alpha+\beta) r\right] e^{-\beta r} \\
R(2p_i) &= N_{2p_i}\, r\, e^{-\gamma_i r} \\
R(3s) &= N_{3s}\left[1 + \mu r + \nu r^2\right] e^{-\delta r} \\
R(3p) &= N_{3p_i}\left[1 - \tfrac{1}{5}(\gamma_i + \eta_i) r\right] r\, e^{-\eta_i r}
\end{aligned}
\qquad (1.2)
$$

where $i = x, y, z$

Also

$$N_{1s}^2 = 4\alpha^3 ; \quad N_{2s}^2 = \frac{12\beta^5}{(\alpha^2 - \alpha\beta + \beta^2)} ; \quad N_{2p_i}^2 = \frac{4}{3}\gamma_i^5$$

$$N_{3s}^2 = \frac{8\delta^7}{\left[2\delta^4 + 6\mu\delta^3 + 6(2\nu + \mu^2)\delta^2 + 30\mu\nu\delta + 45\nu^2\right]}$$

$$N_{3p_i}^2 = \frac{40\eta_i^7}{(9\gamma_i^2 - 12\gamma_i\eta_i + 9\eta_i^2)}$$

$$\mu = \frac{3(\beta+\delta^2)(\delta-\alpha) - (\alpha+\delta)^2\left[3(\beta+\delta) - 5(\alpha+\beta)\right]}{3\left\{(\alpha+\delta)\left[3(\beta+\delta) - 5(\alpha+\beta)\right] - (\beta+\delta)\left[3(\beta+\delta) - 4(\alpha+\beta)\right]\right\}}$$

$$\nu = \frac{(\alpha+\delta)\left\{(\alpha+\delta)(\beta+\delta)\left[3(\beta+\delta) - 4(\alpha+\beta)\right] - 3(\beta+\delta)^2(\delta-\alpha)\right\}}{12\left\{(\beta+\delta)\left[3(\beta+\delta) - 4(\alpha+\beta)\right] - (\alpha+\delta)\left[3(\beta+\delta) - 5(\alpha+\beta)\right]\right\}}$$

The Wave Function and Energy

Using the molecular orbitals defined in (1.1), the total wave function is expressed as a single determinant composed of orthonormal spin orbitals ϕ_k

$$\Psi = \det\{\phi_1, \phi_2, \cdots, \phi_N\} \tag{1.3}$$

The non-relativistic Hamiltonian within the Born-Oppenheimer approximation is utilized:

$$H = \sum_i H_i + \sum_{i>K} \frac{1}{r_{iK}} + \sum_U \frac{Z}{R_u} + \sum_{U>V} \frac{1}{R_{UV}} \tag{1.4}$$

H_i is the Hamiltonian for the ith electron in the nuclear framework alone and is given as

$$H_i = -\frac{1}{2}\nabla_i^2 - \frac{Z}{r_i} - \sum_V \frac{1}{r_{ui}} \tag{1.5}$$

The distances r_i, r_{ui} and r_{ik} are respectively, the distance of the ith electron from the origin, from the uth proton and from the Kth electron. R_u and R_{uv} are the distances of the uth proton from the origin and from the vth respectively.

Using the variational theorem, the total energy of the system is written as

$$E = \frac{\int \Psi^* H \Psi \, d\tau}{\int \Psi^* \Psi \, d\tau} \qquad (1.6)$$

The energy function (1.6) reduces to a sum of integrals of the usual form on introducing the UA wave function into (1.6). All integrals may be solved analytically and details of the integral solutions may be found in the Appendix. To determine the best energy in the context of the variational theorem it only remains to minimise the energy expression with respect to the parameters of the UA wave function. These are of course the exponents in the basis functions and the proton-heavy nucleus distance - the bond length of the system - which may be treated as an additional variational parameter.

Optimisation of the total electronic energy for the ten and eighteen electron systems considered here was carried out on an Elliot 803 computer. Using the optimum wave functions calculations were performed to determine other physical properties. A detailed report of the results of the calculations on AlH_4^-, NeH^+ and AH^+ appears in the next two chapters.

CHAPTER II

PHYSICAL PROPERTIES OF AlH_4^-

The Co-ordinate System

The co-ordinate system used for an XH_4 molecule is shown in Figure 2.1. The bond angle is set equal to the tetrahedral angle θ_T.

From symmetry considerations a reduction in the number of UA wave function parameters can be made by observing that for the co-ordinate system in Figure 2.1 the exponents for the 2p and 3p orbitals must be such that

$$\begin{aligned} \gamma_x = \gamma_y = \gamma_z &= \gamma \\ \eta_x = \eta_y = \eta_z &= \eta \end{aligned} \qquad (2.1)$$

The total number of variational parameters for AlH_4^- is thus reduced from ten to six including the bond length.

In Table 2.1 optimised energies for AlH_4^- at various bond lengths are presented. Included in the table are the results of Albasiny and Cooper[10] who published their findings during the course of this work. These authors adopted a numberical SCF technique within the single-centre approximation. They included spherical harmonics, $S_{lm}(\theta, \phi)$, up to three in l in the expansions of their molecular orbitals and determined the radial factors in the expansions numerically. They report results for spherical and non-

Co-ordinate system for XH_4 molecule

$t = R/\sqrt{3}$

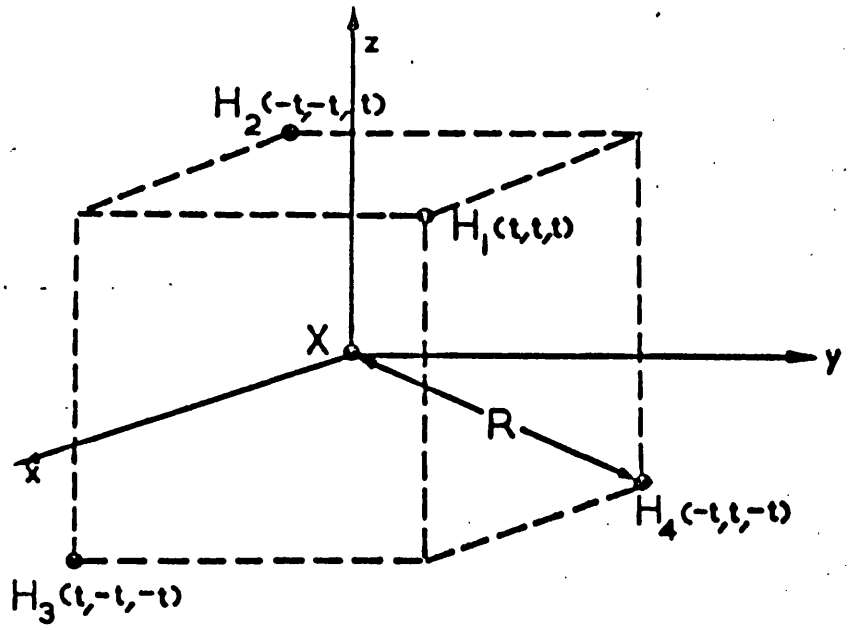

Figure 2.1

Co-ordinate system for XH molecule

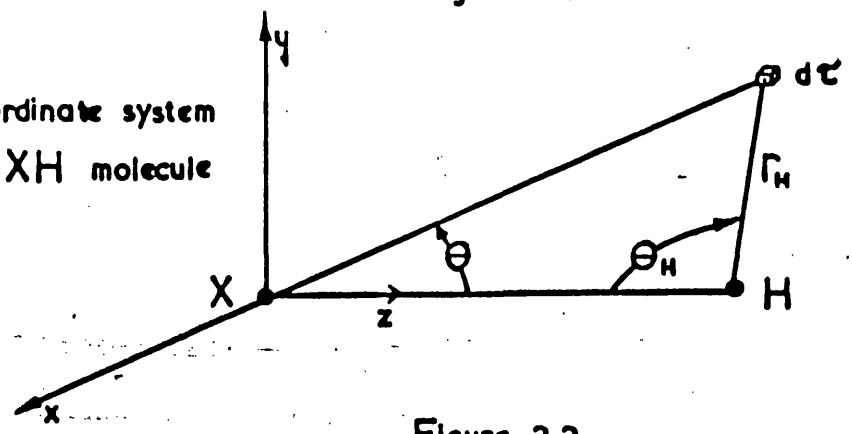

Figure 2.2

TABLE 2.1

ENERGIES[a] AND VARIATIONAL PARAMETERS FOR AlH_4^-

	BOND LENGTH	ENERGY	α	β	γ	δ	η
UA RESULTS	3.1322[b]	-242.0270	12.698	5.091	4.435	1.417	1.143
	3.0	-242.0226	12.696	5.094	4.436	1.453	1.179
	3.2	-242.0258	12.696	5.092	4.434	1.399	1.126
	3.25	-242.0237	12.695	5.092	4.434	1.386	1.114
SCF(S)	3.137[b]	-243.222					
SCF(NS)	2.965[b]	-243.734					

a All quantities in atomic units

b Theoretical bond length

The SCF(S) and SCF(NS) results are those of Albasiny and Cooper (reference 10)

spherical cases; in the former only the first harmonic is retained in each molecular orbital, whilst in the latter the full angular dependence is utilized. The results for these two cases are included under the headings SCF(S) and SCF(NS) respectively in Table 2.1.

The final optimised energies in the UA calculations are such that changes of one unit in the fourth figure of the exponents produced no changes in the seventh figure of the energy, although larger exponent variations would do so.

Physical Properties for AlH_4^-

The simplicity of the UA wave function makes the calculation of several molecular properties quite straight-forward. The evaluation of the X-ray scattering factor, diamagnetic susceptibility and the breathing force constant is discussed in this section.

A. X-Ray Scattering Factor

The X-radiation scattered by molecules of a gas consists of a coherent part, which has the same wavelength as the incident radiation, and an incoherent component which has a continuous spectrum of frequencies less than that of the incident radiation. The incoherent component results from the Compton effect.

Waller and Hartree[11] have made a detailed theoretical investigation of the scattering process and they showed that the total intensity of the scattered radiation is given, for one molecule, by

$$I_{Tot.} = I_{cl} \sum_{m} \left(\frac{\nu'_{nm}}{\nu} \right)^2 \left| D_{nm} \right|^2 \qquad (2.2)$$

where

$$D_{nm} = \int \Psi_n^* \Psi_m \sum_{j=1}^{N} \exp\left\{ \frac{2\pi i}{c} \left(\nu'_{nm} \underline{s}' - \nu \underline{s} \right) r_j \right\} d\tau \qquad (2.3)$$

and I_{cl} is the intensity which would be scattered by a free electron on classical theory. Also ν and ν'_{nm} are the frequencies of the initial and scattered radiation respectively and $\underline{s}$ and $\underline{s}'$ are the vectors defining the directions of the initial and scattered waves. Ψ_n and Ψ_m are the initial and final wave functions of the system and N is the total number of electrons in the molecule. Ψ_n refers to the normal state of the molecule. For the formula to be applicable, relativistic effects must not be important and ν must be higher than the K-absorption frequency of the system. Thus the formula may be appropriately applied to predict X-ray scattering for light atoms and molecules using incident wavelengths with a lower limit in the region of 1 Å.

If coherent scattering alone is considered, then the initial and final states of the system are the same and (2.2) reduces to

$$\bar{I}_{coh} = I_{cl} \left| D_{nn} \right|^2 \qquad (2.4)$$

Substituting for D_{nn} produces an expression for the mean intensity of the coherent radiation

$$\bar{I}_{coh} = I_{cl} \iint \rho(r_1)\, \rho(r_2)\, \frac{\sin x_{12}}{x_{12}}\, d\tau_1\, d\tau_2 \qquad (2.5)$$

where $\rho(r)$ is the electron density for the system and

$$x_{12} = \frac{4\pi\, r_{12} \sin(\theta/2)}{\lambda} = K r_{12} \qquad (2.6)$$

θ being the angle of scatter and λ the incident wavelength

The coherent scattering factor $f(K)$ is defined by

$$f^2(K) = \frac{\bar{I}_{coh}}{I_{cl}} \qquad (2.7)$$

Theoretical investigation of the coherent and incoherent X-ray scattering in atoms has been performed by Freeman[22] and Ibers[23]. Banyard and March[4] have shown that the scattering factor may be expressed in a particularly simple form if the one-electron density $\rho(r, \theta, \phi)$ is expanded in a series of spherical harmonics, that is

$$\rho(r, \theta, \phi) = \sqrt{2} \sum_{l=0}^{\infty} \sum_{m=-l}^{m=+l} \rho_{lm}(r)\, \Theta_{lm}(\theta)\, e^{im\phi} \qquad (2.8)$$

then

$$f^2(K) = \sum_{l=0}^{\infty} \sum_{m=-l}^{m=+l} f_{lm}^{*}(K)\, f_{lm}(K) \qquad (2.9)$$

where

$$f_{lm}(K) = (2\pi)^{3/2} \int \rho_{lm}(r) \frac{J_{l+1/2}(Kr)}{(Kr)^{1/2}} r^2 dr \qquad (2.10)$$

Thus each radial term in the electron density expansion contributes to the coherent scattering factor according to (2.9).

The UA one-electron density for AlH_4^- will be spherically symmetric due to the symmetry constraints imposed on the 2p and 3p orbital exponents. In this case the scattering factor is given by $f_{00}(K)$ where

$$f_{00}(K) = 4\pi \int_0^\infty \rho_{00}(r) \frac{\sin(Kr)}{(Kr)} r^2 dr \qquad (2.11)$$

Defining the radial density distribution $D(r)$ for N electrons by

$$\int_0^\infty D(r)\, dr = N \qquad (2.12)$$

(2.11) may be rewritten as

$$f_{00}(K) = \int_0^\infty D(r) \frac{\sin(Kr)}{(Kr)} dr \qquad (2.13)$$

In Figures 2.3 and 2.4, diagrams are presented showing the radial density distribution and the X-ray scattering curve respectively, computed from the UA wave function at the theoretical bond length of 3.1322 a.u. These results may be compared with those from Albasiny and Cooper's SCF(NS) wave function at a bond length of

2.965 a.u., which are also included in the diagrams. Only the contribution from the spherically symmetric term in the SCF density to the scattering factor is shown in Figure 2.4, since contributions from higher angular terms are small in comparison.

B. Diamagnetic Susceptibility

Van Vleck[12] has shown that the total diamagnetic susceptibility of a molecule in a $^1\Sigma$ state may be written

$$\chi = -\frac{Le^2}{6mc^2}\sum_i r_i^2 + 2L\left(\frac{e}{2mc}\right)^2 \sum_n \frac{\langle n|L_z|0\rangle^2}{E_n - E_0}$$

$$= \chi_r + \chi_p \qquad (2.14)$$

The second term in (2.14), χ_p, represents a temperature independent paramagnetic contribution to χ and entails a knowledge of all excited states for its evaluation. An experimentally based determination of χ_p is possible, as has been shown by Eshbach and Strandberg, if experimental values for the diagonal components of the electronic part of the molecular gyromagnetic tensor are available. The individual contributions, χ_r and χ_p, to the total susceptibility are gauge dependent, i.e. dependent on the gauge chosen for the vector potential, although the total susceptibility is gauge invariant.

For AlH_4^- the diamagnetic contribution, χ_r, to the molar susceptibility is calculated here using the optimum UA wave function

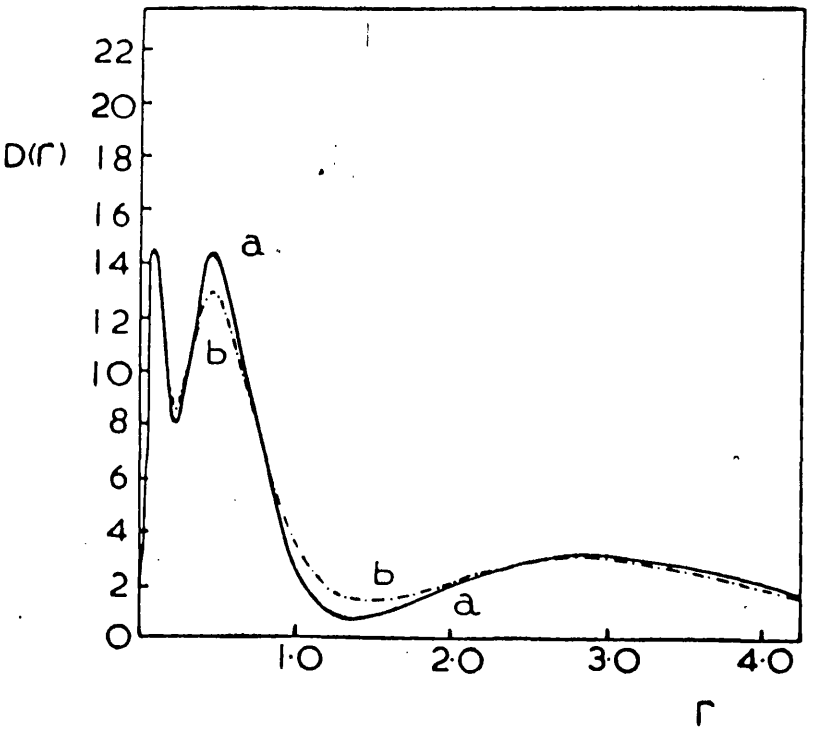

Figure 2.3: Radial Density Distributions for AlH_4^-
Curve a - UA, curve b - SCF(NS)

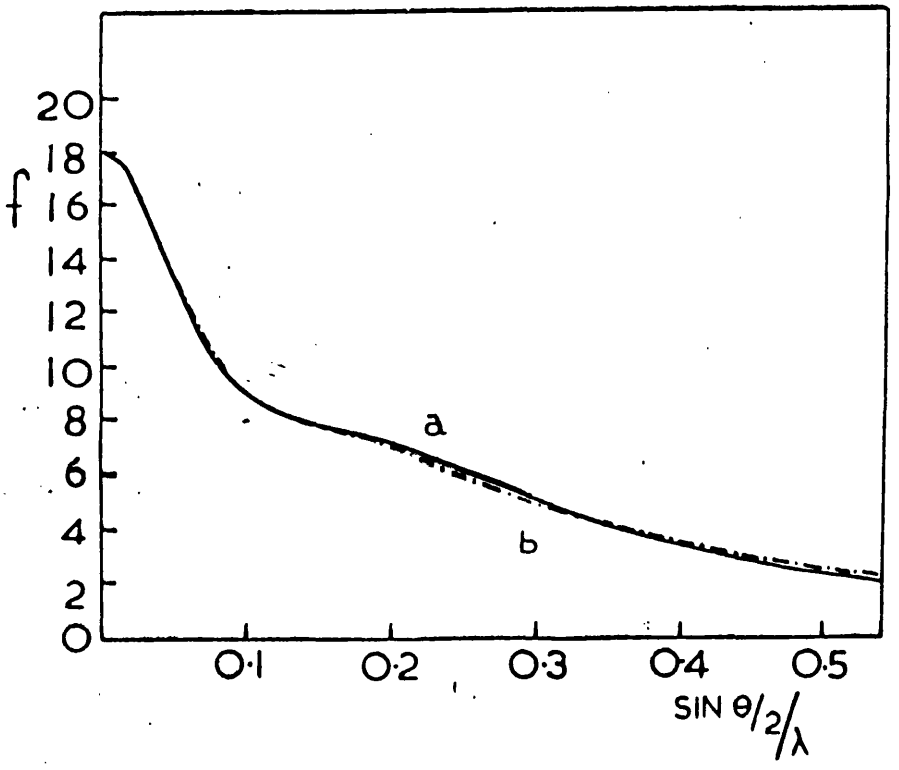

Figure 2.4: X-ray Scattering Factor for AlH_4^-
Curve a - UA, curve b - SCF(NS)

at the theoretical bond length. Introducing the radial density distribution defined in (2.12), χ_r is expressed with respect to the Al nucleus as origin in units of 10^{-6} emu per mole as

$$\chi_r = -0.7923 \int_0^\infty D(r)\, r^2\, dr \qquad (2.15)$$

In Table 2.2 values of χ_r are included for the UA wave function and the SCF functions of Albasiny and Cooper.

C. Force Constant

Within the Born-Oppenheimer approximation, the solution of the wave equation for a molecular system is arrived at by solving first for the motion of the electrons in the fixed nuclear framework and then utilising the electronic solutions to solve for the nuclear motion. In mathematical terms this may be expressed as

$$\begin{aligned} \Psi &= \Psi_n \Psi_e \\ H_e \Psi_e &= E_e \Psi_e \\ (H_n + E_e)\Psi_n &= E_n \Psi_n \end{aligned} \qquad (2.16)$$

The first equation in (2.16) refers to the separation of the problem into nuclear and electronic parts, the total wave function Ψ being written as a product of nuclear and electronic wave functions Ψ_n and Ψ_e respectively. The second and third

equations are the wave equations for the electronic and nuclear motions respectively, the latter including the electronic energy E_e as an extra potential energy term. It is customary to include in E_e the potential energy of interaction of the nuclei and in discussing the variation of E_e with nuclear separation to speak of 'potential energy' curves.

In order to simplify the problem of the solution for the nuclear motions, a number of analytic forms have been suggested to describe the potential energy curve[14], the simplest of which is the Morse potential for diatomics. For polyatomics a good approximation to the potential function in the vicinity of the equilibrium point is given by the quadratic form

$$2V = K_d \sum_i (\Delta d_i)^2 + K_\alpha \sum_i (\Delta\alpha_i)^2 + 2K_{dd} \sum_{i \neq j} (\Delta d_i)(\Delta d_j)$$
$$+ 2K_{\alpha\alpha} \sum_{i \neq j} (\Delta\alpha_i)(\Delta\alpha_j) + 2K_{\alpha d} \sum_{i \neq j} (\Delta\alpha_i)(\Delta d_j) \tag{2.17}$$

where Δd and $\Delta\alpha$ denote small changes in the bond length d and the bond angle α respectively. The force constants may be interpreted as follows; K_d for bond stretching, K_α for bond deformation, K_{dd} for bond-bond interaction, $K_{\alpha\alpha}$ for angle-angle deformation interaction and $K_{\alpha d}$ for angle-bond interaction. Assuming that all $\Delta\alpha$ are zero and all the Δd are equal at all

times enables a definition of breathing force constant to be made from (2.17). Thus utilizing the above conditions for n bonds gives from (2.17)

$$2V = n K_d (\Delta d)^2 + n(n-1) K_{dd} (\Delta d)^2 \qquad (2.18)$$

The breathing force constant, K, is introduced as

$$K = \frac{d^2 V}{d(\Delta d)^2} = n\left[K_d + (n-1) K_{dd}\right] \qquad (2.19)$$

The force constants K_d and K_{dd} may be determined from experimental spectroscopic data, and for AlH_4^- experimentally based predictions[15] for these quantities give K_d = 1.675 and K_{dd} = 0.076, both in units of 10^5 dyne.cm^{-1}.

A UA prediction of the force constant is made here by determining the total electronic energy E at four bond lengths (see Table 2.1). Using a curve fitting routine which fitted a quadratic to the energies determined according to

$$E = a R^2 + b R + c \qquad (2.20)$$

the breathing force constant is determined as

$$K = \left(\frac{d^2 E}{d R^2}\right)_{R_{Th}} = 2a \qquad (2.21)$$

R_{Th} being the theoretical bond length.

In Table 2.2 values of K for AlH_4^- are given for the theoretical treatments discussed, together with the experimentally based value.

D. Discussion of Results for AlH_4^-

The UA results for AlH_4^- may be compared with those of Albasiny and Cooper's SCF calculations in the light of UA and SCF calculations which have been performed for two other tetrahedral systems, SiH_4 and PH_4^+ (5, 10).

Firstly, the UA electronic energy for AlH_4^- when expressed as a fraction of the SCF(NS) prediction is 99.3 percent. The corresponding fraction for SiH_4 and PH_4^+ is 99.4 percent in both cases. It should be remembered in discussing the results for AlH_4^- that this represents the least favourable eighteen electron system from the single-centre point of view. It has been established in previous UA calculations and for other single-centre techniques(16), that the results deteriorate as the number of off-centre nuclei increases and the charge on the heavy nucleus decreases. Hence UA energies get worse in going from HF to CH_4. Such a trend is indicated for the eighteen electron series also, but is obviously not so marked as for the neon series. Comparison with experiment for SiH_4 gives the UA energy as 98.9 percent of the experimental and it is thought that the UA result for AlH_4^- should bear similar comparison.

The theoretical bond lengths given by the UA model are larger than the SCF(NS) values for all three systems. Once again expressing

TABLE 2.2

DIAMAGNETIC SUSCEPTIBILITY AND BREATHING FORCE CONSTANT FOR AlH_4^-

	χ_r [a]	K [b]
UA	-79.8	7.58
SCF(S)	-88.3	6.85
SCF(NS)	-76.5	9.96
EXPT.[c]	-	7.61

a χ_r is expressed with respect to the Al nucleus in units of 10^{-6} emu/mole.

b K is given in units of 10^5 dyne/cm

c See reference 15.

the UA values as fractions of the SCF(NS) results, the figures 105.6 percent, 103.9 percent and 102.6 percent are arrived at for AlH_4^-, SiH_4 and PH_4^+ respectively. From Table 2.1 it is seen that the UA theoretical bond length is closer to the SCF(NS) value than is the SCF(S) prediction. Similar behaviour occurs in theoretical bond length predictions for PH_4^+ and SiH_4 .

The radial density distribution curves (Fig. 2.3) shows the UA model to predict a larger density in the L shell region when compared with the SCF distribution. It should be emphasized when discussing these curves that they correspond to different bond lengths and are thus not strictly comparable. Previous comparisons of D(r) as predicted by the UA method with results from extended basis set calculations[16] have indicated that the radial density distribution predicted is too small in the outer regions of the molecule. This results in a UA value for χ_r which is too small since this quantity is sensitive to the density in the outer regions. This behaviour is not shown for AlH_4^- however, the UA prediction for being larger than the SCF(NS) value. Strict comparison again is not possible, since different bond lengths apply.

The only experimental result available for AlH_4^- is the value of the breathing force constant[15]. The UA approximation has tended to produce values which are too large for this property, indicating a potential curve which is too sharp in the region of the minimum. For AlH_4^- however, the value of K given by the UA approximation is 99.6 percent of the experimental result. This may be compared

with the SCF(NS) result which is 130 percent of the experimental. The closeness of the UA force constant to the experimental result is thought to be fortuitous.

Taken as a whole, the results of this application of the UA approximation have further illustrated its usefulness as a simple and therefore computationally attractive technique. The use of a minimal single-centre basis set - the gross approximation which forms the crux of the method - still yields results for molecular properties which compare favourably with those of much lengthier calculations, as has been seen in this application to AlH_4^-.

CHAPTER III

THE RARE-GAS HYDRIDE IONS NeH^+ AND AH^+

Co-ordinate System

The co-ordinate system used for the UA study of NeH^+ and AH^+ is shown in Figure 2.2. The choice of exponents for the 2p and 3p orbitals is immediately obvious. Thus $\gamma_x = \gamma_y = \gamma$, $\gamma_z = \gamma'$ and $\eta_x = \eta_y = \eta$, $\eta_z = \eta'$. The variational problem for NeH^+ and AH^+ is therefore one in five and eight variational parameters (including bond length) respectively.

Table 3.1 includes the UA energies for the rare-gas hydride ions, along with optimum parameter values. The results of Moran and Friedman[17], who used a modification of the Platt electrostatic model[18] to predict diatomic force constants and internuclear distances, are also included in Table 3.1. The only energy calculation which is useful for comparison with the UA results is that of Peyerimhoff[19] who performed an LCAOSCF calculation on NeH^+. The energy and theoretical bond length given by this calculation are included in Table 3.1.

In Table 3.2 the force constants for NeH^+ and AH^+ given by the UA and Platt models are presented. Also included in this table is the force constant for NeH^+ from the LCAOSCF calculation and the results for χ_r predicted by the UA method for NeH^+ and AH^+.

TABLE 3.1

ENERGIES[a] AND VARIATIONAL PARAMETERS FOR NeH^+ AND AH^+

UA RESULTS

SYSTEM	BOND LENGTH	ENERGY	α	β	γ	γ'	δ	η	η'
AH^+	3.113[b]	-524.5752	17.683	7.680	7.033	7.023	3.235	2.686	2.574
	2.9	-524.5748	17.684	7.679	7.035	7.020	3.235	2.692	2.560
	3.0	-524.5751	17.685	7.681	7.036	7.020	3.235	2.689	2.568
	3.2	-524.5751	17.686	7.680	7.036	7.023	3.235	2.683	2.577
NeH^+	2.331[b]	-127.5703	9.710	3.573	2.910	2.833			
	2.1	-127.5699	9.710	3.574	2.926	2.826			
	2.2	-127.5702	9.711	3.574	2.919	2.828			
	2.45	-127.5703	9.710	3.573	2.904	2.836			

OTHER CALCULATIONS

SYSTEM	METHOD	BOND LENGTH	ENERGY
AH^+	PLATT[c]	2.15[b]	-
NeH^+	LCAOSCF[d]	1.83[b]	-128.6284
	PLATT	1.53[b]	-

a All quantities in atomic units

b Theoretical bond length

c Results of Moran and Friedman, reference 17

d Results of Peyerimhoff, reference 19

TABLE 3.2

PROPERTIES FOR NeH^+ AND AH^+

SYSTEM	METHOD	K^a	χ_r^b
NeH^+	UA	0.17	-5.58
	PLATT	5.52	-
	LCAOSCF	5.29	-
AH^+	UA	0.18	-16.84
	PLATT	5.53	-

a The units of K are 10^5 dyne-cm^{-1}

b χ_r is referred to the heavy nucleus in units of 10^{-6} emu/mole

Discussion of Results

A. General Remarks

The UA results for the systems under study here show a marked departure from expected trends established in previous calculations on XH_n systems. The UA theoretical bond lengths are considerably in excess of those resulting from the other theoretical studies. For AH^+ the UA theoretical bond length is 145 percent of the Platt model result, whilst for NeH^+ the corresponding figure, using the LCAOSCF result, is 127 percent. IN HF and HCl , which seem appropriate systems with which to compare the present results, the UA approximation gave bond lengths which were 90.2 percent and 100.7 percent of the experimental values respectively.

The UA force constants are also markedly at variance with the LCAOSCF and Platt model results. For NeH^+, the UA force constant is just 3 percent of the LCAOSCF value. As the energies in Table 3.1 show, the UA potential energy curve is very flat in the equilibrium region for both systems. The optimum energies are very close to the UA rare-gas atom results of -524.5736 a.u. and -127.5664 a.u. for A and Ne respectively.

The overall performance of the UA method when applied to NeH^+ and AH^+ is thus seen to be disappointing, particularly in its prediction of bond lengths where the approximation has met with some success in other studies. It will be seen in the discussion which follows, that an investigation of the forces acting on the protons in both systems is invaluable in elucidating the failure of the approximation in the

present applications.

B. Forces on the Nuclei in a Molecule

The expectation value of the force on a nucleus N in a molecule is given by

$$F_N = -\nabla_N E \tag{3.1}$$

where differentiation is carried out with respect to the co-ordinates of the nucleus N. The Born-Oppenheimer approximation has been assumed in the definition of F_N, so that the electronic energy E represents the effective potential in which the nuclei move. Introducing the normalized wave function for the system, Ψ , and the energy function

$$E = \langle \Psi | H | \Psi \rangle \tag{3.2}$$

F_N is given by

$$F_N = -\left\{ \langle \nabla_N \Psi | H | \Psi \rangle + \langle \Psi | \nabla_N H | \Psi \rangle + \langle \Psi | H | \nabla_N \Psi \rangle \right\} \tag{3.3}$$

Using the Hermitian property of H, the sum of the first and third terms in (3.3) can be shown to be equal to

$$-\int \nabla_N \Psi^* H \Psi d\tau - \int \nabla_N \Psi H^* \Psi^* d\tau \tag{3.4}$$

The expression (3.4) is identical to zero for a normalized eigenfunction of the Hamiltonian. This is a special application of the Hellmann-Feynman theorem[20,21], for the particular case where differentiation is carried out with respect to the nuclear co-ordinates. Thus for an exact eigenfunction Ψ, the force on the nucleus is given by

$$F_N = -\langle \Psi | \nabla_N H | \Psi \rangle \qquad (3.5)$$

When Ψ represents an approximate wave function the terms considered above do not necessarily vanish, so that (3.5) may not be equivalent to (3.1). For the particular case of the Hartree-Fock wave function the two definitions of force represented by (3.1) and (3.5) have been shown to be equivalent and it will now be shown that this is true for the optimised UA wave function. Consider the Z component of force, F_N^Z. From (3.1) it follows that

$$F_N^Z = -\left\{ \left\langle \frac{\partial \Psi}{\partial Z_N} \middle| H \middle| \Psi \right\rangle + \left\langle \Psi \middle| \frac{\partial H}{\partial Z_N} \middle| \Psi \right\rangle + \left\langle \Psi \middle| H \middle| \frac{\partial \Psi}{\partial Z_N} \right\rangle \right\} \qquad (3.6)$$

For the UA wave function Ψ depends on the nuclear co-ordinates implicitly through the dependence of the variational parameters, μ_n, on the nuclear geometry. Considering again the first and third terms in the force expression (3.6) for the UA wave function which contains p variational parameters, the sum of these terms

may be written

$$-\left\{\left\langle \sum_{n=1}^{p}\left(\frac{\partial\Psi}{\partial\mu_n}\right)\left(\frac{\partial\mu_n}{\partial Z_N}\right)\middle|H\middle|\Psi\right\rangle + \left\langle\Psi\middle|H\middle|\sum_{n=1}^{p}\left(\frac{\partial\Psi}{\partial\mu_n}\right)\left(\frac{\partial\mu_n}{\partial Z_N}\right)\right\rangle\right\} \tag{3.7}$$

For the optimum UA energy, E

$$\left(\frac{\partial E}{\partial\mu_n}\right) = 0 \qquad n = 1, \cdots, p \tag{3.8}$$

(3.8) may be re-written as

$$\left\langle\frac{\partial\Psi}{\partial\mu_n}\middle|H\middle|\Psi\right\rangle + \left\langle\Psi\middle|H\middle|\frac{\partial\Psi}{\partial\mu_n}\right\rangle = 0 \qquad n=1,\cdots,p \tag{3.9}$$

Thus it is seen that for the UA wave function the expression (3.7) is zero and that (3.5) is indeed equivalent to the original definition of force (3.1) for the case of this approximation.

Consider now the case of a diatomic hydride XH with charge Z on the heavy nucleus. Using (3.5) with the notation of Figure 2.2, the force on the proton, F_H, is given by

$$F_H = -\left\langle\Psi\middle|-\frac{Z}{R^2} + \sum_{i=1}^{N}\frac{\cos\theta_H^i}{(r_H^i)^2}\middle|\Psi\right\rangle \tag{3.10}$$

where the summation over i goes over N electrons. In (3.10) F_H represents the non-zero component of force along the Z axis and R the bond length

of the system. Introducing the one-electron density defined as

$$\rho(r, \theta, \phi) = N \int \Psi^* \Psi \, d\tau_1, \ldots, d\tau_N \qquad (3.11)$$

N is the number of electrons in the problem. In (3.11) integration over all spin variables has been assumed. The force on the proton can now be written as

$$F_H = \frac{Z}{R^2} - \int \frac{\rho(r, \theta, \phi) \cos \theta_H \, d\tau}{r_H^2} \qquad (3.12)$$

A similar expression holds for the force on the X nucleus. The expression for proton force (3.12) is precisely that which would be obtained by using classical electrostatics with $\rho(r, \theta, \phi)$ representing a continuous charge distribution. This is an expression of the electrostatic theorem which enables a calculation of nuclear force from a straight forward application of electrostatics.

C. Force Calculation Using UA Wave Function

Having established that for the UA wave function the expression for proton force (3.12) is compatible with the original definition given in (3.1), the forces on the protons in NeH^+ and AH^+ are now investigated. The UA electron density may be expanded in spherical harmonics about the heavy nucleus in the following way

$$\rho(r, \theta, \phi) = \rho_{00}(r) \, \Theta_{00}(\theta) \, \Phi_0(\phi) + \rho_{20}(r) \, \Theta_{20}(\theta) \, \Phi_0(\phi) \qquad (3.13)$$

The limited basis set used in the approximation results in a density expansion which consists of a spherically symmetric term and a d-type term. Using (3.13) in (3.12) F_H reduces to

$$F_H = \frac{Z}{R^2} - \frac{2\sqrt{\pi}}{R^2}\int_0^R \rho_{00}(r)r^2 dr - 6\sqrt{\frac{\pi}{5}}\frac{1}{R^4}\int_0^R \rho_{20}(r)r^4 dr$$

$$+ 4\sqrt{\frac{\pi}{5}}\, R\int_R^\infty \frac{\rho_{20}(r)}{r}\, dr \qquad (3.14)$$

The force on the heavy nucleus, F_X, is given by

$$F_X = -\frac{Z}{R^2} + \int \frac{\rho(r,\theta,\phi)}{r^2}\cos\theta\, d\tau \qquad (3.15)$$

This force simply reduces to $-Z/_R{}^2$ for the UA density which is therefore not able to account for the expected equality (in magnitude) of the forces on the X and H nuclei.

Using optimised wave functions at various bond lengths, the proton forces in NeH^+ and AH^+ have been determined using (3.14). Figure 3.1 shows the proton force plotted as a function of the bond length for the two systems.

D. The Proton Force Results

The proton force curves (Figure 3.1) show the expected variation of the force with bond length. For NeH^+, the force on the proton

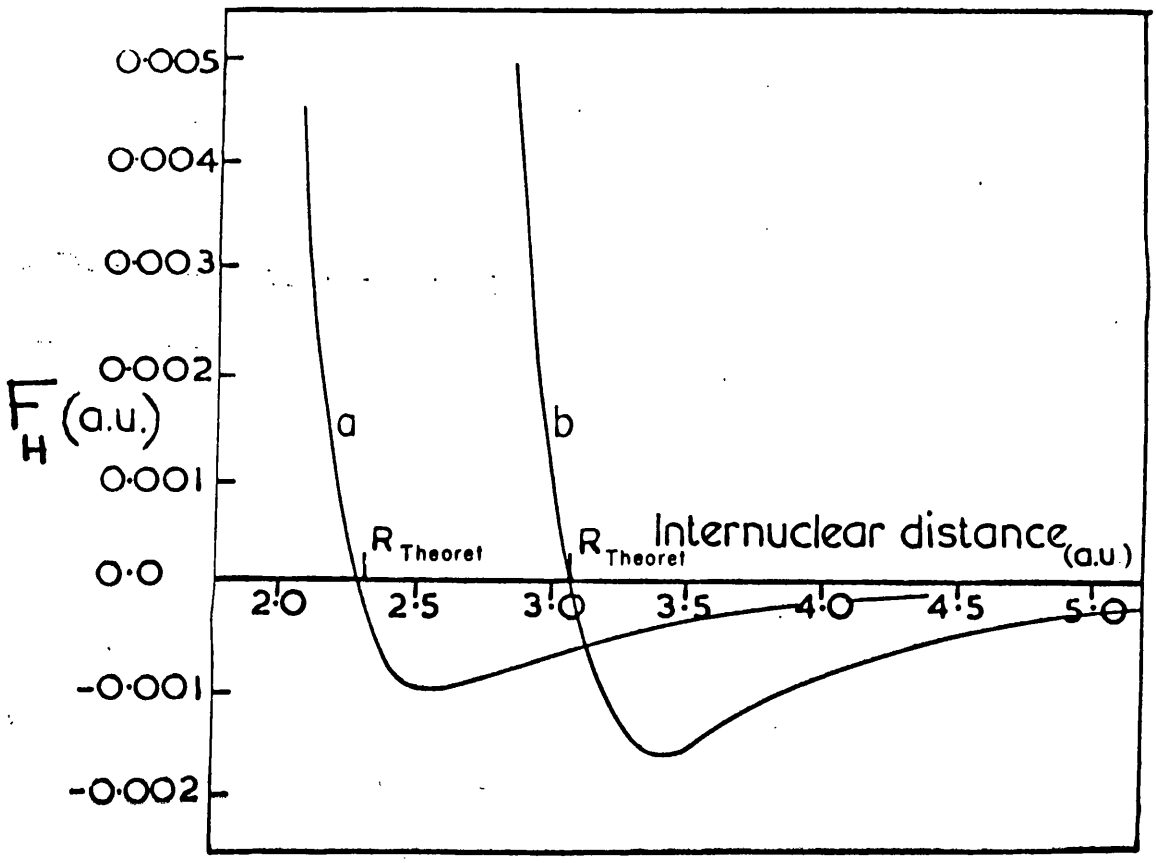

Figure 3.1: UA Proton Force for a - NeH^+, b - AH^+

evaluated at the theoretical bond length is -0.0002 a.u., while for AH^+ the corresponding figure is zero to within four decimal places. These figures result from extensive optimisation of the variational parameters entering the wave function.

A consideration of (3.14) is useful in discussing the poor performance of the UA approximation when applied to NeH^+ and AH^+. The first two terms in the expression for F_H may be interpreted on electrostatic grounds. These terms represent the contributions to the proton force made by the heavy nucleus and the spherically symmetric term in the electron density. The charge on the heavy nucleus is screened by the electronic charge contained within a radius equal to the bond length. The remaining two terms in the expression for F_H give the contribution of the angular term in the UA density to this quantity.

Consider now the expression for F_H which results from a central-field study. In this case, only the first two terms on the right hand side of (3.14) contribute to F_H since there are no angular terms in the electron density. Electrostatic equilibrium is established when

$$Z = 2\sqrt{\pi} \int_0^{R_{Th}} \rho_{00}(r)\, r^2\, dr \qquad (3.16)$$

where R_{Th} is the theoretical bond length. Such central-field studies have been performed for a number of XH_n systems where $Z < 10$ (or 18) and have yielded reasonable bond lengths, e.g. in

the application to AlH_4^- in Chapter I. For the rare-gas hydrides, however, a consideration of (3.16) shows that such a central-field approach would lead to infinite bond lengths. This is so because for these systems, Z, the charge on the heavy nucleus, is equal to the total number of electrons and hence R_{Th} must be increased to infinity to completely screen the heavy nucleus. It follows that in order for a finite bond length to be predicted for the rare-gas hydrides, angular terms must be present in the electron density and these terms play a more important role in the bonding process than in other applications of the UA approach to XH_n systems where, as mentioned above, their presence is not essential for the prediction of a satisfactory bond length. The addition of a single d-type term in the UA density for NeH^+ and AH^+ brings the proton in from infinity to the exaggeratedly large bond lengths given in Table 3.1. At these bond lengths the proton is barely penetrating the electronic charge distribution (17.96 electrons are contained within R_{Th} for AH^+) and it is thus not surprising that the force constants calculated are very small since the proton is situated in a region of very small and slowly varying density.

This discussion has shown that the failure of the UA method when applied to NeH^+ and AH^+ is due to the deficient description of density angularity inherent in the method. This feature of the approximation, although not serious in applications of the UA method to other XH_n systems, assumes major importance in the studies of the

rare-gas hydride ions and results in the atypically poor predictions of bond lengths and force constants reported here.

PART II

ONE ELECTRON EXPECTATION VALUES AND ELECTRON DENSITIES FROM HFR WAVE FUNCTIONS FOR HF AND CH_4

CHAPTER 4

WAVE FUNCTIONS FOR HF AND CH_4

Introduction

The matrix formulation of the Hartree-Fock approach to molecular problems - the Hartree-Fock-Roothean method (HFR)[24] - has been utilized extensively in recent times. A great deal of theoretical information on atoms and molecules has thus been gathered since the HFR method was developed as a tractable computational approach to the Hartree-Fock problem. Even at present, at a time when a great deal of attention is being given to the problem of describing electronic correlation, the HFR approach is still recognized as an extremely useful prototype method capable of providing significant results. At this point it should be mentioned that the HFR method, using a truncated basis set, provides an approximate solution of the Hartree-Fock problem[25]. With the use of an extensive, flexible, well optimised basis set however, 'Hartree-Fock limit' solutions may be reached within the HFR approach. These solutions (and now the discussion is restricted to 'closed-shell' systems) have additional significance which is highlighted in the theorems of Moller and Plesset[26] and Brillouin[27]. Thus Hartree-Fock limit solutions provide electron densities and one-electron expectation values which are correct to second order in a perturbation treatment of electron correlation. Thus physical properties which may be represented by one-electron operators should be quite accurately determined using good HFR functions. The theorems referred to above give no indication

of the magnitude of the error expected in one-electron expectation values derived from good solutions of the Hartree-Fock equations, although recent work[28] has been done on the evaluation of expectation value error bounds. No simple general result has emerged however.

This study will be concerned with HFR results for the ground states of HF and CH_4, both of which have received a considerable amount of attention within the HFR scheme. Thus the $^1\Sigma^+$ state of HF[1,16,29-35] and the $^1A_1$ state of CH_4[16,36-40] have been the subjects of a plethora of HFR calculations, each differing in the choice of basis set. This aspect of the HFR calculation - the choice of basis - is considerably arbitrary, although authors tend to be guided by the results of appropriate atomic HFR calculations and by other molecular HFR bases.

The molecules considered here are both suitable for single-centre calculations and have been the subject of such HFR studies. In what follows the single-centre HFR functions will be referred to as OCE (one-centre expansion of molecular orbitals) to distinguish them from the results of the more common poly-centre calculations (PCE).

The purpose of the present study should be established at this point. First it is proposed to evaluate some one-electron expectation values from several HFR bases for HF and CH_4. Some of these expectation values will be related to physical properties of the systems which may be measured experimentally. As has been mentioned, good HFR solutions should provide good one-electron expectation values. A comparison with experiment should furnish a check of this conclusion. The other objective of this work is an electron density based analysis of the

OCE HFR functions for HF and CH_4 to be introduced later in this chapter. The largest PCE basis results will be used to provide an appropriate measure of the effectiveness of the OCE bases in describing the electron density in HF and CH_4. Having given the aims of the present investigation the rest of this chapter will be taken up with a description of the HFR bases to be utilized.

HFR Wave Functions and Energies for HF and CH_4

The closed-shell electronic configurations for HF and CH_4 are described in the following way:

$$HF(^1\Sigma^+) : \phi^2(1\sigma)\,\phi^2(2\sigma)\,\phi^2(3\sigma)\,\phi^2(1\pi_+)\,\phi^2(1\pi_-)$$

$$CH_4(^1A_1) : \phi^2(1A_1)\,\phi^2(2A_1)\,\phi^2(T_{2x})\,\phi^2(T_{2y})\,\phi^2(T_{2z})$$

The molecular orbitals (MO's) for both systems are labelled in the usual way according to the irreducible representation of the appropriate symmetry point group ($C_{\infty v}$ for HF and T_d for CH_4) to which they belong. Orbital degeneracy exists for both systems with a doubly degenerate orbital eigenvalue giving rise to the π MO's in HF and a triply degenerate level in CH_4 resulting in the T_2 MO's. The latter set of MO's are labelled according to their C_2 symmetry about the co-ordinate axes (see Figure 2.1 for the co-ordinate system used for all the CH_4 wavefunctions to be used in this section).

The basis functions used for all calculations appearing here are Slater-type functions (STF's) defined as

$$STF(n,l,m,\zeta) = \sqrt{\frac{(2\zeta)^{2n+1}}{(2n)!}}\, r^{n-1} e^{-\zeta r} S_{lm}(\theta,\phi) \tag{4.1}$$

where $S_{lm}(\theta,\phi)$ is either a real or imaginary normalized spherical harmonic. An MO of symmetry species λ , sub-species α is written as

$$\phi_{i\lambda\alpha} = \sum_{p} C_{i\lambda p}\, \chi_{p\lambda\alpha} \tag{4.2}$$

in which the $\chi_{p\lambda\alpha}$ are STF's or linear combinations of STF's of the appropriate symmetry. The coefficients $C_{i\lambda p}$ occur as eigenvectors in the HFR equations and are solved for iteratively.

The basis sets and energies for HF and CH_4 will now be introduced starting with PCE bases.

PCE Bases

One of the earliest extensive basis HFR calculations on CH_4 was that of Woznick[39]. Five basis sets used by Woznick are included here labelled as PCE(1-5). The largest basis (PCE(5)) is of particular interest from the point of view of the evaluation of one-electron expectation values. The other bases (PCE(1-4)) are used to illustrate the convergence properties of the PCE basis from an expectation value point of view. In Table 4.1 the total energy is recorded for each basis. Also shown is the orbital energy eigenvalue of the T_2 orbitals (ϵ_{T_2}) which corresponds to the first ionization potential. The experimental nuclear configuration was used with a bond length of

TABLE 4.1 : HFR ENERGIES FOR CH_4

Function	Number of STF's	$-\epsilon_{T2}$	$-E^{a}_{TOTAL}$
PCE(1)[b]	9	0.57196	40.073
PCE(2)	12	0.58185	40.096
PCE(3)	13	0.54460	40.164
PCE(4)	17	0.54401	40.180
PCE(5)	21	0.54341	40.181
OCE(1)[c]	22	0.43272	39.52841
OCE(2)	28	0.48269	39.74423
OCE(3)	40	0.50175	39.87488
OCE(4)	47	0.51849	39.99588
OCE(5)	55	0.52523	40.03873
OCE(6)	63	0.52888	40.06563

$$E_{TOTAL}(\text{OBS.}) = -40.522$$

a All energies (in au) corresponding to R = 2.0665 au

b Results of Woznick (Ref. 39)

c Results of Hoyland (Ref. 40)

TABLE 4.2 : HFR ENERGIES FOR HF

Function	Number of STF's	$-\epsilon_\pi$	$-E^a_{TOTAL}$
PCE(1)[b]	6	0.46858	99.536145
PCE(2)	13	0.64514	100.03508
PCE(3)	23	0.65145	100.06051
PCE(4)	32	0.65008	100.07030
OCE(1)[c]	28	0.61609	99.88611
OCE(2)	43	0.64170	100.01996
OCE(3)	46	0.64823	100.05294
OCE(4)	48	0.64935	100.05925

$$E_{TOTAL}(\text{OBS.}) = -100.530$$

a All energies are in au. The OCE results correspond to R = 1.733 au whereas the PCE results were evaluated at R = 1.7328 au.

b The results of Cade and Huo (Ref. 35)

c The results of Hoyland (Ref. 40)

TABLE 4.3 : PCE BASES FOR CH_4[a]

Function	A1 MO'S	T2 MO'S
PCE(1)	$1S_c$, $2S_c^3$, $1S_h^2$	$2p_c^2$, $1S_h^1$
PCE(2)	$1S_c$, $2S_c^2$, $2S_c^3$, $1S_h^1$	$2p_c^1$, $2p_c^2$, $1S_h^1$
PCE(3)	$1S_c$, $2S_c^2$, $2S_c^3$, $1S_h^1$, $1S_h^2$	$2p_c^1$, $2p_c^2$, $1S_h^1$, $1S_h^2$
PCE(4)	$1S_c$, $2S_c^1$, $2S_c^2$, $2S_c^3$, $1S_h^1$, $1S_h^2$	$2p_c^1$, $2p_c^2$, $2p_c^3$, $1S_h^1$, $1S_h^2$
PCE(5)	$1S_c$, $2S_c^1$, $2S_c^2$, $2S_c^3$, $2S_c^4$, $1S_h^1$, $1S_h^2$	$2p_c^1$, $2p_c^2$, $2p_c^3$, $2p_c^4$, $1S_h^1$, $1S_h^2$

a The results of Woznick (Ref. 39)

BASIS KEY

$1S_c$ = $0.03926\ 1S_c\ (9.8) + 0.35946\ 1S_c\ (6.5) + 0.61493\ 1S_c\ (4.7)$

$2S_c^1$ = $2S_c\ (3.96)$

$2S_c^2$ = $2S_c\ (2.38)$

$2S_c^3$ = $2S_c\ (1.55)$

$2S_c^4$ = $2S_c\ (1.04)$

$2p_c^1$ = $2p_c\ (3.26)$

$2p_c^2$ = $2p_c\ (1.58)$

$2p_c^3$ = $2p_c\ (1.01)$

$2p_c^4$ = $2p_c\ (0.78)$

$1S_h^1$ = $1S_h\ (1.0)$

$1S_h^2$ = $1S_h\ (1.5)$

TABLE 4.4 : PCE BASES FOR HF[a]

Function	σ MO'S	π MO'S
PCE(1)	$1s_f(8.7)$, $2s_f(2.6)$, $2p_f(2.7)$, $1s_h(1.3)$	$2p_f(2.5)$
PCE(2)	$1s_f(8.3)$, $2s_f(2.7)$, $2s_f(10.5)$, $2p_f(2.0)$ $2p_f(4.5)$, $1s_h(1.5)$, $2p_h(0.8)$	$2p_f(1.9)$, $2p_f(4.3)$, $2p_h(1.1)$
PCE(3)	$1s_f(7.9)$, $1s_f(14.2)$, $2s_f(1.7)$, $2s_f(3.0)$ $3s_f(9.9)$, $2p_f(1.5)$, $2p_f(3.0)$ $2p_f(6.2)$, $3p_f(3.9)$, $1s_h(1.7)$, $1s_h(2.0)$ $2s_h(1.2)$, $2p_h(2.1)$	$2p_f(1.1)$, $2p_f(3.1)$, $2p_f(6.2)$ $3p_f(2.1)$, $2p_h(1.5)$
PCE(4)	$1s_f(7.9)$, $1s_f(14.1)$, $2s_f(1.9)$, $2s_f(3.2)$ $3s_f(9.9)$, $2p_f(1.4)$, $2p_f(2.4)$ $2p_f(4.3)$, $2p_f(9.0)$, $3d_f(1.8)$ $3d_f(3.4)$, $4f_f(2.7)$, $1s_h(1.4)$ $1s_h(2.5)$, $2s_h(2.5)$, $2p_h(2.9)$	$2p_f(1.4)$, $2p_f(2.3)$ $2p_f(4.3)$, $2p_f(9.3)$ $3d_f(2.1)$, $4f_f(2.8)$ $2p_h(1.8)$, $3d_h(3.3)$

a Results of Cade and Huo (Ref. 35)

2.0665 au . In Table 4.3 the basis set for each calculation is illustrated using a straight forward notation, i.e. $1s_H$ signifies an STF based on the hydrogen with n = 1, l = 0 and m = 0. The STF's are listed according to the MO's in which they appear. Thus the s-type functions on the hydrogens appear in both the A1 and T_2 MO's in different linear combinations. The smallest basis, PCE(1), is not minimal due to the presence of a $1s$ carbon core function taken from an HFR carbon calculation[41]. No attempt has been made by Woznick to optimise non-linear parameters (orbital exponents) in the basis. The choice of orbital exponents for the s functions on the hydrogens was arbitrary, whereas the exponents for the carbon-based orbitals were taken from the carbon atom HFR calculation mentioned above.

In the case of HF, the calculations of Cade and Huo[35] provide a quintessential example of the application of the HFR technique. The functions for HF used here are chosen from an extensive study of first-row diatomic hydrides made by the authors which is remarkable for its clarity and thoroughness. Four PCE bases are shown in Table 4.2, each corresponding to a bond length of 1.7328 au - the experimental value. Extensive optimisation of non-linear parameters was carried out for all functions. The smallest basis, PCE(1), is minimal whereas the other two intermediate bases, PCE(2) and PCE(3) are described as double-zeta and saturated s and p respectively. In Table 4.4 the PCE bases are given.

The OCE Bases

The OCE HFR calculations on HF and CH_4 undertaken by Hoyland[40], represent attempts to reach the HF limit with an OCE basis. A major

problem which has to be overcome in OCE calculations is the representation of orbitals on the off-centre nuclei by STF's on the expansion centre. This necessitates the presence of high n, l values in the STF's of the OCE basis in order to accumulate density at the protons, Hoyland solves the problem in a systematic way which will be illustrated by referring to HF. The results of Cade and Huo already described indicate that the most important function of σ symmetry centred at the hydrogen nucleus is a $1s$ function with ζ value of about 1.4. This function was variationally expanded in terms of a set of STF's centred at a distance 1.733 au from the hydrogen (i.e. at the fluorine nucleus) using a hydrogen-like Hamiltonian with $z = 1.4$. The STF's used for the expansion have harmonics through $l = 8$. A similar procedure was used for the π orbitals, although harmonics up to $l = 3$ only were used here. The STF's arrived at in this way were added to the Cade, Huo fluorine basis to complete the OCE basis for HF. In the case of CH_4 a similar procedure was adopted using a Hamiltonian with $z = 1.2$ to determine the OCE representation of the hydrogenic orbitals, utilizing a bond length of 2.0665 au. The CH_4 OCE basis included harmonics up to $l = 6$ on the carbon, the carbon basis being taken from an earlier OCE calculation[16].

In Tables 4.2 and 4.6 OCE energies and bases for HF will be found, whereas Tables 4.1 and 4.5 show the results for CH_4. Four OCE bases are included for HF (OCE(1-4)) and six for CH_4 (OCE(1-6)). Some description of the basis set nomenclature used in the tables is required here. The basis sets are listed according to the largest l value (l_{max}) occurring in the MO expansions. Thus for CH_4, the six OCE bases

TABLE 4.5 : OCE BASES FOR CH_4[a]

Function	l	A1 MO'S	T2 MO'S
	0	(1,5.5)[b], (1,9.5), (2,1.5) (4,2.0), (4,3.0), (6,2.3) (22,10.2)	
OCE(1)	1		(2,1.37), (3, 2.95) (4,2.95), (4, 2.26) (8,2.68)
OCE(2)	2		(4,1.64), (14,6.31)
OCE(3)	3	(5,1.98), (19,8.65)	(5,1.98), (19,8.65)
OCE(4)	4	(11,4.78)	(11,4.78)
OCE(5)	5		(14,6.18)
OCE(6)	6	(20,9.0)	(20,9.0)

a Results of Hoyland (Ref. 40)

b The figures in brackets give the (n, ζ) values of the radial STF associated with the tetrahedral harmonic of l value shown in the second column.

TABLE 4.6 : OCE BASES FOR HF[a]

Function	l	MO'S	MO'S
	0	(1,7.9)[b], (1,14.1), (2,1.9), (2,3.3), (3,9.93) (1,2.5), (2,1.3), (6,3.1), (34,19.0)	
OCE(1)	1	(2,1.41), (2,2.37), (2,4.28), (2,8.97), (3,1.66) (8,4.00), (25,13.97)	(2,1.16), (2,1.36) (2,2.33), (2,4.26) (2,9.30), (5,2.37)
	2	(3,1.84), (3,3.37), (5,2.49), (23,12.64)	(3,2.13), (5,2.28)
OCE(2)	3	(4,2.70), (5,2.36), (19,10.27)	(4,2.79), (6,2.25)
	4	(12,6.22)	
	5	(14,7.37)	
OCE(3)	6	(18,9.63)	
	7	(24,13.0)	
OCE(4)	8	(30,16.48)	

a Results of Hoyland (Ref. 40)

b The figures in brackets give the (n, ζ) values of the radial STF associated with the spherical harmonic of l value shown in the second column.

have $l_{max} = 1 - 6$, whereas the four HF bases correspond to $l_{max} =$ 1, 3, 6 and 8. The radial Slater parameters (n, ζ) associated with successive l values (which defines a tetrahedral harmonic occurring in the MO expansion for CH_4) are shown in brackets alongside the value with which they are associated. In forming the basis with $l_{max} = 1$ the basis having $l_{max} = 1 - 1$ is simply added to the new functions associated with $l_{max} = 1$. In this way Hoyland's results for HF and CH_4 illustrate the convergence properties of the OCE bases as a function of l_{max} - the largest spherical harmonic l value occurring in them.

Comments

This chapter will be concluded with a few comments on the energies and basis sets introduced. First, of all the HFR calculations included, the Cade, Huo results for HF (the largest basis set - PCE(4)) represent the closest approach to a true Hartree-Fock solution. Indeed the authors state emphatically that their best calculation is at most 0.001 au above the HF limit for HF. This result is due to the large, flexible, optimised basis set used, including d and f functions on the fluorine. The necessity of using such functions has been known for some time[42], in order for a successful attack on the Hartree-Fock problem to be made. The largest PCE basis for CH_4 (PCE(5)) gives an energy of -40.181 au. This may be compared with an estimate[43] of the Hartree-Fock limit for this molecule of -40.22 au. Thus the PCE attack on CH_4 is less successful than that on HF due of course to the somewhat restricted basis used by Woznick. It should be mentioned at this point that a more recent calculation has been made on CH_4 yielding an energy of -40.204 au.[44]

Results from this calculation will be referred to in later chapters.

The OCE results show the largest basis set for HF (OCE(4)) yielding an energy very close to the result given by the largest PCE basis (0.011 au higher). This result is achieved with 48 STF's compared with 32 STF's in the PCE basis. Thus the dimensions of the secular equations giving the MO's are considerably increased in going from a PCE to an OCE basis. This factor is off-set of course by simpler integral evaluation in the OCE case. Machine time comparison between OCE and PCE calculations is not possible here. The OCE performance in the case of CH_4 is less successful, with the largest basis yielding a total energy of -40.0665 au compared with the PCE result of -40.181 au. Factors governing the performance of OCE calculations in XH_n systems will be discussed in chapter 6; suffice it to say that the energies tabulated in this chapter certainly indicate the superiority of the OCE attack on HF to that on CH_4.

This chapter has been concerned with defining objectives and presenting basis sets. In Chapter 5 the expectation values evaluated will be introduced and tabulated and electron density expansions for HF and CH_4 (to be used in discussing the OCE densities) will be defined.

CHAPTER 5

ELECTRON DENSITY EXPANSIONS AND EXPECTATION VALUES

The Electron Density Expansions

The one-particle density, which will be used extensively in what follows, is defined as

$$\rho(x_1) = N \int \Psi^*(q_1, q_2, \cdots, q_N)\Psi(q_1, q_2, \cdots, q_N)\, ds_1\, dq_2 \cdots dq_N \tag{5.1}$$

in which Ψ represents a normalized wave function and integration is carried out over the co-ordinates (space and spin (x and s)) of all electrons but one. The resulting electron density is spinless (due to the integration over s_1) and integrates over all space to N, the number of electrons in the system.

The two molecular ground states which are of interest in this study, the $^1\Sigma^+$ state of HF and the $^1A_1$ state of CH_4, are represented by wave functions which transform according to one dimensional, fully symmetric, irreducible representations of the symmetry point groups involved ($C_{\infty v}$ for HF and T_d for CH_4). Consider the action of a symmetry operator R on the electron density for such states. R is defined as

$$HR = RH \tag{5.2}$$

and the operation considered is

$$R\rho(x_1) = NR \int \Psi^*(q_1, q_2, \cdots, q_N)\Psi(q_1, q_2, \cdots, q_N)\, ds_1 \cdots dq_N \tag{5.3}$$

The operator R may be taken inside the integration sign without altering the result of the integration. Also the infinitessimals dq are not changed by R due to its arthogonal character. Hence

$$R\rho(x_1) = N\int R\left\{\Psi^*(q_1,q_2,\cdots,q_N)\Psi(q_1,q_2,\cdots,q_N)\,ds_1\cdots dq_N\right\} \quad (5.4)$$

Now due to the linearity of R, $R\{\phi_1\phi_2\} = R\{\phi_1\}R\{\phi_2\}$

so that

$$R\rho(x_1) = N\int R\left\{\Psi^*(q_1,q_2,\cdots,q_N)\right\}R\left\{\Psi(q_1,q_2,\cdots,q_N)\right\}ds_1\cdots dq_N \quad (5.5)$$

Since, as has been stated, the states of interest transform according to fully symmetric one dimensional irreducible representations, it follows that

$$R\,\Psi(q_1,q_2,\cdots,q_N) = \Psi(q_1,q_2,\cdots,q_N) \quad \text{for all } R \quad (5.6)$$

Hence using (5.6) in (5.5)

$$R\rho(x_1) = \rho(x_1) \quad (5.7)$$

Thus the one electron density possesses the same symmetry as the wave functions considered. This fact is of considerable importance in developing electron density expansions for CH_4 and HF which will be useful in comparing the OCE and PCE results. Thus the type of expansion envisaged separates the radial and angular co-ordinates of the electron:

$$\rho(r,\theta,\phi) = \sum_{l=0}^{\infty} R_l(r)\, A_l(\theta,\phi) \tag{5.8}$$

The discussion so far has indicated that the electron densities for HF and CH_4 transform according to the one dimensional, fully symmetric, representations of the respective point groups. The angular functions appearing in the expansion (5.8) must also possess this symmetry.

In the case of HF, such functions are well known. They are the spherical harmonics (to be defined later) $Y_l^{0,c}$, so that for this system the appropriate electron density expansion is

$$\rho(r,\theta,\phi) = \sum_{l=0}^{\infty} R_l(r)\, Y_l^{0,c} \tag{5.9}$$

In the case of CH_4, the angular functions $A_l(\theta,\phi)$ appearing in the electron density expansion must transform according to the A_1 representation of T_d. In the next section these functions (the tetrahedral harmonics) will be evaluated.

The Tetrahedral Harmonics

In this derivation of the tetrahedral harmonics, the method proposed by Altmann[45] is used. The general theory (which follows Altmann's presentation) is introduced first, followed by an application to the tetrahedral group T_d.

Altmann's approach uses a well known group theoretical result which allows a function possessing a particular symmetry to be formed by projection. Thus using the spherical harmonics Y_l^m as generator functions, suppose the transformations of Y_l^m, RY_l^m

under all operations of a point group are known. Then a function ϕ^i which transforms according to the ith irreducible representation may be generated according to the equation

$$\phi^i = \sum_R \chi^{i*}(R) R Y_l^m \tag{5.10}$$

where the $\chi^i(R)$ are the characters of the ith irreducible representation. If R is a pure rotation, then using the fact that the spherical harmonics span (2l + 1) - dimensional representations of the rotation group allows $R Y_l^m$ to be written as:

$$R Y_l^m = \sum_R D^l_{m'm}(R) Y_l^{m'} \tag{5.11}$$

The matrix representatives $D^l_{m'm}(R)$ have been given by Wigner[46]. Altmann modifies Wigner's results for use with unnormalized spherical harmonics defined as

$$Y_l^m(\theta, \phi) = P_l^m(\cos\theta)\, e^{im\phi} \tag{5.12}$$

A rotation is specified by Euler angles α, β, γ ($0 \leq \alpha < 2\pi$; $0 \leq \beta \leq \pi$; $0 \leq \gamma < 2\pi$). Then, using the unnormalized form of the spherical harmonics, the matrix representatives, $D^l_{m'm}(R) \equiv D^l_{m'm}[R(\alpha, \beta, \gamma)]$, may be written as

$$D^l_{m'm}[R(\alpha, \beta, \gamma)] = C_{m'm}\, e^{im'\gamma}\, e^{im\alpha}\, S^l_{m'm}(\beta) \tag{5.13}$$

where

$$C_{m'm} = i^{|m'|+m'} \, i^{|m|+m}$$

and

$$S^{l}_{m'm}(\beta) = \sum_{r=0}^{r_m} K^{l}_{\mu\nu}(r) \cos^{\nu-\mu+2r}(\beta/2) \sin^{2l-(\nu-\mu+2r)}(\beta/2) \tag{5.14}$$

Also

$$K^{l}_{\mu\nu}(r) = \frac{(-1)^{\mu-r} (l+|m|)!\,(l-|m'|)!}{(\nu-\mu-r)!\; r!\; (\mu-r)!\; (2l-\nu-r)!}$$

in which

$$\begin{aligned} \mu &= \min(1 - m', 1 + m) \\ \nu &= \max(1 - m', 1 + m) \\ r_m &= \min(\mu, \; 2l - \nu) \end{aligned} \tag{5.15}$$

In the case of point group operators R' which are not pure rotations, e.g. rotary reflections, then the operation may always be written as a product of the inversion and a rotation, i.e. $R' = i R$. The matrix representative of the inversion in the chosen basis is $(-1)^l$ (-1 being the unit matrix) so that the matrix representative of R^1 may be obtained by multiplying the rotation result by $(-1)^l$. Hence the result (5.10) may be used to project a function of the desired symmetry for any (finite) point group. After choosing a generator harmonic. Y^m_l , the function belonging to the ith irreducible representation is given by combining (5.10_1 11 and 13) as

$$\phi^i = \sum_R \chi^{i*}(R) \sum_{m'} C_{m'm} e^{im'\gamma} e^{im\alpha} S^l_{m'm}(\beta) Y_l^{m'} \qquad (5.16)$$

In order to simplify (5.16) the group G is divided into sets G^β, all elements of which have the same β angle. The sets G^β are partitioned into subsets $G^{\beta,C}$ which belong to the same class (the whole class need not be included in $G^{\beta,C}$). An element of the group will be labelled $R^{\beta_r C_{s,t}}$, t being a running index over those elements having the same β angle and belonging to the same class. The α and γ angles of the operations are denoted by α_t and γ_t. The expression (5.16) may thus be re-written

$$\phi^i = \sum_r \sum_{m'} S^l_{m'm}(\beta_r) \left\{ \sum_s \chi^{i*}(C_s) C_{m'm} \sum e^{im'\gamma_t} e^{im\alpha_t} \right\} Y_l^{m'} \qquad (5.17$$

For operations which involve the inversion, the term $e^{im'\gamma_t} e^{im\alpha_t}$ must be multiplied by $(-1)^l$. Equation (5.17) will be the fundamental result used in this section.

The values of β occurring for point groups are 0, $\pi/2$ and π. Altmann shows that for the special cases $\beta = 0$ and $\beta = \pi$ considerable simplification occurs in the application of (5.17). For $\beta = \pi$ the only spherical harmonic occurring on the RHS of (5.11) is that for $m' = -m$ and only one term survives in the coefficient $S^l_{-mm}(\pi)$. Similar behaviour occurs for $\beta = 0$; in this case only $m' = m$ occurs in the summation over m'. These two results are summarized below where the two terms in the sum over r are presented

$$\beta_r = 0 \qquad \sum_s \chi^i(C_s)^* \sum_t e^{im\gamma_t} e^{im\alpha_t} Y_l^m \tag{5.18}$$

$$\beta_r = \pi \qquad \sum_s \chi^i(C_s)^* \sum_t (-1)^l e^{-im\gamma_t} e^{im\alpha_t} Y_l^{-m}$$

The above theory is now applied to the present problem, i.e. the generation of tetrahedral harmonics of type A_1. In this case all $\chi^i(R) = 1$. Tabulation of the sum over t for all the T_d operations in (5.17) (which depends on l only through a sign coefficient $(-1)^l$ for non-rotations) shows that this term has a periodic structure, so that only certain values of m and m' need be considered. The values m' takes are - 1 to + 1 for a generator Y_l^m. The tabulation referred to establishes the following behaviour: for even l the only values of m leading to no-zero values of the sum over s (for all β angles) are m = 0, $\pm$ 4, $\pm$ 8 etc. or m = $\pm$ 4n. Thus only generator functions Y_l^0, $Y_l^{\pm 4}$, $Y_l^{\pm 8}$ etc. need be considered in generating even l functions. Also the values of m' which appear are restricted to the values m' = $\pm$ 4n. Thus the even l tetrahedral harmonics will be linear combinations of spherical harmonics Y_l^0, $Y_l^{\pm 4}$, $Y_l^{\pm 8}$ etc. The coefficient tables also establish the following for odd l generators: the only values of m leading to finite coefficients are m = $\pm$ 2, $\pm$ 6, $\pm$ 10 etc. The values of m' are restricted to the same values.

For the values of m and m' mentioned above, the summation over t is indicated in the table below. Included in brackets in the table is

the sum over s (over those elements with the same β angle). The T_d operations are divided according to their β angles. The twenty four operations in five classes consist of 3 C_2 rotations about the co-ordinate axes (see Figure 2.1.), six S_4 rotary reflections, 12 C_3 rotations and six reflections.

Projection of Tetrahedral Harmonics

Generator function Y_l^m

		l even, $m = \pm 4n$		l odd, $m = \pm (2 + 4n)$	
		$m' = m$	$m' = -m$	$m' = m$	$m' = -m$
$\beta = 0$	E	1		1	
	C_{2_z}	1 (4)		1 (4)	
	$S_{4_z}^+$	2		2	
	$S_{4_z}^-$				
$\beta = \pi$	C_{2_x}		2 (4)		-2 (-4)
	C_{2_y}				
	σ_5		2		-2
	σ_6				

The $\beta = \pi/_2$ coefficients are:

	l even $m = \pm 4n$	l odd $m = \pm (2 + 4n)$
	$m' = \pm 4n$	$m' = \pm (2 + 4n)$
C_{3a}		
C_{3b}		
C_{3c}		
C_{3d}	8	-8
C_{3a}^2		
C_{3b}^2		
C_{3c}^2		
C_{3d}^2	(16)	(-16)
S_{4x}^+		
S_{4x}^-	4	-4
S_{4u}^+		
S_{4y}^-		
σ_1		
σ_2		
σ_3	4	-4
σ_4		

As an illustration of the use of the table consider the generator Y_2^0. Then the $\beta = 0$ and $\beta = \pi$ contributions to the sum over r in (5.17) according to (5.18), using the tabulated coefficients, is

$$4Y_2^0 + 4Y_2^0$$

The $\beta = \pi/2$ elements give the contribution

$$16\, Y_2^0\, S_{00}^2(\pi/2)$$

The total projected function is thus

$$T_2(\theta, \phi) = 8Y_2^0 + 16\, S_{00}^2(\pi/2)\, Y_2^0$$

The coefficient $S_{0,0}^2$ is $-\frac{1}{2}$ so that $T_2(\theta, \phi) = 0$. Thus there is no A_1 type harmonic for $l = 2$. This is true for $l = 1$ and 5 also.

Altmann generates all A_1 type tetrahedral harmonics up to $l = 12$. This list is extended here up to $l = 16$. In Table 5.1 the coefficients occurring in the harmonics are presented (the coefficients $S_{m',m}^1(\pi/2)$ were evaluated by computer). The spherical harmonics occurring in the tabulated functions are normalized real spherical harmonics:

$$Y_l^{m,c} = \sqrt{\frac{(2l+1)\,(l-|m|)!}{2\pi\,(l+|m|)!\,(1+\delta_{l0})}}\; P_l^m(\cos\theta)\cos m\phi$$

$$Y_l^{m,s} = \sqrt{\frac{(2l+1)\,(l-|m|)!}{2\pi\,(l+|m|)!}}\; P_l^m(\cos\theta)\sin m\phi \qquad (5.19)$$

In which δ_{l0} = 1 if m = 0 and 0 otherwise. The tetrahedral harmonics presented are normalized to unity and have the general form:

<u>even l</u>

$$T_l(\theta,\phi) = \sum_{m'} c_{lm'} Y_l^{m',c} \qquad m' = 0,4,8\cdots \leq l$$

(5.20)

<u>odd l</u>

$$T_l(\theta,\phi) = \sum_{m'} c_{lm'} Y_l^{m',s} \qquad m' = 2,6,10\cdots \leq l$$

In the case where more than one tetrahedral harmonic is associated with a given l value the functions have been arthogonalized by a technique suggested by Altmann. Thus

$$\int T_l^{j}(\theta,\phi)\, T_{l'}^{j'}(\theta,\phi)\, d\Omega = \delta_{ll'}\, \delta_{jj'}$$

where the superscript distinguishes between those harmonics with the same l value. The coefficients $C_{lm'}$ are presented in the tables to ten significant figures.

The electron density expansion for CH_4 is thus written:

$$\rho(r,\theta,\phi) = \sum_{l=0}^{\infty} R_l(r)\, T_l(\theta,\phi) \qquad (5.21)$$

in which the summation over those tetrahedral harmonics associated with a given l value is implicitly assumed.

Diagrams of the tetrahedral harmonics up to l = 9 are shown in Figure 5.1. The diagrams show the functions in the plane containing

TABLE 5.1

TETRAHEDRAL HARMONIC COEFFICIENTS $C_{l,m'}$

m'	2	6	10	14
1				
3	1			
7	-0.7359800722	-0.677003200		
9	0.4330127019	-0.901387887		
11	0.6653633093	0.4592793268	0.5885186205	
13	0.4973890161	-0.4934466368	-0.7135226579	
15	0.6349468892	0.3181615852	0.4830185352	0.5121608617
	0	-0.6486492596	0.7121026823	-0.2686334081

m'	0	4	8	12	16
1					
0	1				
4	-0.7637626158	-0.6454972244			
6	0.3535533906	-0.9354143467			
8	0.7180703308	0.3818813079	0.5818433352		
10	0.4114253679	-0.5863019700	-0.6978389260		
12	0.6955026659	0.31412556680	0.3484495380	0.5442279759	
	0	-0.5589793742	0.8062675082	-0.1935839985	
14	0.4400964620	-0.457681183	-0.4911323014	-0.5963484807	
	0.6813616833	0.2758680227	0.2904898698	0.3275697469	0.5176454259
	0	-0.6370482146	0.3299903488	0.6479807485	-0.2557281593

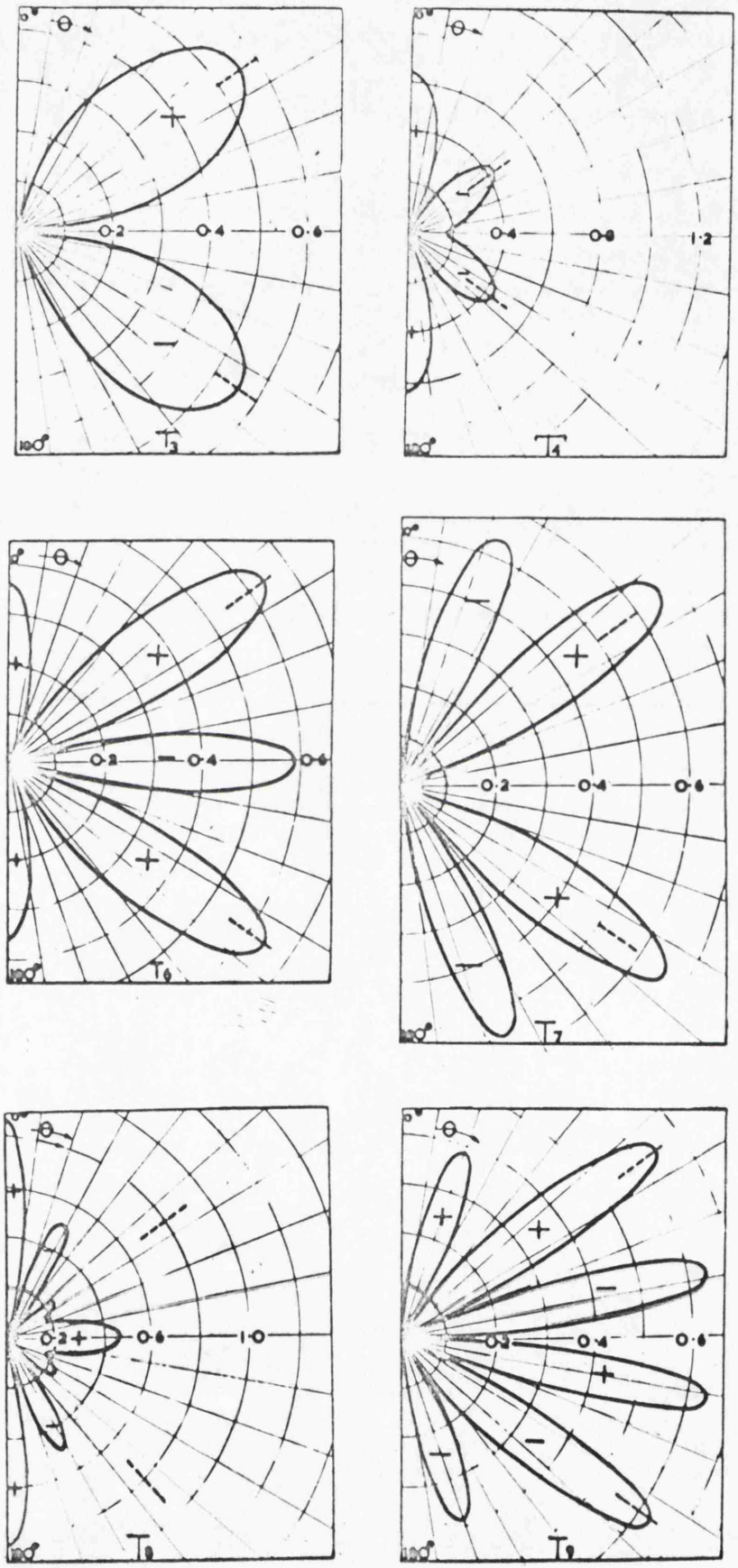

Figure 5.1: Tetrahedral Harmonics

H1, H2 and the C nucleus in Figure 2.1 (Chapter 2, Part I). This is the plane for which $\phi = \pi/4$, defining ϕ in the usual way with respect to the cartesian's shown in the diagram. The left hand edge of each diagram is coincident with the z axis, about which the figures are invariant under a C_2 rotation. The θ angles $\theta = \theta_T/2$ and $\pi - \theta_T/2$ (θ_T being the tetrahedral angle) are indicated in dotted lines for all the diagrams. The proton lies in the direction $\theta = \theta_T/2 = 54^\circ\ 44^1$ for the chosen plane.

Expectation Values

Having established the electron density expansion for HF (in the case of HF, normalized spherical harmonics $Y_l^{0,c}$ (5.19) are used in the expansion) and CH_4, the expectation values determined for both molecules will now be discussed. Where possible the expectation values will be expressed in terms of the radial terms $R_l(r)$ in the electron density expansions. The numerical techniques involved in the evaluation of the radial terms will be given at the end of this chapter.

The one electron density resulting from the closed-shell HFR wave functions under study is given as

$$\rho(r,\theta,\phi) = 2\sum_{k=1}^{N/2} \phi_k^*(r,\theta,\phi)\,\phi_k(r,\theta,\phi) \qquad (5.22)$$

where the ϕ_k are the doubly occupied MO's of the system.

For HF, the radial terms are given as

$$R_l(r) = \int \rho(r,\theta,\phi)\, Y_l^{0,c}\, d\Omega \qquad (5.23)$$

Also for CH_4

$$R_L(r) = \int \rho(r,\theta,\phi)\, T_L(\theta,\phi)\, d\Omega$$

The radial density distributions, which will feature in the discussion of results in the next chapter, are defined as

$$D(r) = \sqrt{4\pi}\, R_0(r)\, r^2$$
$$\int D(r)\,dr = N \qquad (5.24)$$

Expectation values of the form $\langle r^n \rangle$ are given as

$$\langle r^n \rangle = \int D(r)\, r^n\, dr \qquad (5.25)$$

The values of n chosen here are -2, -1, 2 and 4. The expectation values $\langle r^{-1} \rangle$, $\langle r^{-2} \rangle$ are related to magnetic properties of the systems. The other two n values are included to stress the extreme inner and outer portions of the $D(r)$ curve which will be useful for comparison purposes.

The purely diamagnetic contribution to the susceptibility, χ^d, has already been introduced in Chapter 2. This quantity is given in terms of the unperturbed ground state wave function of a molecule in a homogeneous magnetic field, i.e.

$$\bar{\chi}^d = -\left(e^2/4mc^2\right)\left\langle \Psi_0 \middle| \sum_k r_k^2 \bar{I} - \bar{r}_k \bar{r}_k \middle| \Psi_0 \right\rangle \qquad (5.26)$$

For most systems only the rotational average of χ^d is known, which is related to the principle-axis components of χ^d as

$$\langle \chi^d \rangle_{Av} = -\frac{1}{3}\left(\chi^d_{xx} + \chi^d_{yy} + \chi^d_{zz}\right)$$

$$= -\frac{e^2}{6mc^2}\left\langle \Psi_0 \middle| \sum_k r_k^2 \middle| \Psi_0 \right\rangle$$

The molar susceptibility is given here as

$$\chi_r = \langle \chi^d \rangle_{Av} = -\frac{L e^2}{6mc^2}\int_0^\infty D(r) r^2 \, dr \qquad (5.27)$$

The magnetic shielding constant, σ, determines the magnetic field at a nucleus n in a molecule placed in a magnetic field, H_{ext}. Thus the field at nucleus n is determined as

$$H_n = H_{ext}(1 - \sigma_n) \qquad (5.28)$$

As with the diamagnetic susceptibility, the magnetic shielding constant is appropriately treated by means of perturbation theory and results in an expression for σ which is the sum of a diamagnetic and paramagnetic contribution:

$$\sigma_n = \sigma_n^d + \sigma_n^p$$

The diamagnetic contribution is given in terms of the unperturbed wave function as

$$\sigma_n^d = \frac{e^2}{3mc^2}\left\langle \Psi_0 \middle| \sum_k r_k^{-1} \middle| \Psi_0 \right\rangle \qquad (5.29)$$

which may be expressed as

$$\sigma_n^d = \frac{e^2}{3mc^2} \int \frac{D(r)}{r} dr \qquad (5.30)$$

Expectation values of the form $\langle r^n \rangle$ are presented for all the HFR bases in Tables 5.2 and 5.3. Also included are the χ_r referred to the fluorine and carbon nuclei. The diamagnetic shielding factor is also presented for the heavy nuclei in both molecules. The experimental results for χ_r shown in the tables were determined from the experimental total χ and a knowledge of the rotational magnetic moment of both molecules which enabled a determination of χ^{P}(47), to be made.

Multipole Moments

The multipole moment definitions used here are those of Buckingham(48) and Kielich(49). Thus

$$\mu_\alpha = \int \rho \, r_\alpha \, d\tau$$

$$\Theta_{\alpha\beta} = \frac{1}{2} \int \rho \left[3 r_\alpha r_\beta - r^2 \delta_{\alpha\beta} \right] d\tau$$

$$\Omega_{\alpha\beta\gamma} = \frac{1}{2} \int \rho \left[5 r_\alpha r_\beta r_\gamma - r^2 \left(r_\alpha \delta_{\beta\gamma} + r_\beta \delta_{\gamma\alpha} + r_\gamma \delta_{\alpha\beta} \right) \right] d\tau$$

TABLE 5.2

$\langle r^n \rangle$ [a] FOR HF

Function	$\langle r^{-2} \rangle$	$\langle r^{-1} \rangle$	$\langle r^{2} \rangle$	$\langle r^{4} \rangle$	χ_r [b]	σ_F^d [c]
OCE(1)	331.14	27.228	13.689	58.737	-10.846	48.330
OCE(2)	331.00	27.184	13.803	58.710	-10.937	48.252
OCE(3)	330.99	27.172	13.830	58.571	-10.958	48.231
OCE(4)	330.99	27.170	13.834	58.531	-10.961	48.227
PCE(1)	327.50	27.131	12.100	41.621	- 9.5872	48.158
PCE(2)	330.77	27.170	13.741	59.080	-10.887	48.227
PCE(3)	330.98	27.165	13.848	58.414	-10.972	48.218
PCE(4)	330.98	27.168	13.805	57.824	-10.938	48.223
OBSERVED					- 9.2[d]	

a All $\langle r^n \rangle$ in au, referred to F nucleus.

b χ_r referred to F nucleus, in units of 10^{-6} emu/mole

c σ_F^d units of 10^{-5} emu.

d Reference 55

TABLE 5.3

$\langle r^n \rangle$ [a] FOR CH_4

Function	$\langle r^{-2} \rangle$	$\langle r^{-1} \rangle$	$\langle r^{2} \rangle$	$\langle r^{4} \rangle$	χ_r [b]	σ_c^d [c]
OCE(1)	138.81	16.826	36.121	305.22	-28.620	29.866
OCE(2)	138.84	16.771	36.367	303.74	-28.815	29.769
OCE(3)	138.61	16.731	36.490	302.48	-28.912	29.698
OCE(4)	138.55	16.713	36.386	297.58	-28.830	29.666
OCE(5)	138.56	16.707	36.337	295.61	-28.791	28.655
OCE(6)	138.54	16.702	36.327	294.70	-28.783	29.646
PCE(1)	132.02	16.191	37.951	320.91	-30.070	28.739
PCE(2)	136.49	16.528	38.898	349.57	-30.820	29.337
PCE(3)	136.38	16.582	36.207	289.19	-28.690	29.433
PCE(4)	138.82	16.667	36.329	293.71	-28.785	29.584
PCE(5)	138.39	16.670	36.252	290.92	-28.724	29.589
OBSERVED			-33.69 ± 0.72 [d]			

a All $\langle r^n \rangle$ in au, referred to C nucleus

b χ_r referred to C nucleus, in units of 10^{-6} emu/mole

c σ_c^d in units of 10^{-5} emu

d Reference 47

$$\Phi_{\alpha\beta\gamma\delta} = \frac{1}{8}\int \rho\Big[35\, r_\alpha r_\beta r_\gamma r_\delta - 5r^2\big(r_\alpha r_\beta \delta_{\gamma\delta} + r_\alpha r_\gamma \delta_{\beta\delta}$$

$$+ r_\alpha r_\delta \delta_{\beta\gamma} + r_\beta r_\gamma \delta_{\alpha\delta} + r_\beta r_\delta \delta_{\alpha\gamma} + r_\gamma r_\delta \delta_{\alpha\beta}\big)$$

$$+ r^4\big(\delta_{\alpha\beta}\delta_{\gamma\delta} + \delta_{\alpha\gamma}\delta_{\beta\delta} + \delta_{\alpha\delta}\delta_{\beta\gamma}\big)\Big]\, d\tau \tag{5.31}$$

or, in general

$$M_{\alpha,\beta,\ldots,\mu} = \frac{(-1)^m}{m!}\int \rho\, r^{2m+1} \frac{\partial^m}{\partial r_\alpha \partial r_\beta \quad \partial r_\mu}\left(\frac{1}{r}\right) d\tau$$

where μ_α, $\Theta_{\alpha\beta}$, $\Omega_{\alpha\beta\gamma}$, $\Phi_{\alpha\beta\gamma\delta}$ and $M_{\alpha,\beta,\ldots,\mu}$ are components of the dipole, quadrupole, octupole, hexadecapole and general m^{th} rank tensors respectively. In the equations (5.28) is the charge density (including the charge on the nuclei) at the point (X, Y, Z). The subscripted r's are X, Y or Z depending on whether the subscripts have the value 1, 2 or 3. The δ's are Kronecker δ's.

The potential due to a system of charges, at a point outside the distribution, is simply related to the multipole moments of the charge system. Consider a distribution of charges e_i at points X_i, Y_i, Z_i represented by vectors $\bar{r}_i$ from an origin O. The potential at P(X, Y, Z), represented by $\bar{R}$, where $\bar{R} > \bar{r}_i$ for all i, may be written

$$V_P = \sum_i \frac{e_i}{|\bar{R} - \bar{r}_i|}$$

The distance between e_i and P, R_i, may be expended in terms of derivatives

with respect to $r_{i\alpha}$ (X_i, Y_i or Z_i) at the origin. Thus

$$V_P = \sum_i e_i \left[\frac{1}{R} + \left(\frac{\partial \left(\frac{1}{R_i}\right)}{\partial r_{i\alpha}} \right)_0 r_{i\alpha} + \frac{1}{2} \left(\frac{\partial^2 \left(\frac{1}{R_i}\right)}{\partial r_{i\alpha} \partial r_{i\beta}} \right)_0 r_{i\alpha} r_{i\beta} \right.$$
$$\left. + \frac{1}{6} \left(\frac{\partial^3 \left(\frac{1}{R_i}\right)}{\partial r_{i\alpha} \partial r_{i\beta} \partial r_{i\gamma}} \right) r_{i\alpha} r_{i\beta} r_{i\gamma} + \cdots \right.$$

Then evaluating the derivatives occurring in the above expression gives

$$V_P = \frac{q}{R} + \frac{\mu_\alpha R_\alpha}{R^3} + \frac{\Theta_{\alpha\beta}}{3R^5}\left(3R_\alpha R_\beta - R^2 \delta_{\alpha\beta}\right)$$
$$+ \frac{\Omega_{\alpha\beta\gamma}}{5R^7}\left[5R_\alpha R_\beta R_\gamma - R^2\left(R_\alpha \delta_{\beta\gamma} + R_\beta \delta_{\gamma\alpha} + R_\gamma \delta_{\alpha\beta}\right)\right] + \tag{5.32}$$

For an axially symmetric charge distribution, each multipole moment is determined by a single scalor quantity (viz., q, μ, Θ, Ω, $\cdots$)
In this case (5.32) becomes

$$V_P = \frac{q}{R} + \frac{\mu \cos\theta}{R^2} + \frac{\Theta}{2R^2}\left(3\cos^2\theta - 1\right) + \frac{\Omega}{2R^4}\left(5\cos^3\theta - 3\cos\theta\right) + \cdots \tag{5.33}$$

in which P is now the point (R, θ) relative to an origin on the axis of the charge distribution. Equations (5.32) and 5.33) show that the potential outside a charge distribution is the sum of contributions from a charge, dipole, quadrupole etc. located at the origin. The interaction of a charge distribution with an external field may also be written in a multipole expansion and the interaction between two non-overlapping distributions may be treated in the same way. Early attempts to explain the attractive forces between molecules in a gas used static and induced

multipoles to account for this phenomenon. Although these interactions are now known to be overshadowed by quantum mechanical induction (dispersion forces) they are, nevertheless, important whenever the molecules are in fact polar.

In this study, the dipole and quadrupole moments of HF have been determined for all the HFR bases and included in Table 5.4. The OCE results are Hoyland's, although these were redetermined here to check the numerical technique used with the OCE bases. Expressing the electronic contributions to the multipoles in terms of specific radial terms gives

$$\mu^e = \mu_z^e = -\int \rho(r,\theta,\phi)\, z\, d\tau = -\sqrt{\frac{4\pi}{3}} \int_0^\infty R_1(r) r^3\, dr$$

$$\Theta^{e'} = \Theta_{zz}^{e'} = -2\,\Theta_{yy}^{e'} = -2\,\Theta_{zz}^{e'} = -\sqrt{\frac{4\pi}{5}} \int_0^\infty R_2(r) r^4\, dr \qquad (5.34)$$

Both formulae (5.34) refer the moments to the F nucleus as origin. For comparison with experiment it is convenient to express Θ with respect to the centre of mass of the system (located 0.08736 au from the F nucleus). In order to accomplish this, the following transformation is used:

$$\Theta = \Theta' - Z\mu R$$

where the origin Θ is referred to has co-ordinates (0, 0, R) with respect to the F nucleus. The dipole moment is independent of origin. Table 5.4 shows the separate nuclear and electronic contributions to μ

and Θ , together with the total values.

For CH_4, all components of the dipole and quadrupole moments are zero (due to the absence of $R_1(r)$, $R_2(r)$ in the electron density expansion already discussed). Also

$$\Omega = \Omega_{xyz}$$

and

$$\Phi = \Phi_{xxxx} = \Phi_{yyyy} = \Phi_{zzzz} = -16\,\Phi_{zzxx} = -16\,\Phi_{zzyy} = -16\,\Phi_{xxyy}$$

Once again expressing the electronic contributions to Ω and Φ , Ω^e and Φ^e , in terms of radial terms gives

$$\Omega^e = -\sqrt{\frac{5\pi}{21}} \int_0^\infty R_3(r)\, r^5\, dr \qquad (5.35)$$

$$\Phi^e = -\sqrt{\frac{7\pi}{27}} \int_0^\infty R_4(r)\, r^6\, dr$$

The results for CH_4, giving Ω and Φ in units of 10^{-34}esu cm^3 and 10^{-42}esu cm^4 respectively, referred to the carbon nucleus as origin, are presented in Table 5.5 for the six OCE bases and five PCE bases.

All the experimental moments presented (except the dipole moment of HF - see reference 53) are taken from the tables of Stogryn and Stogryn[50]. These authors suggest 'recommended' values for the moments of many molecules; the recommended values being the average of experimental and theoretical predictions. Some comments on these experimental values will be made in the following chapter.

TABLE 5.4

DIPOLE[a] AND QUADRUPOLE[b] MOMENTS FOR HF

Function	μ^e	μ^T	Θ^e	Θ^T
OCE(1)[c]	-0.386	4.019	-0.166	3.466
OCE(2)	-2.249	2.156	-1.045	2.587
OCE(3)	-2.421	1.984	-1.257	2.375
OCE(4)	-2.448	1.957	-1.285	2.347
PCE(1)	-2.9661	1.4379	-2.1751	1.4560
PCE(2)	-2.5037	1.9003	-1.5949	2.0362
PCE(3)	-2.3204	2.0836	-1.3978	2.2333
PCE(4)	-2.4624	1.9416	-1.2803	2.3507
OBSERVED		1.8195[e]		2.60[d]

a The total and electronic contribution to the dipole moment (μ^T and μ^e respectively) are tabulated in Debye (10^{-18} esu em)

b The quadrupole moments are presented in units of 10^{-26} esu em^2

c The OCE results are those of Hoyland (Ref. 40)

d The results of Stogryn (Ref. 50)

e Reference 53.

TABLE 5.5

OCTAPOLE[d] AND HEXADECAPOLE MOMENTS[b] FOR CH_4

Function	Ω^e	Ω^T	Φ^e	Φ^T
OCE(1)[c]	0	12.087	0	10.684
OCE(2)	-5.548	6.539	-1.2125	9.471
OCE(3)	-7.773	4.314	-4.690	5.993
OCE(4)	-9.568	2.519	-5.933	4.750
OCE(5)	-9.918	2.169	-6.926	3.757
OCE(6)	-10.12	1.967	-7.242	3.441
PCE(1)	-10.214	1.8733	-8.2966	2.3869
PCE(2)	-11.130	1.0569	-9.1825	1.5010
PCE(3)	-10.844	1.2430	-8.9102	1.7733
PCE(4)	-10.610	1.4770	-8.6324	2.0511
PCE(5)	-10.665	1.4216	-8.6769	2.0066
OBSERVED		4.5[d]		

a The electronic contribution to and the total octapole moment (Ω^e and Ω^T respectively) tabulated in units of 10^{-34} esu cm^3

b The hexadecapole moment is given in units of 10^{-42} esu cm^4

c The OCE moments tabulated are those of Hoyland (ref. 40)

d The results of Stogryn (Ref. 50).

The Bond Moment for CH_4

Performing a unitary transformation on the HFR MO's leaves the wave function unchanged and thus represents the same physical situation. The bonding situation in CH_4 may be described by performing such a transformation which produces four MO's which each have C_3 symmetry about each CH bond. The transformation envisaged assumes the inner shell MO ($\phi(1A_1)$), which is largely $1s_c$, to be coalesced with the carbon nucleus. The remaining four MO's $\phi(2A_1)$, $\phi(T_{2x})$, $\phi(T_{2y})$ and $\phi(T_{2z})$ are transformed to form 'equivalent' orbitals which have the symmetry described. The centroid of electronic charge for one such orbital, which has C_3 symmetry about CH_1 (See Figure 2.1) is given as

$$\bar{c} = \frac{1}{2}\int r_{H_1}\left\{\phi(2A_1) + \phi(T_{2x}) + \phi(T_{2y}) + \phi(T_{2z})\right\}^2 d\tau \tag{5.36}$$

in which r_{H1} represents distance measured along the $C-H_1$ direction. The bond dipole moment may be formed according to

$$\mu_B = 2e\left(\bar{c} - \frac{R}{2}\right)$$

where R is the bond length. The bond moment thus defined is calculated here for all the HFR functions used. Table 5.6 shows μ_B expressed in Debye.

X-Ray Scattering Factor

In Chapter 2(Part I), the coherent X-ray scattering factor, f(k), was defined as

TABLE 5.6

BOND MOMENT FOR CH_4

Function	$\bar{c}$ (au)[a]	μ_c (D)
OCE(1)	0.9067	-0.6433[b]
OCE(2)	1.2638	1.1729
OCE(3)	1.3387	1.5542
OCE(4)	1.3582	1.6507
OCE(5)	1.3672	1.6965
OCE(6)	1.3753	1.7371
PCE(1)	1.3812	1.7676
PCE(2)	1.4314	2.0218
PCE(3)	1.3944	1.8337
PCE(4)	1.3842	1.7829
PCE(5)	1.3853	1.7880

a $\bar{c}$ gives the centroid of electronic charge derived from an equivalent orbital measured along a CH bond.

b The negative moment recorded for OCE(1) signifies polarity C^-H^+.

TABLE 5.7

COHERENT X-RAY SCATTERING FACTORS FOR HF AND CH_4

HF^a

$K = \sin\theta/2/\lambda$	f_o	f_1	f_2	f_3	$f = \sqrt{\sum_{i=0}^{3} f_i^2}$
0.05	9.1611	0.2905	0.0565	0.0114	9.1659
0.10	7.2833	0.3287	0.1426	0.0609	7.2924
0.20	3.9802	0.0275	0.0815	0.1181	3.9829
0.30	2.4423	-0.0591	-0.0401	-0.0459	2.4438
0.40	1.8150	-0.0263	-0.0453	-0.0045	1.8158
0.45	1.6495	-0.0154	-0.0354	-0.0027	1.6500

$CH_4{}^b$

$K = \sin\theta/2/\lambda$	f_o	f_3	f_4	$f = \sqrt{\sum_{i=0}^{4} f_i^2}$
0.05	7.9512	0.0819	-0.0147	7.9516
0.10	4.4721	0.3492	-0.1313	4.4876
0.20	1.8728	0.3019	-0.2929	1.9195
0.30	1.6031	-0.0050	-0.0508	1.6031
0.40	1.3546	0.0000	0.0163	1.3547
0.45	1.2255	0.0086	0.0009	1.2255

a The x-ray scattering factor for HF is calculated for wave function PCE(4) - Cade-Huo (Ref. 35)

b For CH_4 the scattering factor is presented for PCE(5) - Woznik (Ref. 39)

$$f^2(K) = \sum_{l=0}^{\infty} \sum_{m=-l}^{m=+l} f_{lm}^*(K)\, f_{lm}(K)$$

where

$$f_{lm}(K) = (2\pi)^{3/2} \int_0^{\infty} \rho_{lm}(r)\, \frac{J_{l+1/2}(Kr)}{(Kr)^{1/2}}\, r^2 dr$$

These results were obtained using the electron density expansion

$$\rho(r, \theta, \phi) = \sqrt{2} \sum_{l=0}^{\infty} \sum_{m=-l}^{m=+l} \rho_{lm}(r)\, \Theta_{lm}(\theta)\, e^{im\phi}$$

For the cases of HF and CH_4, using the electron density expansions defined here for these systems ((5.9) and (5.21)), the X-ray scattering factor is expressed as:

a) HF

$$f^2(K) = \sum_{l=0}^{\infty} f_l^2(K)$$

where

$$f_l(K) = \sqrt{2}\,\pi \int_0^{\infty} R_l(r)\, \frac{J_{l+1/2}(Kr)}{(Kr)^{1/2}}\, r^2 dr \qquad (5.37)$$

b) CH_4

$$f^2(K) = \sum_{l=0}^{\infty} f_l^2(K)$$

where

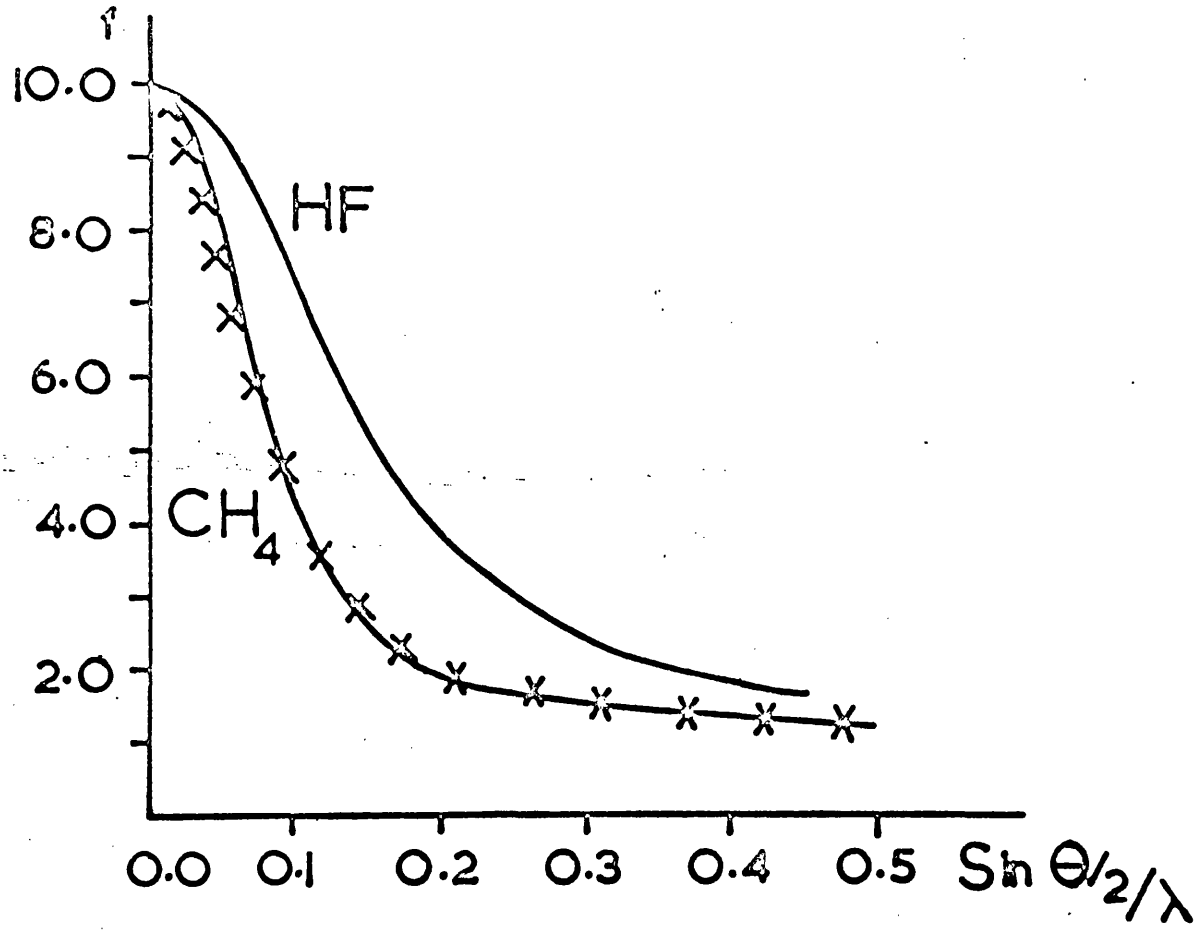

Figure 5.2: X-Ray Scattering Factors for HF and CH_4. The crosses correspond to a fit of Thomer's experimental results for CH_4 (Ref. 51).

$$f_l(K) = \sum_{m'=0,4,8\ldots} C_{lm'}\,\pi\sqrt{1+\delta_{l0}}\int_0^\infty R_l(r)\,\frac{J_{l+1/2}(Kr)}{(Kr)^{1/2}}\,r^2dr \quad \ldots \text{l even}$$

$$= \sum_{m'=2,6,10\ldots} C_{lm'}\,\pi\int_0^\infty R_l(r)\,\frac{J_{l+1/2}(Kr)}{(Kr)^{1/2}}\,r^2dr \quad \ldots \text{l odd}$$

(5.38)

The coefficients $C_{lm'}$ are those appearing in the tetrahedral harmonics (5.20).

In order to investigate contributions to the scattering factor made by angular terms in the electron density, the first four terms in the summation over l in (5.37) have been calculated for the largest PCE basis for HF. These are presented in Table 5.7 for several values of $K = \sin\theta/2/\lambda$. For CH_4, again for the largest PCE basis, the contributions f_0, f_3 and f_4 to the scattering factor are presented in Table 5.7. The total scattering factors are presented in Figure 5.2. The crosses represent a fitting of Thomer's[51] experimental results for CH_4.

Numerical Techniques

The numerical methods used to determine the radial terms occurring in the electron density expansions for HF and CH_4 will be described in this section. The computer programmes written to evaluate the radial terms were used to determine many of the expectation values introduced in this chapter, since, as has been shown, these expectation values depend on individual radial terms. Two distinct approaches were followed. In the case of the OCE bases the R_l (r) were determined by a very economic

numerical technique which will be described in the next section. For the PCE bases numerical integration over angles was used to yield the $R_l(r)$.

Determination of the $R_l(r)$ for OCE Functions

The problem at hand is the evaluation of the radial terms, $R_l(r)$, occurring in the electron density expansions for HF and CH_4, which will be written in the general form:

$$\rho(r, \theta, \phi) = \sum_{L=0}^{L} R_L(r)\, A_L(\theta, \phi) \qquad (5.39)$$

The summation over l is truncated for the OCE basis since the MO's are finite expansions in spherical harmonics ($L = 2l_{max}$, where l_{max} is the maximum l value in the MO expansions).

Let the density be determined at M θ, ϕ, values for a given , where M is the number of terms occurring in the sum over l in (5.39). The M values of ρ, $\rho(r, \theta_1, \phi_1)$, $\rho(r, \theta_2, \phi_2) \cdots, \rho(r, \theta_M, \phi_M)$ may be considered to constitute a vector $\bar{\rho}$ in M dimensional space. The angular functions, $A_L(\theta, \phi)$, may also be determined at the same M θ, ϕ values, so that the vectors $\bar{A}_1$, $\bar{A}_2$, ...,$\bar{A}_m$ (changing the sum over l to one over j, where j goes from 1 to M) may be formed. The vectors $\bar{A}_1$, $\bar{A}_2$, ..., $\bar{A}_M$ may be said to span an M dimensional space. The components of the vector $\bar{\rho}$ in this basis are just the radial terms which are required, i.e. R_1, R_2, ..., R_M. So rewriting (5.39) according to the vector interpretation just described gives

$$\bar{\rho} = \sum_{j=1}^{M} R_j\, \bar{A}_j \qquad (5.40)$$

The scalar product of two vectors in the space spanned by the basis $\bar{A}_1$ ....., $\bar{A}_m$ is written as:

$$(V1, V2) = \sum_{j=1}^{M} V1(j)\, V2(j) \tag{5.41}$$

Consider now a change of basis which produces an orthonormal basis $\bar{O}_j$. The procedure used is the well-known Schmidt orthogonalization process. Thus,

$$\begin{aligned}
\bar{O}'_1 &= \bar{A}_1 \\
O'_2 &= \bar{A}_2 - \left(\frac{\bar{A}_2 \cdot \bar{A}_1}{\bar{A}_1 \cdot \bar{A}_1}\right) \bar{A}_1 \\
\bar{O}'_3 &= \bar{A}_3 - \left(\frac{\bar{A}_3 \cdot \bar{A}_2}{\bar{A}_2 \cdot \bar{A}_2}\right) \bar{A}_2 - \left(\frac{\bar{A}_3 \cdot \bar{A}_1}{\bar{A}_1 \cdot \bar{A}_1}\right) \bar{A}_1 \\
&\;\;\vdots
\end{aligned} \tag{5.42}$$

Normalization of the vectors $\bar{O}'_j$ resulting from (5.42) produces an orthonormal basis $\bar{O}_j$, i.e.

$$(\bar{O}_i, \bar{O}_j) = \delta_{ij} \tag{5.43}$$

Each of the $\bar{O}_j$ may be written

$$\bar{O}_j = \sum_{K=1}^{j} s_{jK}\, \bar{A}_K \tag{5.44}$$

where s_{jK} are elements of the transformation matrix (lower triangular

in form). The vector $\bar{\rho}$ may now be expressed in terms of the orthonormal basis, i.e.

$$\bar{\rho} = \sum_{j=1}^{M} c_j \bar{O}_j \tag{5.45}$$

where the components of $\bar{\rho}$ in the $\bar{O}_j$ basis are immediately given as

$$c_j = (\bar{\rho}, \bar{O}_j) \tag{5.46}$$

Expressing (5.45) in terms of the initial basis $\bar{A}_j$ by using the transformation (5.44) gives

$$\bar{\rho} = \sum_{j=1}^{M} c_j \sum_{k=1}^{j} s_{jk} \bar{A}_k \tag{5.47}$$

Comparing (5.47) and (5.40) gives R_j as

$$R_j = \sum_{k=j}^{M} c_k s_{kj} \tag{5.48}$$

Thus (5.48) determines all R_j for a given r. The process is extended to other r values by redetermining the $\bar{\rho}$ vector for each r; in each case the same basis $\bar{O}_j$ is then used to determine the components c_j and hence the R_j according to (5.48). Thus once the angular functions have been determined at the M distinct values of θ, ϕ and the Schmidt process carried out, only M values of the density are required at each r value to determine all the radial terms at each r.

The Schmidt process described above was carried out in double-precision arithmetic to guard against accumulative round-off error. The largest OCE basis for HF, OCE(4), has seventeen terms in the electron

density expansion ($l = 0 - 16$), whereas the largest CH_4 basis, OCE(6), has eleven radial terms. In order to obtain good orthonormalization, the whole θ range ($0 \leq \theta \leq \pi$) was used. The final orthogonal basis was found to be orthogonal to double-precision accuracy (20 significant figures). The OCE expectation values tabulated in this chapter were obtained by numerical integration over individual radial terms evaluated by the technique described in this section (except in the case of the bond-moment, which was found by numerical integration over three dimensions). The quadrature over radial terms was tested for accuracy by checking normalization. For all OCE bases, normalization was achieved to at least six significant figures. The OCE expectation values are presented and are expected to be accurate to five significant figures (except in the case of the moments were Hoyland's four figure results are presented).

The PCE Bases

The evaluation of the radial terms in the case of the PCE bases will be illustrated by considering CH_4. In this case, the radial terms required are given by the integral over angles:

$$R_l(r) = \int \rho(r, \theta, \phi)\, T_l(\theta, \phi)\, d\Omega \qquad (5.49)$$

Equation (5.49) will be rewritten for the purposes of this discussion as

$$R_l(r) = \int F(r, \theta, \phi)\, d\Omega \qquad (5.50)$$

The integral over ϕ implicit in (5.50) may be reduced to the range

$-\pi/4 \leq \phi \leq \pi/4$ (see Figure 2.1, Chapter 2, for the co-ordinate system used for CH_4, defining spherical polars in the usual way with respect to the cartesian co-ordinate system shown). The integral over this range of ϕ will be $^1/4$ of the integral over all due to the symmetry of the integrand, so that

$$R_L(r) = 4 \int_{\theta=0}^{\pi} \int_{\phi=-\pi/4}^{\phi=\pi/4} F(r, \theta, \phi) \sin\theta \, d\theta \, d\phi \qquad (5.51)$$

The integral over co-ordinate θ is conveniently split into three ranges, i.e. $\theta = (0 - \theta_T/2)$, $(\theta_T/2 - (\pi - \theta_T/2))$ and $((\pi - \theta_T/2) - \pi)$, where θ_T is the tetrahedral angle. In this way, the cusps in the density at the hydrogens occur at the ends of the θ ranges which is suitable for numerical integration. The integrals (over θ, ϕ) for $\theta = 0 - \theta_T/2$ and $\theta = (\pi - \theta_T/2) - \pi$ are in fact equal, so that only two ranges of θ need be considered. Thus (5.51) may be written as:

$$R_L(r) = 8 \int_{\theta=0}^{\theta_T/2} \int_{\phi=-\pi/4}^{\pi/4} F(r, \theta, \phi) \sin\theta \, d\theta \, d\phi + 4 \int_{\theta=\theta_T/2}^{\pi-\theta_T/2} \int_{\phi=-\pi/4}^{\pi/4} F(r, \theta, \phi) \sin\theta \, d\theta \, d\phi \qquad (5.52)$$

The numerical integration technique used is that of gaussian quadrature, i.e.

$$\int_{-1}^{+1} f(x) \, dx \doteq \sum_{i=1}^{NPOINT} w_i f(x_i) \qquad (5.53)$$

where the weights, w_i, and the arguments, x_i, for an NPOINT gaussian quadrature are given in tables[52]. In order to generalize the result (5.53) for an integral over the range $b \leq x \leq a$, a transformation of argument is required, i.e.

If $$x = \frac{(b-a)t + (b+a)}{2}$$

$$f(x) = f'(t)$$

Then

$$\int_a^b f(x)\,dx = \frac{(b-a)}{2}\int_{-1}^{1} f'(t)\,dt$$

$$\doteqdot \frac{(b-a)}{2}\sum_{i=1} w_i f'(t_i)$$

$$\doteqdot \frac{(b-a)}{2}\sum_{i=1}^{NPOINT} w_i f\left[\frac{(b-a)t_i + (b+a)}{2}\right] \qquad (5.54)$$

Extending the formula to two dimensions, gives

$$\int_a^b\int_c^d f(x,y)\,dx\,dy \doteqdot \frac{(b-a)(d-c)}{4}\sum_{i,j=1}^{NPOINT} w_i w_j f(x_i, y_i) \qquad (5.55)$$

in which $$x_i = \frac{(b-a)t_i + (b+a)}{2}, \quad y_i = \frac{(d-c)t_i + (c+a)}{2}$$

In (5.55), the same NPOINT quadrature formula is used over both dimensions (x, y). This quadrature formula was the one used to evaluate

the integrals required (5.52). Some experimentation with the number of points, NPOINT, used in the quadrature formula was undertaken. For NPOINT = 20, the results for $R_l(r)$ $(l = 0 - 8)$, were changing at most by three digits in the sixth figure, when compared with the results for NPOINT = 16. It was decided to use NPOINT = 20 for the evaluation of angular terms. The expectation values $\langle r^n \rangle$, Ω, Φ etc required a further numerical integration over radial co-ordinate r. In order to provide some kind of check on the results, the expectation values provided by Pitzer[54] for CH_4 were re-evaluated. In all cases, the results checked to five figures - the PCE results presented in the tables in this chapter are given to this accuracy .

CHAPTER 6

DISCUSSION OF RESULTS

The interpretation of HFR wave functions has been carried out along the lines of SCF population analysis[56] suggested by Mullikan. Difficulties in interpretation within the population analysis scheme occur when the wave functions being compared are constituted from widely differing basis sets of STF's. An extreme example of this problem arises when comparing the results of OCE and PCE bases - which is present in this study of HFR calculations for HF and CH_4. For this reason the population analysis scheme is not resorted to in this discussion of results; the PCE and OCE results will be related by straight-forward comparison of expectation values and by comparing electron densities and the electron density expansions introduced in Chapter 5. The discussion of expectation values tabulated in Chapter 5 is started with a consideration of the PCE results for HF and CH_4.

The PCE Results

This discussion of PCE results for HF and CH_4 will be opened with a few remarks on the incomplete PCE basis results, starting with CH_4.

The three smallest PCE bases for CH_4 - PCE(1-3) - mainly illustrate the effect of changing the hydrogenic contribution to the MO's of the system. The smallest basis - PCE(1) (not minimal due to the presence of the $1s_C$ atomic SCF core orbital) has a significant contribution from the STF $1s_H$ (1.0) in the T_2 orbitals (see Table 4.3 for the PCE bases for CH_4). This results in the expectation values $\langle r^2 \rangle$ and $\langle r^4 \rangle$

(Table 5.3, Chapter 5) being larger than the values given by the largest PCE basis - PCE(5). In going to the function PCE(2) even larger values of $\langle r^2 \rangle$ and $\langle r^4 \rangle$ are recorded together with significant increases in the electronic contributions to the multipole moments (Table 5.5). The function PCE(2) has a single s function on the proton ($1s_H$ (1.0)) and this accounts for the behaviour noted above (all other functions have contributions from $1s_H$ (1.5) which falls off more rapidly than $1s_H$ (1.0)). Thus PCE(2) has significantly larger contributions from $1s_H$ (1.0) in the MO's $\phi(2A_1)$ and $\phi(T_2$ X, Y, Z) producing larger densities in the outer regions than any of the other bases. The function PCE(3) includes both $1s_H$ (1.0) and $1s_H$ (1.5) in all its MO's with the former dominating the latter in the T_2 orbitals and vice-versa in the A_1 orbitals. The inclusion of $1s_H$ (1.5), with a diminution in the contribution from $1s_H$ (1.0) accounts for the decrease in $\langle r^2 \rangle$ and $\langle r^4 \rangle$ in going from PCE(2) to PCE(3). The functions PCE(3-5) illustrate the effect of adding 2s and 2p functions to the carbon. The largest PCE basis for CH_4 - PCE(5), which yields an energy of -40.181 au compared with an estimated HF limit of -40.22 au is deficient in that it does not include any STF's with higher n and l values than those found in the minimal basis. The more recent HFR calculation of Moccia et al[44] on CH_4, referred to in Chapter 4, which utilizes s and p functions on the hydrogens and d and f functions on the carbon yields for the octapole moment, Ω^T, $1.3905 \cdot 10^{-34}$ esu-cm^3. This calculation gives χ_r as $-27.071 \cdot 10^{-6}$ emu and a value for $\langle r^2 \rangle$ of 35.303 au. These expectation values correspond to a bond length of 2.067 au. These functions are required to describe the distortion of atomic densities which accompanies molecular binding

and also to reach the Hartree-Fock limit. Woznick has not attempted to minimize orbital exponents, although it would appear that this factor decreases in importance as the size of the basis is increased[35]. The results for the incomplete bases for HF (see Table 4.4) are difficult to rationalize without going into detail, since the bases differ considerably. Suffice it to say that the minimal basis - PCE(1) gives results which are somewhat at variance with those from the three other PCE bases. This function is characterised by values of $\langle r^{-2} \rangle$, $\langle r^{-1} \rangle$ which are smaller than those results given by any other basis and smaller values of $\langle r^2 \rangle$ and $\langle r^4 \rangle$ (see Table 5.2, Chapter 5). An investigation of densities at the nuclei show PCE(1) to have a smaller density at the fluorine nucleus and a larger density at the proton than any of the other PCE basis predictions. This factor is evident when comparing dipole moments for the PCE bases (Table 5.4). Incomplete PCE bases, such as those considered here for HF and CH_4, have diminished in significance as more calculations have been performed which use large flexible bases (of the quality of that used by Cade and Huo for HF - PCE(4)) which provide more accurate information, within the HFR scheme.

A comparison of theoretical and experimental results is now in order. Experimental knowledge is not plentiful for either system. In the case of CH_4 an experimental value $\langle r^2 \rangle$ [47] is available (Table 5.3), together with a result for the octapole moment[50] (Table 5.5). The experimental X-ray scattering curve, which represents a fit of Thomer's[51] experimental results is shown in Figure 5.2. Taking theoretical predictions for the largest CH_4 basis (PCE(5)), a comparison with experiment for $\langle r^2 \rangle$ (and χ_r) shows a theoretical value which

is 8 per cent larger than the experimental. In the case of the octapole moment the theoretical value is only 32 per cent of the experimental. The experimental result in this case is highly dubious. Stogryn and Stogryn[50] list multipole moments for many molecules and tabulate 'recommended' moments which are averages of experimental and theoretical results. One such recommended value is the octupole moment, Ω^T, of $4.5.10^{-34}$ esu cm^3 included in Table 5.5 The theoretical predictions used in producing the recommended value are those from single-centre calculations. which are inappropriate for determining multipole moments (see discussion of OCE results in this chapter). An experimental value for Ω^T of $1.56.\ 10^{-34}$ esu cm^3 is listed by Stogryn and Stogryn which is much closer to the theoretical prediction made here of $1.42.10^{-34}$ esu cm^3. No experimental determination of the hexadecapole moment of CH_4 has been made - the theoretical result of $2.0066.10^{-42}$ esu cm^4 is, as far as is known, the only PCE HFR determination of this quantity to have been made. The experimental and theoretical X-ray scattering curves (Figure 5.2) are seen to agree rather well. This is to be expected as previous determinations[4, 5] of this property have shown it to be fairly insensitive to the quality of the wave function for XH_n systems, depending, as it does, largely on the spherically symmetric term in the electron density. The contributions to the scattering factor made by the angular terms shown in Table 5.7 support the conclusion that these contributions are insignificant and may be safely neglected.

For HF the only experimental results are those for the dipole[53] and quadrupole moments[50] and $\langle r^2 \rangle$ (χ_r)[55]. Comparison with experiment shows the largest PCE basis giving a dipole moment which is

only 0.7 per cent in excess of the experimental value (Table 5.4). (All of the expectation values for the largest basis for HF together with others have been determined by McLean and Yoshamine[57].) The quadrupole moment is 10 per cent less than the recommended value (Table 5.4) whilst the theoretical prediction of $\langle r^2 \rangle$ (and χ_r) is 19 per cent in excess of the experimental result (Table 5.2).

The dipole moment prediction for HF is especially pleasing - in full accordance with what might be expected for this calculation in the light of the Moller-Plesset[26] theorems for Hartree-Fock wave functions. The quadrupole moment and $\langle r^2 \rangle$ are certainly less accurately determined although there is some doubt about the experimental 'recommended' value for Θ^T. Both HFR calculations for HF and CH_4 give $\langle r^2 \rangle$ to be significantly larger than the experimental values - the error of 19 per cent for HF would appear to be rather large and to throw doubt on the validity of the experimental value in this case.

A good check on the accuracy of HFR expectation values would appear to require more experimental work on a variety of properties including some not included here, e.g. polarzabilities and quadrupole coupling constants.

This discussion of PCE results is concluded with a consideration of radial terms in the electron density expansions for HF and CH_4 introduced in Chapter 5. The D(r) curves (Figure 6.1), in which the largest PCE basis results are shown in dashed lines, illustrate well the relative diffuseness of the electron density distribution in CH_4 relative to that in HF. The radial terms as far as $l = 6$ in HF and $l = 8$ in CH_4 are shown in Figures 6.2 and 6.3 respectively. These radial terms, together with their angular parts, constitute elements in a sum which produces a total

D(r) for HF

----- PCE(4)

——— OCE(4)

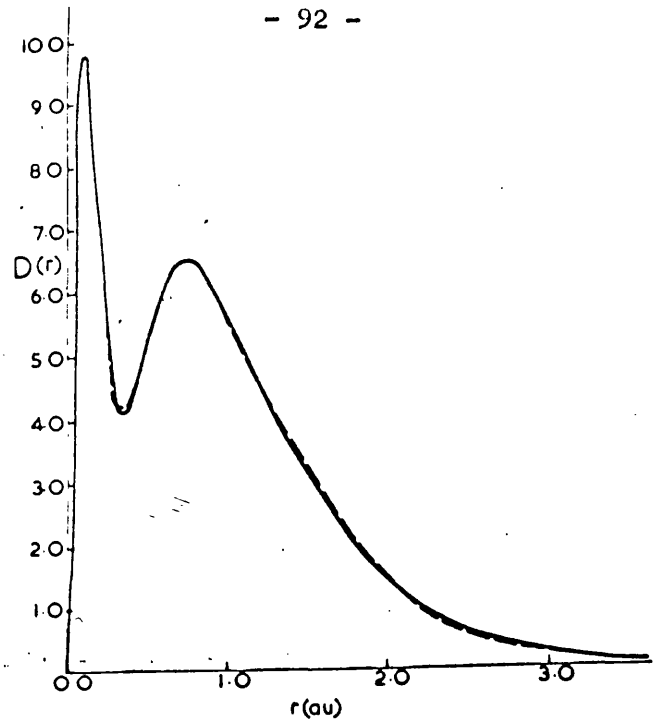

D(r) for CH_4

——— OCE(1)

— • — OCE(6)

----- PCE(5)

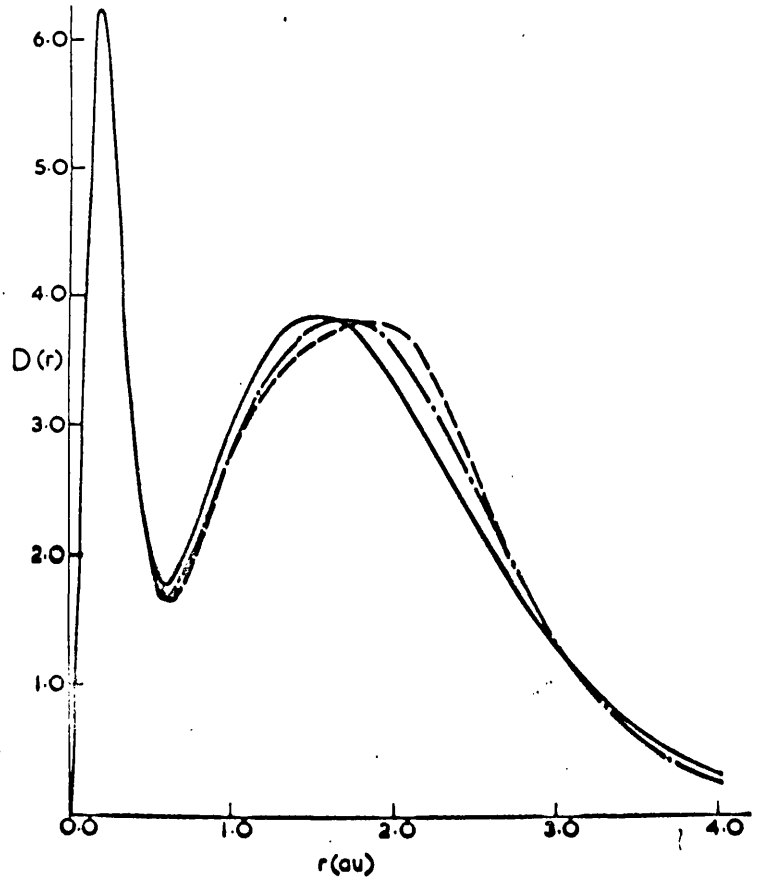

Figure 6.1: Radial Density Distributions for HF and CH_4

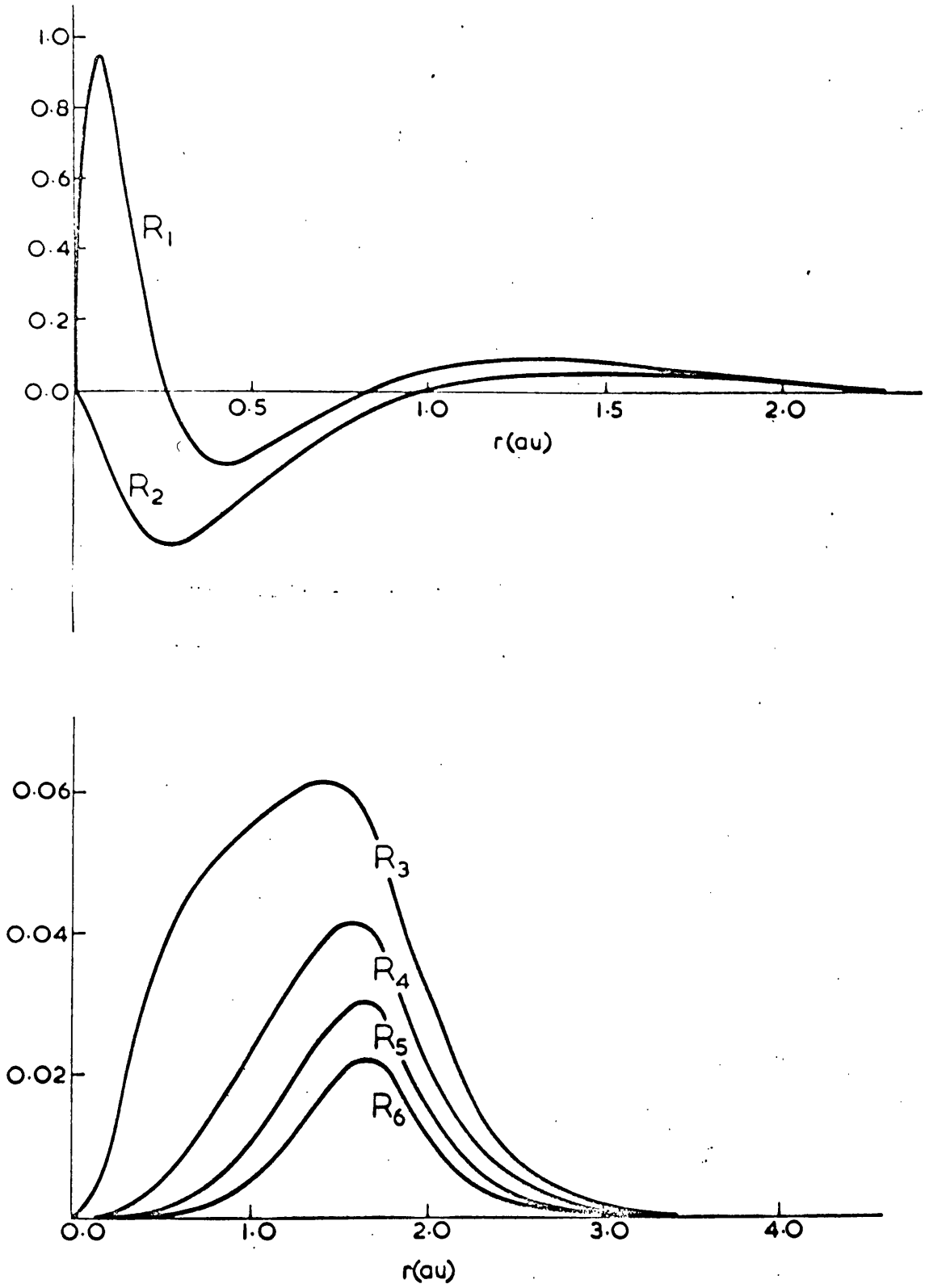

Figure 6.2: Radial Terms R_1 - R_6 in Electron Density Expansion for HF. Function PCE(4)

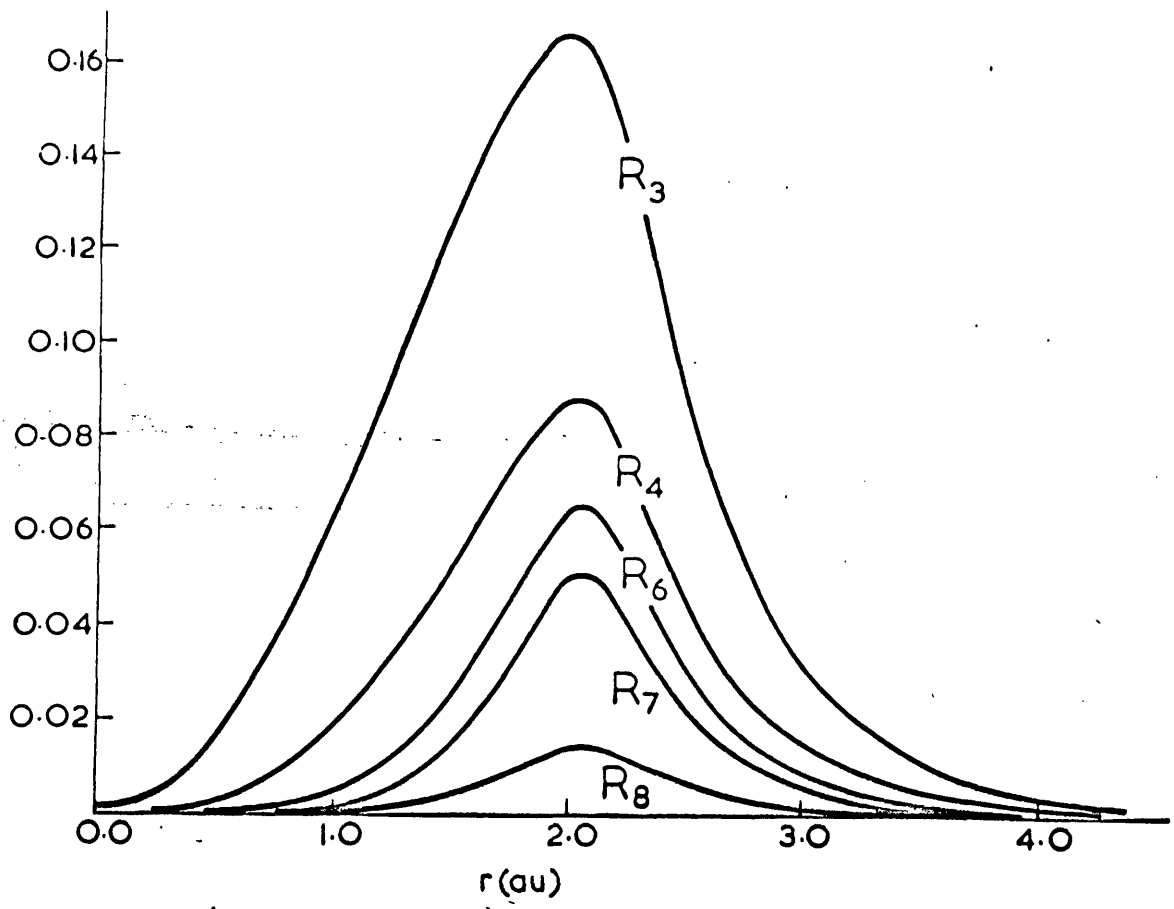

Figure 6.3: Radial Terms R_3 - R_8 in Electron Density Expansion for CH_4. Function PCE(5)

electron density of the appropriate symmetry for both systems. It will be noted that for CH_4, from which the l = 1, 2 and 5 terms are missing in the electron density expansion (see definition of tetrahedral harmonics in Chapter 5), the radial terms peak at approximately the bond length and thus are responsible for describing deviations from spherical symmetry in the electron density at the protons. For HF, the PCE radial terms (Figure 6.2), indicate the presence of a strong dipole term (R_1'). This term, in conjunction with its angular counterpart ($\propto \cos\theta$), would appear to be responsible for moving a considerable amount of charge from behind the fluorine (F) nucleus into the bond region close to (within 0.2 au) the F nucleus. The radial terms $R_3' - R_6'$ (Figure 6.2) should produce effects in the deposition of charge near the proton (at Z = 1.7328 au). The rather remarkable behaviour of R_3' is noted and this radial term, together with the d-type spherical harmonic it is associated with, will place significant amounts of charge in the bond region.

The radial terms just discussed will be reconsidered in the discussion of OCE results in the next section.

The OCE Results

In this section the convergence of radial terms in the electron density expansions for HF and CH_4 given by the OCE bases will be illustrated and compared with the PCE results. The expectation values tabulated in Chapter 5 will be called upon to illustrate the discussion. Before launching in on this appraisal of OCE results a few comments will be made on factors influencing the OCE performance in XH_n molecules. (A detailed exposition of these factors has been given by Moccia[16].) First an obvious parameter affecting the accuracy of the OCE calculation is the

charge on the neavy nucleus, X. (This consideration applies only to OCE calculations using the heavy nucleus as the expansion centre, as in XH_n molecules.) Thus the UA (united-atom) single-centre approach, which was utilized in Part I, performs better in the argon series of hydrides than in the neon series[5, 6]. The greater the charge on the heavy nucleus, the greater is the inner shell energy contribution to the molecular energy - which the OCE method can approximate rather well. A second obvious factor is simply the number of protons - since the OCE technique meets great difficulty in describing density cusps at off centre nuclei, the number of such cusps will obviously influence the energetic performance of the technique. Both these factors place HF in an advantageous position over CH_4 as far as the OCE technique is concerned. Thirdly the larger the bond length, the worse the OCE performance. This factor has been highlighted in the off-centre hydrogen atom calculations of Hoyland et al[58] which show the energy and dipole moment convergence (as a function of spherical harmonic l value) to progressively get slower as the expansion centre - proton distance is increased. Lastly, the nature of the cusps at the protons and the density in the immediate vicinity of the protons is important. The state of affairs existing in ionic species or in certain excited states where large amounts of charge are removed from the proton regions - leaving a significantly smaller cusp than that found in the isolated hydrogen atom is a favourable one as far as the OCE technique is concerned. Taking the largest PCE basis results for HF and CH_4 the charge density at the proton(s) in both molecules is 0.4217 au and 0.4860 au respectively. Hence it would appear that all four factors favour HF over CH_4 from a

single-centre calculation point of view. The fact that CH_4 possesses a symmetry advantage over HF in that the $l = 1$, 2 and 5 terms are missing from its density expansion, would appear to be overridden by the factors mentioned above.

The OCE Electron Density Expansions

To open this appraisal of the OCE results for HF and CH_4, the radial density distributions, D(r), given in Figure 6.1 are considered. To illustrate changes in the distributions as a function of the OCE basis set the additional diagrams found in Figure 6.4 have been included. These latter diagrams indicate the change in D(r), Δ D(r), relative to the distribution given by the smallest basis set - OCE(1) - for both molecules. The Δ D(r) curves are labelled by l_{max} - the maximum spherical harmonic l value in the basis considered. Thus for both systems the distribution in the inner and outer regions would appear to increasingly diminish on increasing the size of the basis set, this behaviour being accompanied by an increase in D(r) in intermediate regions. (The above description ignores the small increase in D(r) for OCE(2) in CH_4 very close to the carbon.) The expectation values $\langle r^n \rangle$ given in Tables 5.2 and 5.3 (Chapter 5) for the OCE bases appear to support the general pattern evident from the Δ D(r) curves. Thus $\langle r^{-2} \rangle$, $\langle r^{-1} \rangle$ and $\langle r^4 \rangle$ for both HF and CH_4 diminish monotonically as the size of the basis is increased (ignoring once again the small increase in $\langle r^{-2} \rangle$ for CH_4). The first two operators emphasize inner portions of D(r) whereas $\langle r^4 \rangle$ magnifies extreme outer regions. The positive peaks in the ΔD(r) curves account for the

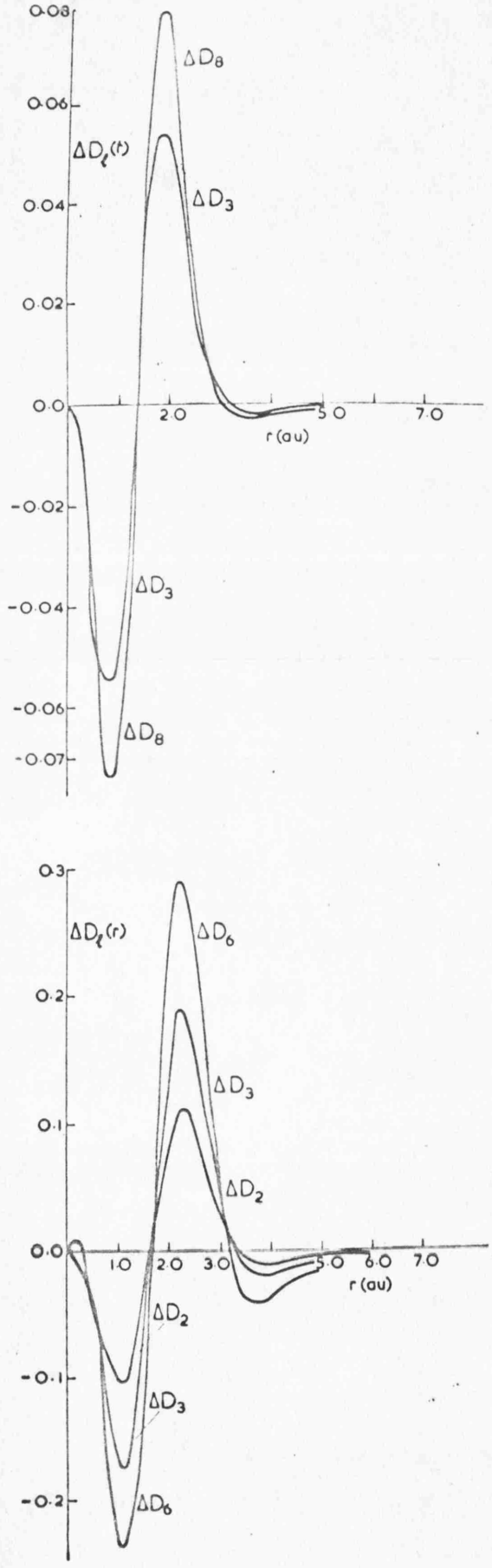

Figure 6.4: $\Delta D(r)$ from OCE distributions for HF and CH_4.

trend in $\langle r^2 \rangle$ for both molecules. The total D(r) curves for HF show the best OCE result approximating the PCE distribution closely all over space. Comparison between the best OCE and PCE results for $\langle r^n \rangle$ (Table 5.2, Chapter 5) show the OCE results to differ from the PCE results by less than one per cent. (Since the OCE basis includes the PCE fluorine basis the closeness of $\langle r^{-2} \rangle$ and $\langle r^{-1} \rangle$ given by the two techniques is not surprising.) The D(r) curves for CH_4 (Figure 6.1) show two OCE distributions (OCE(1) and OCE(6)) and the distribution from PCE(5). A rather surprising result which emerges is that for both HF and CH_4 the best OCE predictions of $\langle r^2 \rangle$ and $\langle r^4 \rangle$ are larger than the corresponding PCE results (see Tables 5.2, 5.3, Chapter 5). The supposition that the OCE technique will produce low densities at the protons generally leads to the assumption that at least $\langle r^2 \rangle$ will be underestimated by the single centre method. However the underestimate of electron density at the protons (to be illustrated later in this chapter) has a corollary: electron density must be overestimated elsewhere in space. The OCE results for HF and CH_4 suggest that the low density at the proton sites is compensated by larger densities in the outer regions than that predicted by the best PCE bases.

In summation the OCE functions appear to provide rather accurate radial density distributions for both molecules. The convergence of the OCE distributions is aptly described by the $\Delta D(r)$ curves which show an average movement of charge from inner at outer regions into intermediate regions encompassing the proton sites in both systems. These changes in D(r) reflect the attempt of the OCE functions to build up density in the bond regions - this point will be illustrated later with the aid of

contour diagrams and density profiles.

The radial terms associated with non-spherical contributions to the electron density expansions will now be discussed. Figures 6.5A and 6.5B illustrate the convergence of the radial terms R_1-R_6 for HF, while Figure 6.6 documents the convergence of R_3, R_4 and R_6 for CH_4. The PCE results are shown in broken lines. These radial terms are of importance in that they determine the electronic contributions to the multipole moments of the molecular charge distributions (see Tables 5.4 and 5.5, Chapter 5 for multipole moments).

The dipole and quadrupole moment terms (R_1 and R_2) in HF given by the largest OCE basis - OCE(4) - are so close to the PCE results that only OCE curves are shown in 6.5A. The dipole and quadrupole moment for HF given by the best OCE function (Table 5.4, Chapter 5) differ by about one per cent from the PCE predictions. The l = 3-6 radial terms show larger differences when compared with the PCE results (Figure 6.5B) but, on the whole, the largest OCE basis - OCE(4) - with spherical harmonics up to l_{max} = 8 in its basis, appears to provide a rather good description of the first seven (including R_o) radial terms in the electron density expansion for HF.

In the case of CH_4, the first two radial terms R_3 and R_4, giving rise to the octupole and hexadecapole moments respectively, appear to be quite well described by OCE(6), which has l_{max} = 6. The term R_6 is rather poorly defined and higher terms (not shown) rapidly deteriorate. The best OCE octupole moment is 40 per cent larger than the best PCE result, whereas the hexadecapole moment is 70 per cent larger than the PCE value. Of all the one electron expectation values determined, the

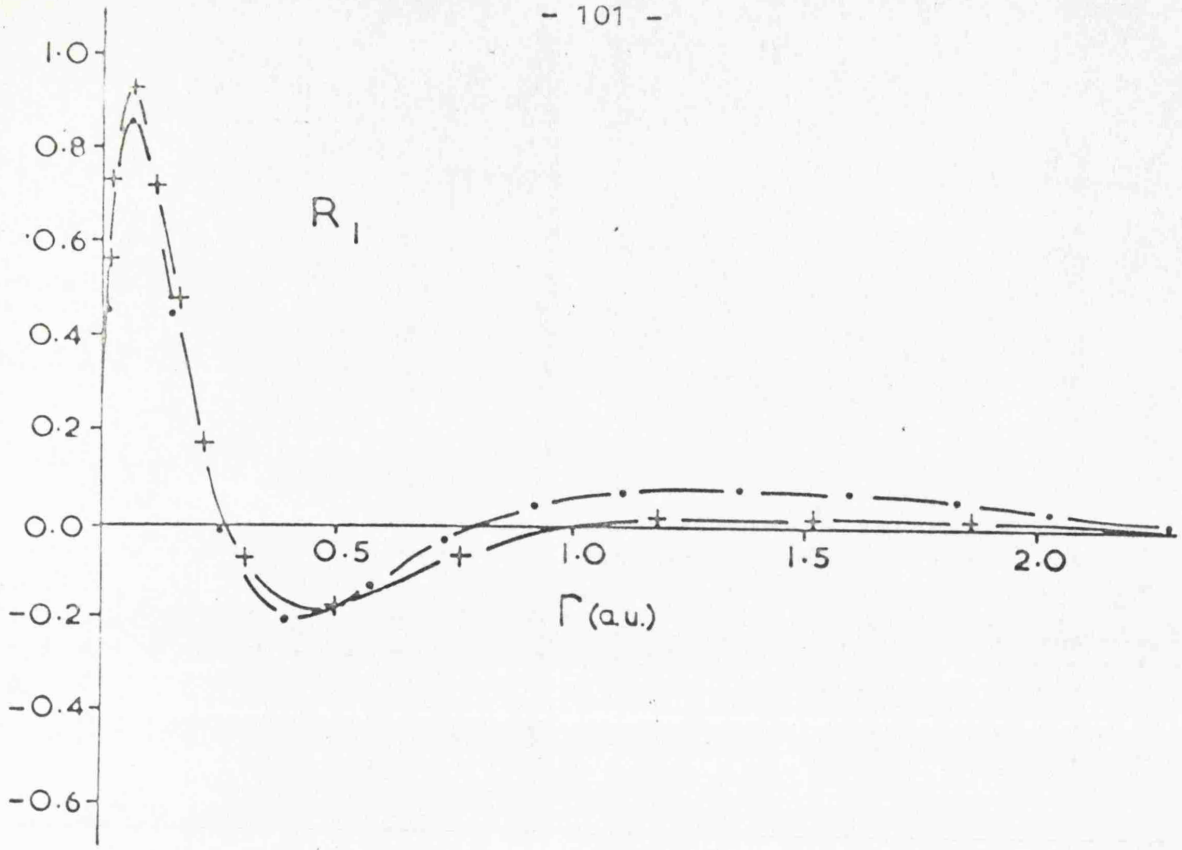

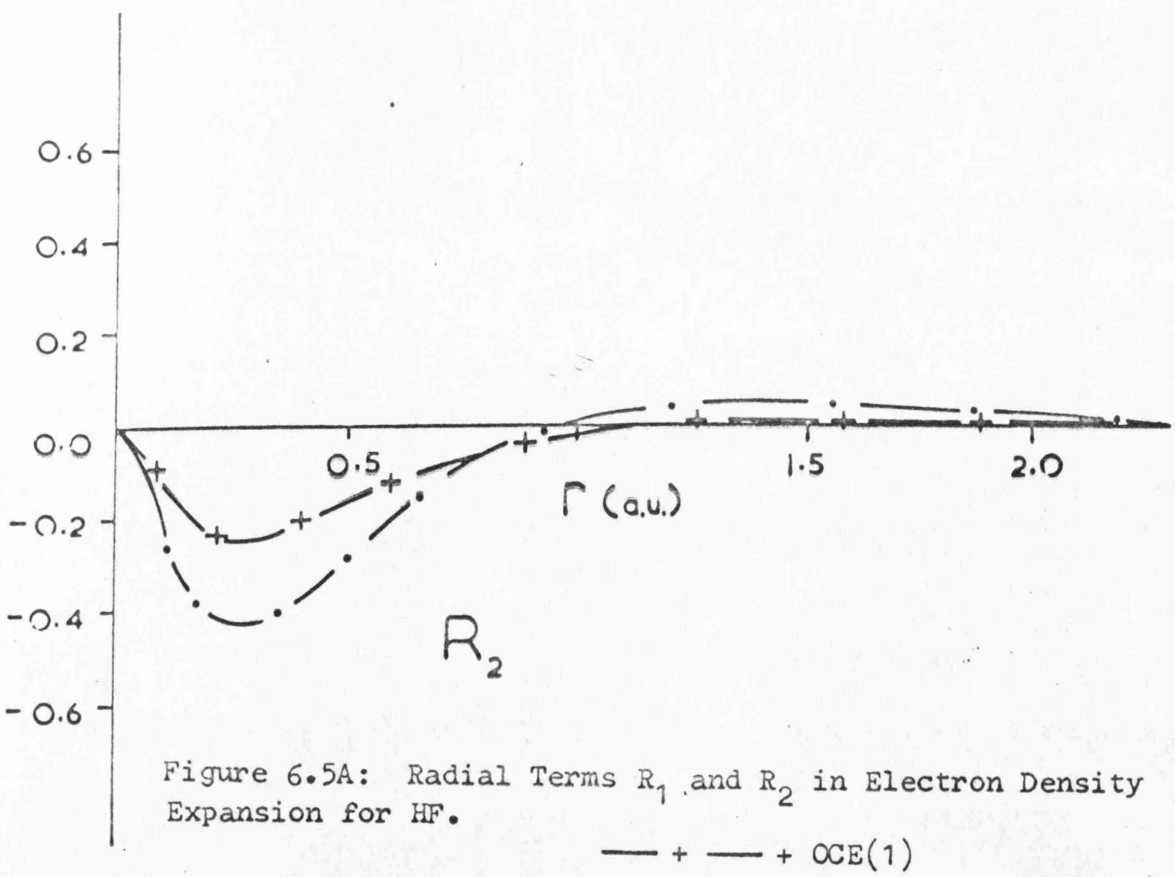

Figure 6.5A: Radial Terms R_1 and R_2 in Electron Density Expansion for HF.

—— + —— + OCE(1)

—— • —— • OCE(4)

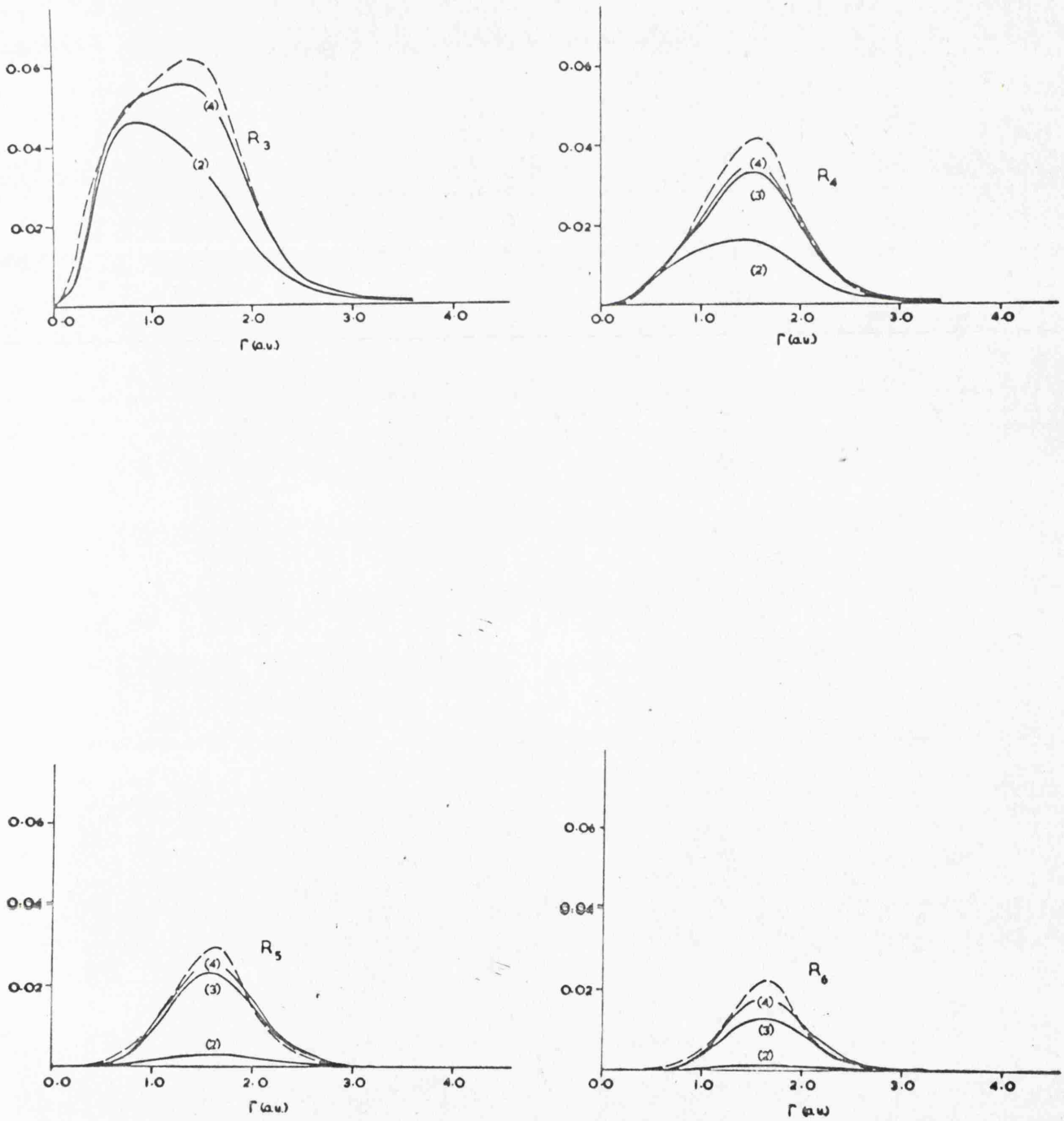

Figure 6.5B: Radial Terms R_3 - R_6 in Electron Density Expansion for HF. OCE results (in solid lines) are labelled according to wave function, e.g. (4) - OCE(4) (See Chapter 4). Dashed curves are those from PCE(4).

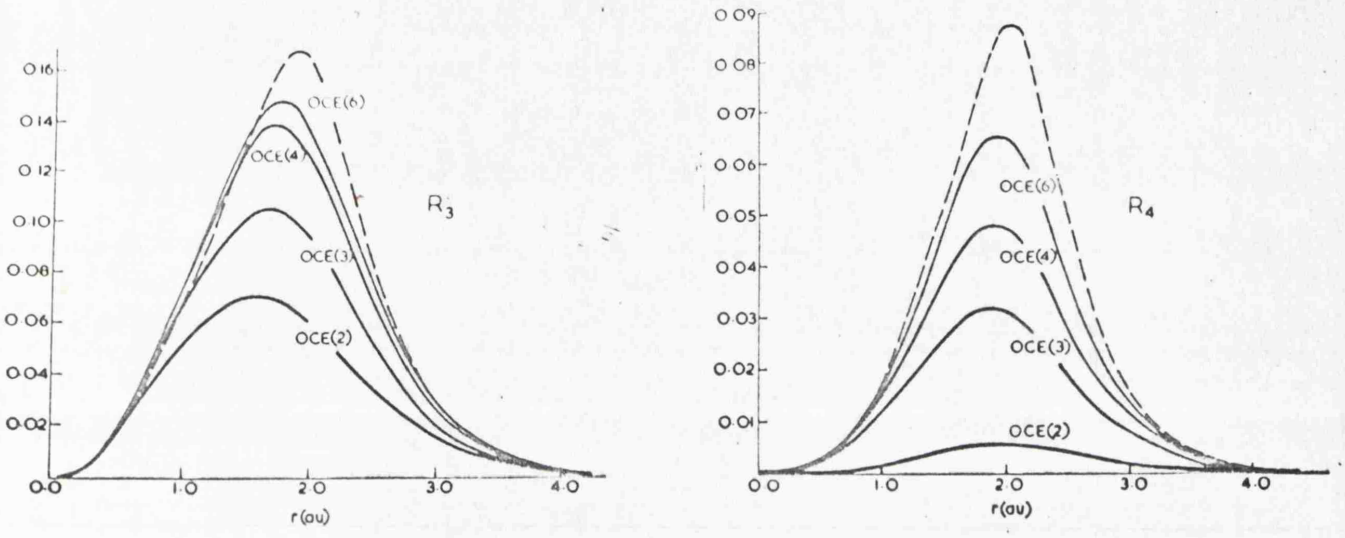

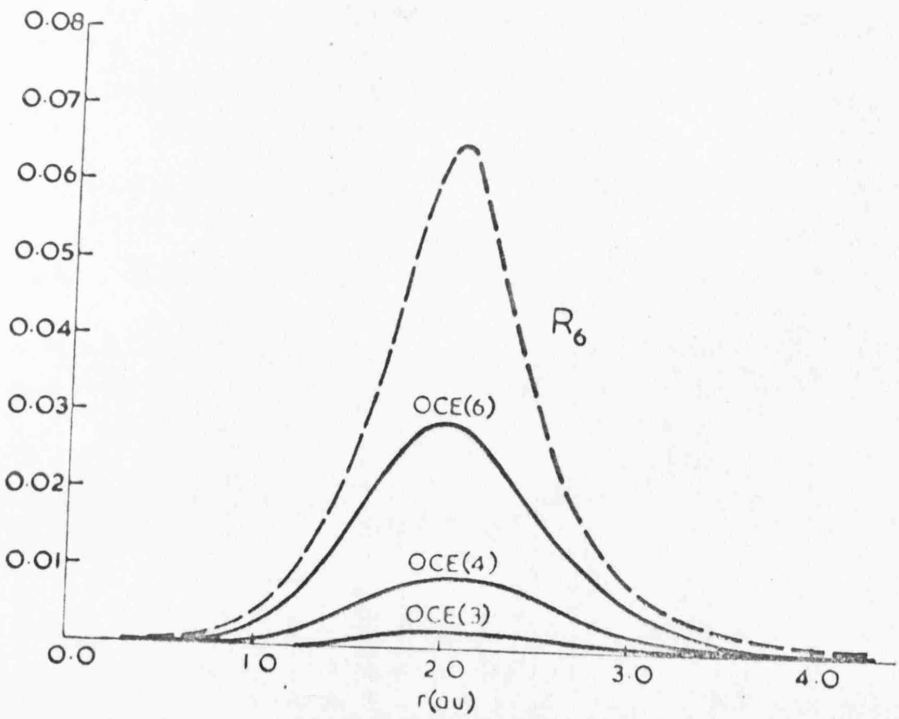

Figure 6.6: Radial Terms R_3, R_4 and R_6 in Electron Density Expansion for CH_4. The dashed curves correspond to results for PCE(5).

multipole moments most severely test the OCE technique, these quantities showing a slow convergence as the OCE basis is extended in CH_4 (Table 5.5, Chapter 5). Earlier work[16] which utilized spherical harmonics up to $l = 3$ (and therefore comparable to the results for OCE(3) here) would appear to be inadequate for describing density angularity in CH_4.

The OCE bond moments (Table 5.6, Chapter 5) show a large variation as the size of the basis is increased. The smallest basis, OCE(1), gives the wrong sign for μ_B (C^-H^+). This quantity depends on the description of the MO's $\phi(2A_1)$ and $\phi(T_{2X,Y,Z})$ which will be shown in contour form in the next section.

The Electron Densities

The figures appropriate to the discussion in this section will be the one electron density contour diagrams for HF and CH_4, given for three OCE bases in the case of HF (OCE(1, 2 and 4)) in Figure 6.7, and for four OCE bases for CH_4 (OCE(1, 3, 4 and 6)) in 6.9.

The CH_4 contours are shown in a 'bonding-plane', one of the two planes containing the carbon nucleus and two hydrogen atoms. The left hand edge of all diagrams in Figure 6.9 coincides with the z axis in the co-ordinate system shown in Figure 2.1 (Part I, Chapter 2). Thus each of the diagrams may be reflected across the left-hand edge. The proton position is clearly marked on each diagram, this being located at $(2.0665, \theta\, T/2)$ in polar co-ordinates centred on the carbon. For HF, the obvious plane containing the molecular axis is shown in Figure 6.7, the bottom edge of the diagram being co-incident with the molecular axis. As additional information which is useful in complementing these

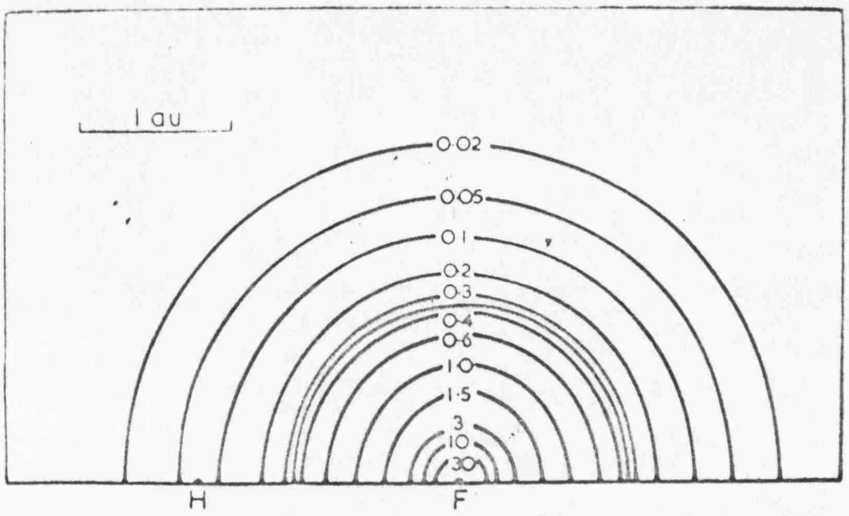

OCE(1)

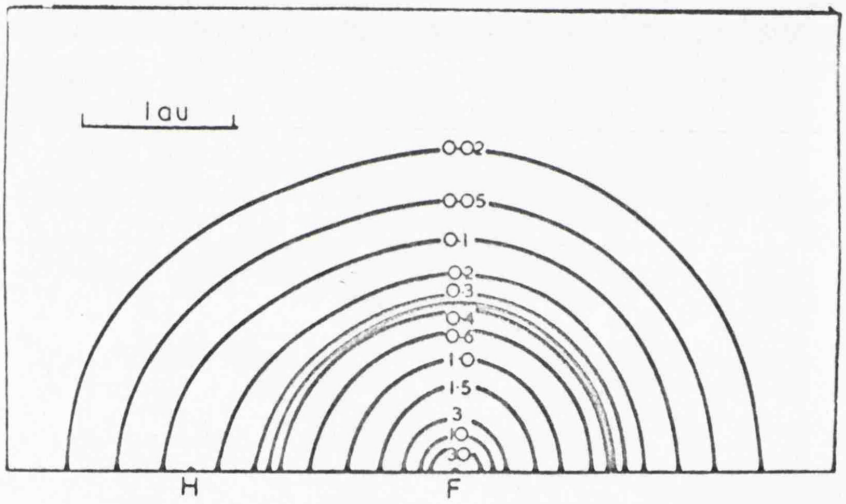

OCE(2)

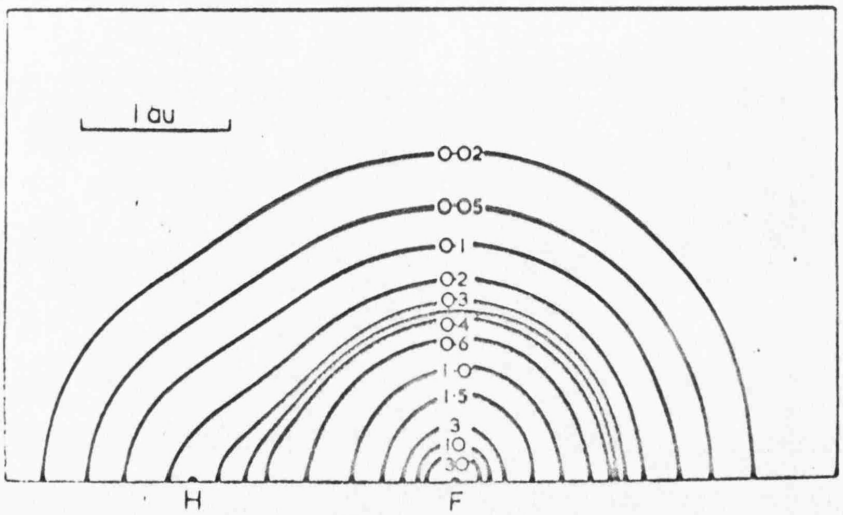

OCE(4)

Figure 6.7: OCE Electron Density Contours for HF.

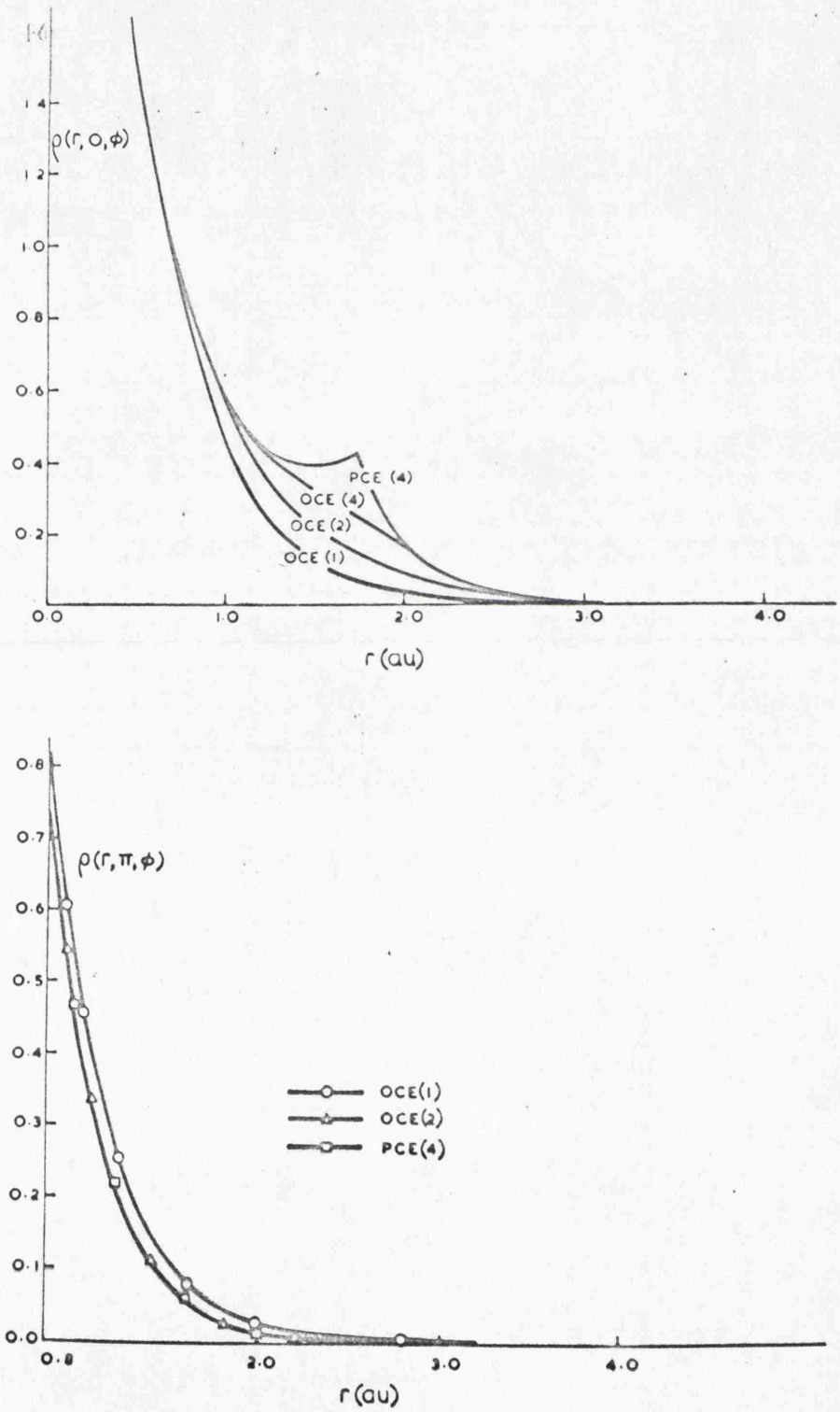

Figure 6.8: Electron Density Profiles for HF.

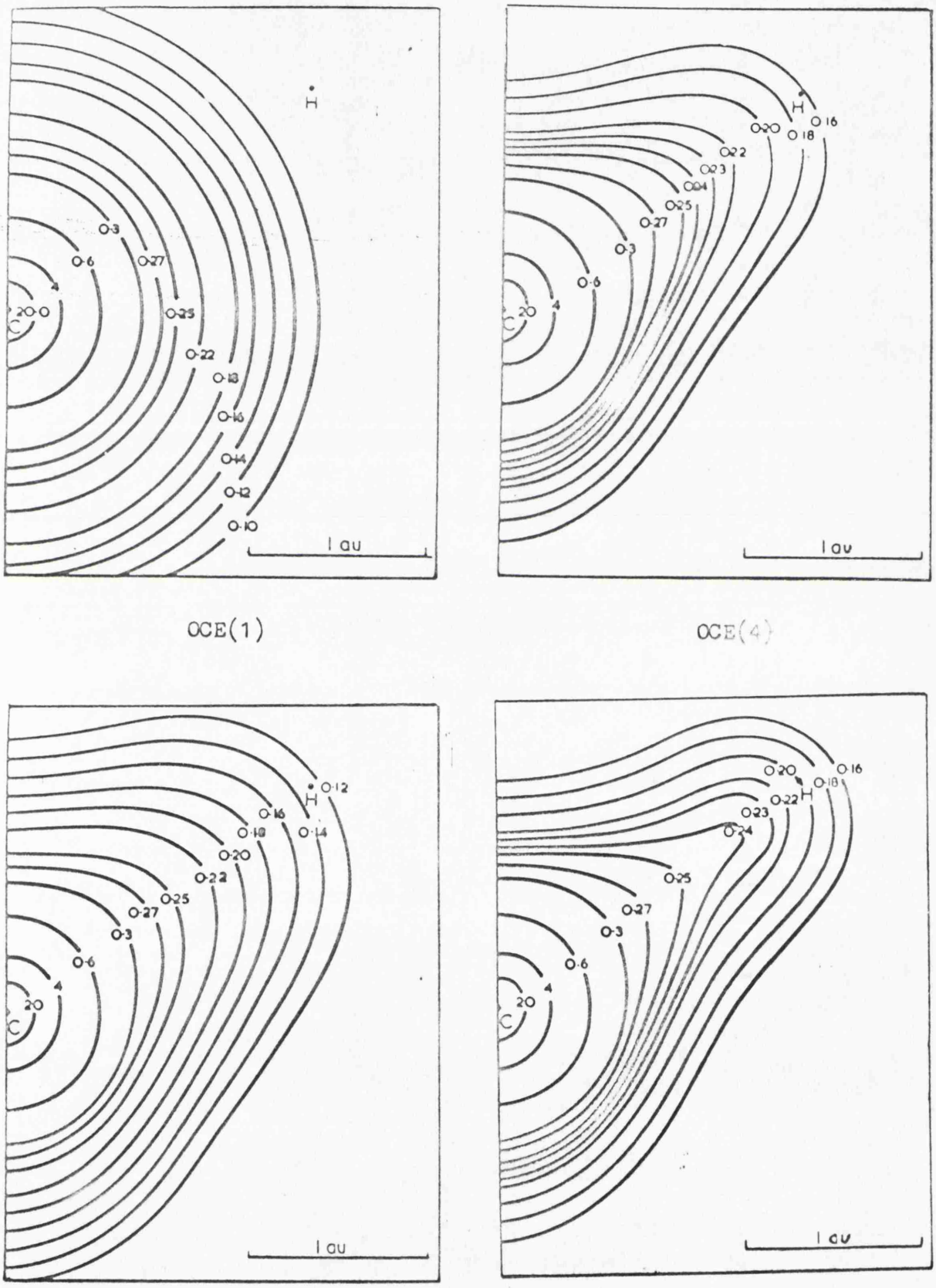

Figure 6.9: OCE Contours for CH_4.

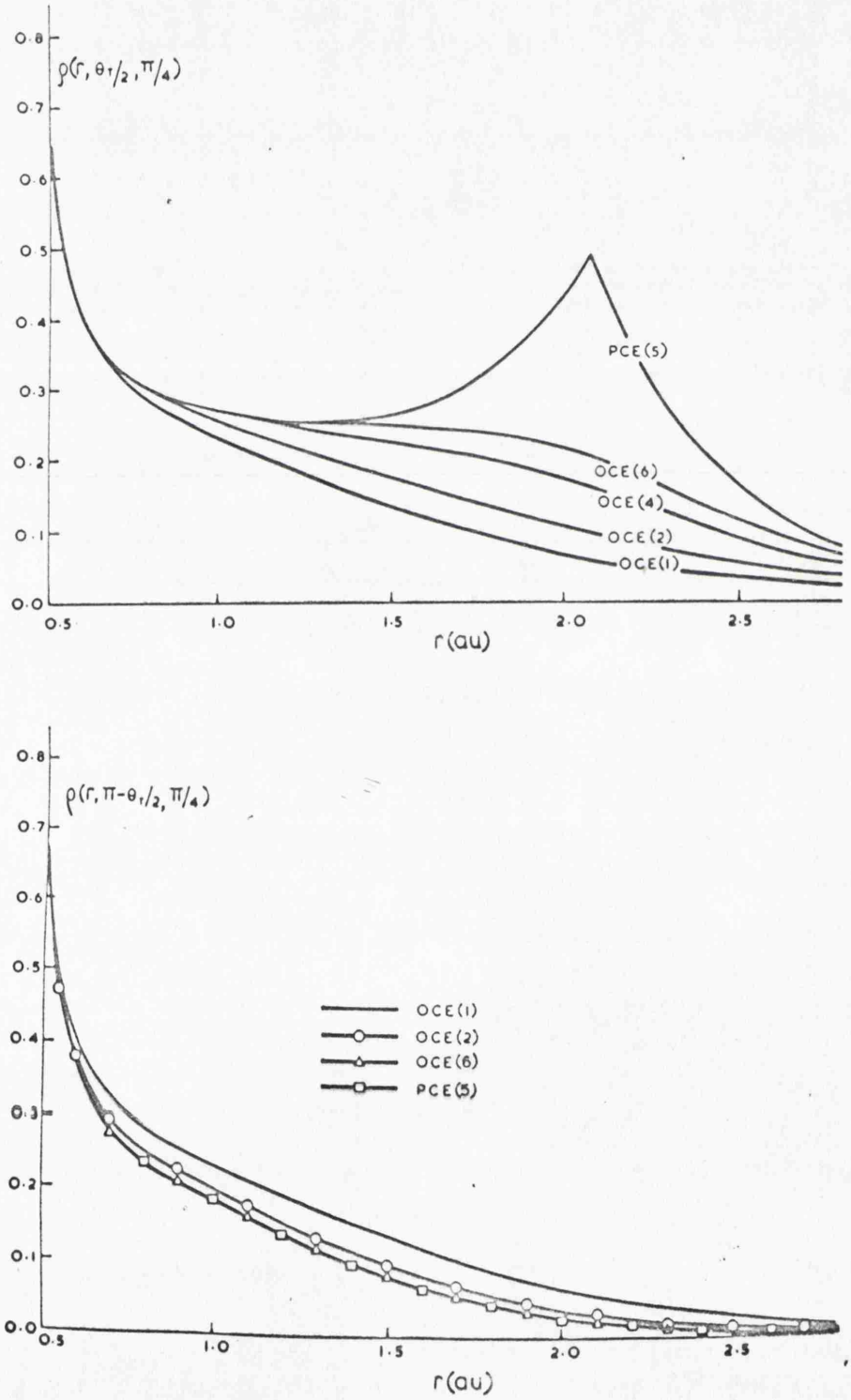

Figure 6.10: Electron Density Profiles for CH_4.

diagrams, two density profiles are shown for both HF and CH_4 (Figure 6.8 and 6.10 respectively). For HF the profiles give the density along the molecular axis in the bond direction ($\rho(r, 0, \phi)$) and behind the fluorine nucleus ($\rho(r, \pi, \phi)$). In the case of CH_4, Figure 6.10, shows profiles in the CH direction ($\rho(r, \theta_{T/2}, \pi/4)$ and in the 'opposite' direction with respect to the carbon ($\rho(r, \pi - \theta_{T/2}, \pi/4)$).

The profiles and contours for CH_4 provide a graphic illustration of the build-up of electronic charge in the bond region for the OCE functions. A measure of the extent to which density is crowded into the bond regions is given by the density at the proton, which in going from OCE(1) to OCE(6), increases from 0.06 au to 0.2 au. The profile $\rho(r, \pi - \theta_{T/2}, \pi/4)$ ('behind' the C nucleus) shows a concomitant decrease in charge in this region accompanying the increase in the bond. Comparison with the PCE profiles reveals the expected disparity at the proton site. The reorganization of OCE density which accompanies the extension of the basis set may be discussed with reference to the tetrahedral harmonics defined in Chapter 5 (Figure 5.1). In going to larger bases more such harmonics are added in to the density expansion for the system. Thus in going from OCE(1) to OCE(2) (l_{max} = 1 and 2 respectively) the harmonics T3 and T4 (Figure 5.1) are added in to what was a spherically symmetric density produced by OCE(1). The harmonic T4 appears to remove charge from the C-H bond direction and the 'unoccupied corner' direction - $\theta = (\pi - \theta_{T/2})$ as shown in the Figure 5.1 (Chapter 5), since it has negative lobes in both directions. However, T3 moves charge from the $\theta = \pi - \theta_{T/2}$ direction into the bond ($\theta = \theta_{T/2}$) - both directions being marked in dotted lines in the diagrams. Since R_3^2 is greater than

R_4 a net amount of charge is moved into the bond and removed from the non-bonded corner, as is shown in the profiles (Figure 6.10). The OCE contours for CH_4 (Figure 6.9) provide a graphic illustration of the build up of a tetrahedral charge distribution from an initially spherical one - OCE(1). The function OCE(1) provides 97.6 per cent of the experimental energy of CH_4. The energy lowering achieved by including harmonics up to $l_{max} = 6$ in OCE(6) is just 0.54 au, to give a total energy of -40.065 au (Table 4.1, Chapter 4). Figure 6.9 shows the innermost contours with respect to the carbon nucleus (20, 4, 0.6) to be largely unaffected as the basis is extended. These contours describe density which is largely due to the non-bonding orbital $\phi(1A_1)$ which peaks strongly at the carbon (composed largely of $1s_c$). Other features of the diagrams to be noted is the 'squeezing in' of contours along the positive z direction and in the unoccupied corner region indicating a steady increase in charge removal from those directions. The largest OCE basis - OCE(6) - is shown together with the PCE contour diagram in Figure 6.12 and affords an impressive illustration of the failure of the OCE technique in building up density at the protons.

The contours and density profiles for HF show the superiority of the OCE attack on this molecule to that in CH_4. (The OCE HF basis is slightly more extensive than that for CH_4, with $l_{max} = 8$ for HF and $l_{max} = 6$ for CH_4. To afford a fair comparison the OCE basis OCE(3) for HF should be compared with OCE(6) for CH_4, both with $l_{max} = 6$. Even taking this into account the single-centre approach is still seen to favour HF over CH_4.) The three contour diagrams (Figure 6.7) together with the profiles (Figure 6.8) show density being removed from behind

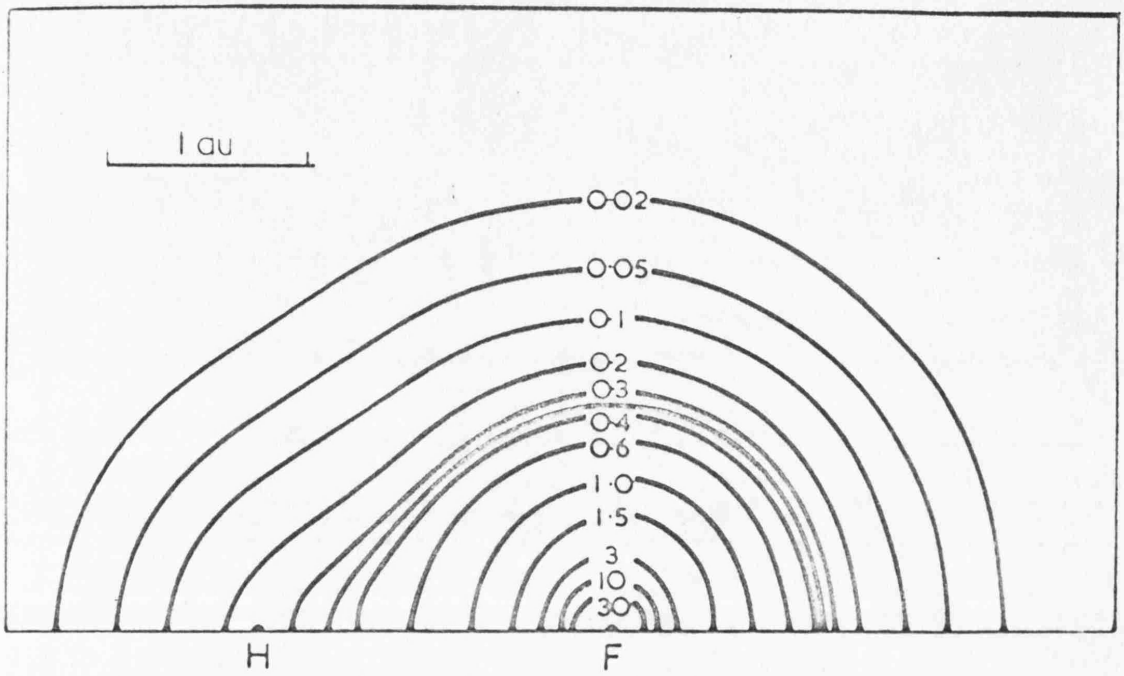

OCE(4)

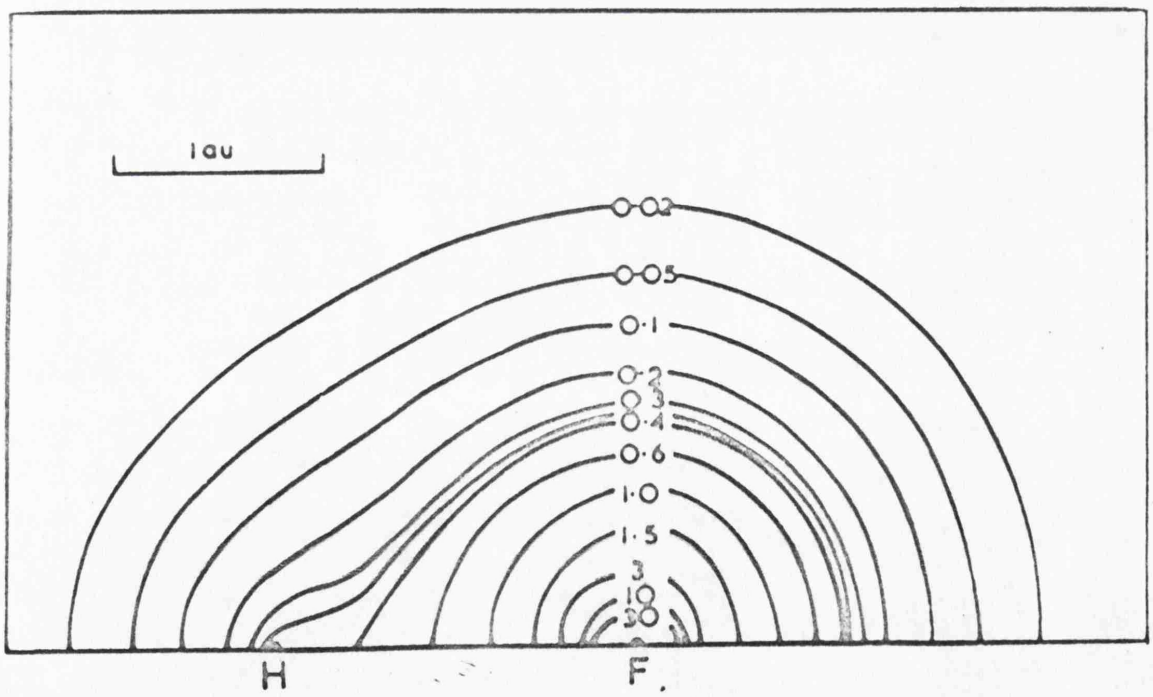

PCE(4)

Figure 6.11: OCE and PCE Electron Density Contours for HF.

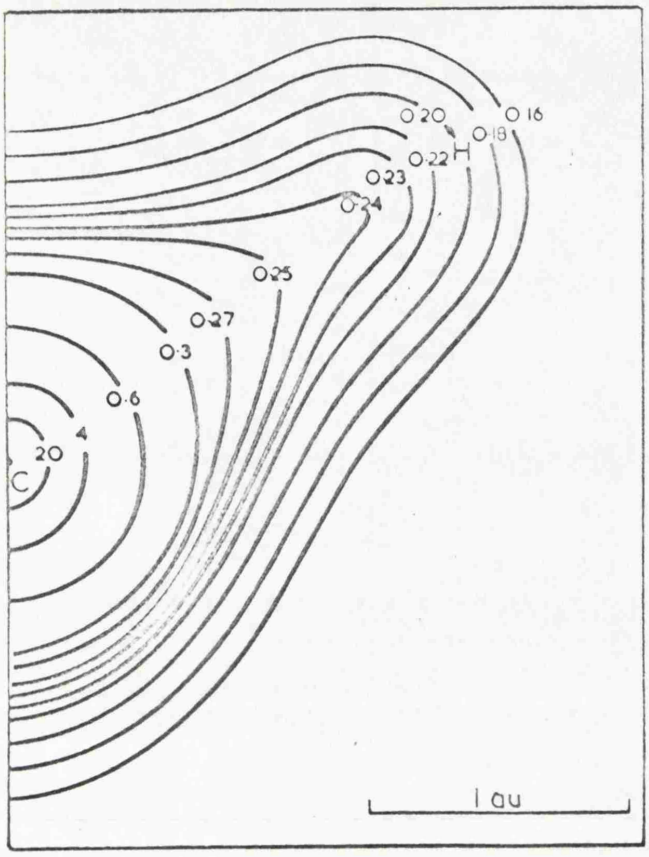

OCE(6)

Figure 6.12: OCE and PCE Electron Density Contours for CH_4.

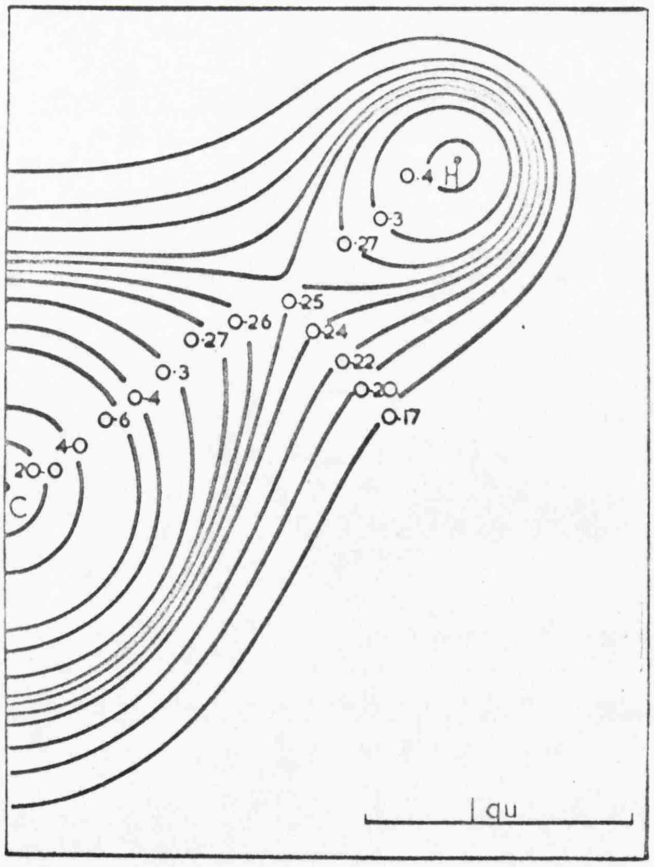

PCE(5)

the fluorine nucleus into the bond region. The largest OCE basis (OCE(4)) is seen to represent the electron density rather well over all space when compared with the PCE contours (Figure 6.11). Apart from the behaviour of the 0.2, 0.3, 0.35 (not valued in diagrams) and 0.4 contours in the region of the proton the overall shape of the contours appears to be very similar.

This discussion of the OCE results is completed with a few comments on the MO contours for CH_4 shown in Figures 6.13 and 6.14. (Diagrams showing MO contours for HF have been given by Cade et al[59]). Three occupied MO's for the system - $\phi(1A_1)$, $\phi(2A_1)$ and $\phi(T_{2z})$ are shown in Figures 6.13 and 6.14. Again the bonding plane ($\phi = \pi/4$) is used to illustrate these orbitals. The MO densities are normalized to two electrons for all diagrams. Comparing OCE and PCE results, the non-bonding MO ($\phi(1A_1)$) appears to be described very similarly by both techniques. This MO is largely $1s_c$. The usual cusp problem shows in the OCE description of the $\phi(2A_1)$ and $\phi(T_{2z})$ MO's which show bonding characteristics. Deviations from spherical symmetry in the density near the proton are clearly evident in both $\phi(2A_1)$ and $\phi(T_{2z})$ with charge being sucked into the bond. The π-like character of the $\phi(T_{2z})$ MO is obvious with the bonded upper-lobes forcing the nodal plane (not shown in diagram) downwards.

Concluding Remarks

At this point a brief summation of the discussion of results attempted in this chapter might be in order. First the largest PCE HFR results for HF and CH_4 have been compared with the few experimental

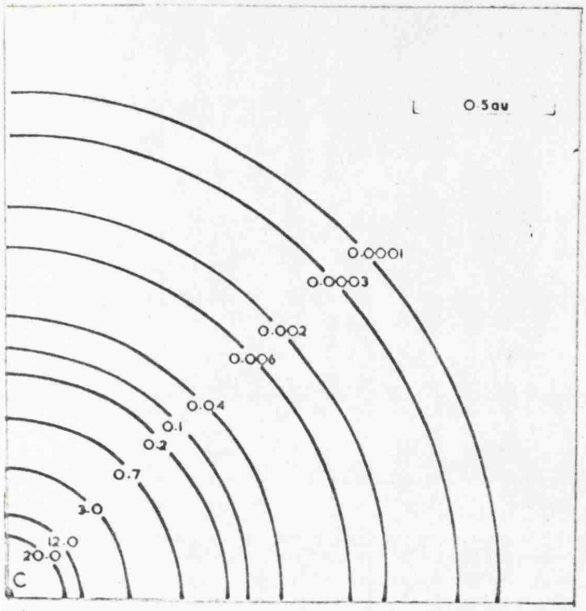

OCE(6)

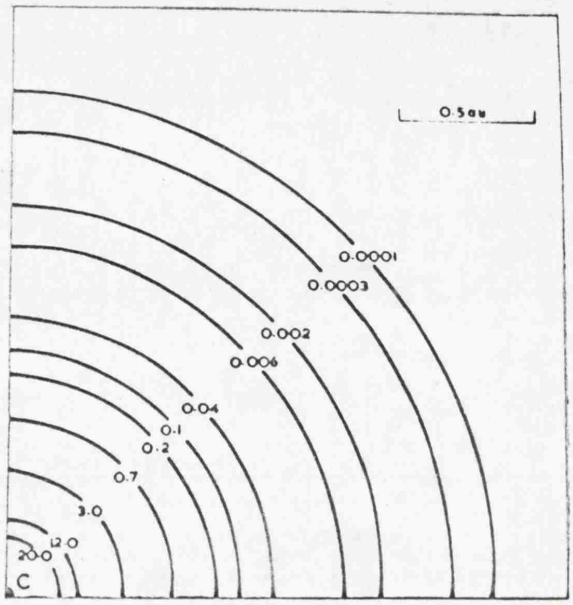

PCE(5)

MO $\phi(1A_1)$

MO $\phi(2A_1)$

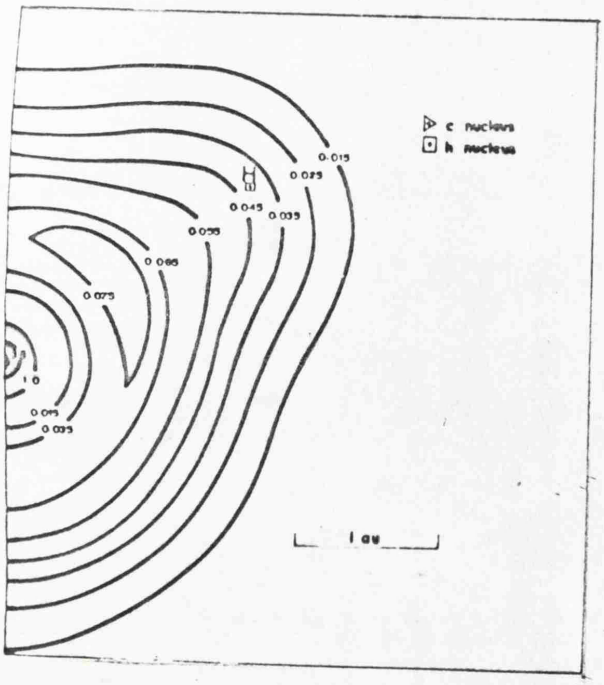

OCE(6)

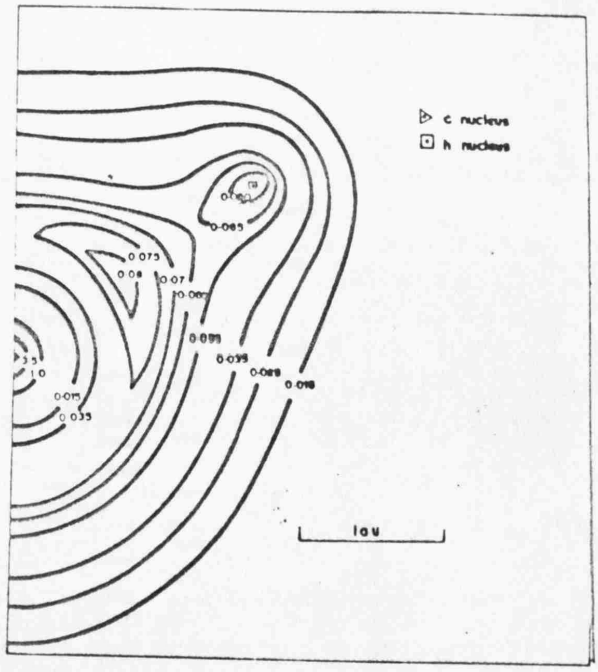

PCE(5)

Figure 6.13: MO's $\phi(1A_1)$ and $\phi(2A_1)$ for CH_4.

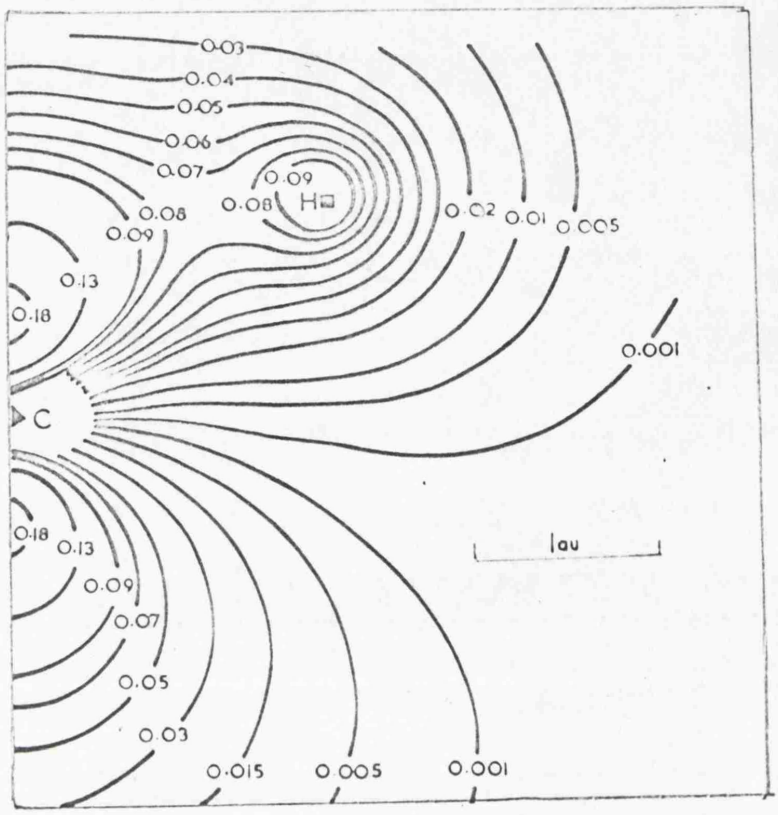

PCE(5)

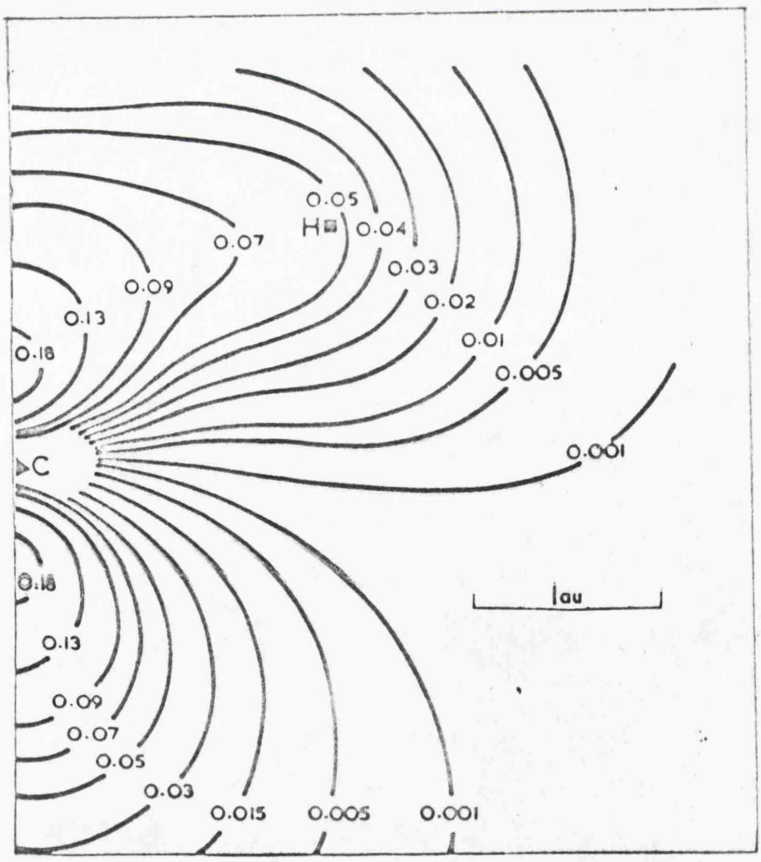

OCE(6)

Figure 6.14: MO $\phi(T_{2Z})$ for CH_4.

results available. Outstanding agreement has been found for the dipole moment of HF, given as 1.9416D by the Cade, Huo function PCE(4), compared with the experimental value of 1.8195D. The theoretical value of quadrupole moment (Θ^T) is approximately 10 per cent less than the experimental result. The theoretical prediction of χ_r, $-10.938.10^{-6}$ emu/mole, is significantly larger (numerically) than the experimental result of $-9.2.10^{-6}$ emu/mole, although the discrepancy here is large enough to throw some doubt on the validity of the experimental value. The quantities mentioned exhaust all known experimental result for HF. The other physical properties mentioned, the fluorine magnetic shielding factor (diamagnetic contribution) and X-ray scattering factor require experimental results for comparison, but on the whole the largest PCE basis for HF appears to perform exceedingly well. In the case of CH_4, the theoretical predictions of octupole moment, χ_r and X-ray scattering factor have been compared with experiment, although the 'observed' value of octupole moment is rather dubious. χ_r for CH_4, as predicted by the largest PCE basis, is about 8 per cent larger than the experimental value, whilst the theoretical and experimental X-ray scattering curves agree quite closely. No experimental results are known for the carbon shielding factor in CH_4, or for the hexadecapole moment of this molecule, although both quantities have been evaluated theoretically here. The largest PCE basis result for Φ^T, the hexadecapole moment in CH_4, is $2.0066.10^{-42}$ esu cm^4. No previous PCE evaluation of this quantity has been made as far as is known.

The discussion of OCE results has utilized the best PCE results for comparison purposes and the electron density expansions and contour

diagrams have illustrated the convergence of the OCE technique as the quality of the basis is improved by adding higher spherical harmonics into the basis. The disparity in the performance of the OCE performance in HF to that in CH_4 has been highlighted, with the superiority of the attack on HF being fully evident. Indeed the OCE HFR performance in HF is very successful:- the technique predicts 99.5 per cent of the Hartree-Fock limit energy and performs very similarly to the largest PCE basis in its prediction of one-electron expectation values. The limitations of the OCE basis used for CH_4 (with $l_{max} = 6$ for OCE(6)) has been shown via the electron density contours and profiles indicating the insufficiency of the basis in coping with the 'cusp problem' presented at the hydrogens. A rather surprising result to emerge from the OCE calculations is the values of $\langle r^2 \rangle$ and $\langle r^4 \rangle$ which are larger than the PCE values for both molecules.

The future of the single-centre approach, of which the OCE HFR calculations here are one example, is somewhat doubtful as a general technique. Since the evaluation of multicentre two electron integrals is no longer an obstacle, (this factor led to the increasing employment of the single-centre approach) the role of the single-centre method would appear to be a specialized one, where the know factors influencing its performance operate to its advantage. The Hoyland OCE HFR calculations on HF certainly show the technique to be capable of yielding successful results when applied to an appropriate system.

A full vindication of the HFR technique requires much more detailed, accurate experimental work on a variety of molecular properties. The PCE results presented in this work have gone some way to illustrate its

potential worth as a predicter of one-electron expectation values. The work of Bader et al[59] which utilizes HFR wave functions to illustrate the bonding process via one-electron densities also presents an interesting example of the use to which the technique may be put. The computational problems inherent in accounting for electronic correlation, even in molecules of the size dealt with here, will for some time yet, leave the HFR technique in a commanding position, as a proven method of general applicability.

APPENDIX

MOLECULAR INTEGRALS

The evaluation of the UA energy integral necessitates the evaluation of four distinct integral types:

$$F(\alpha|\beta) = \iint \phi_\alpha^*(i)\, \phi_\alpha(i) \frac{1}{r_{ij}} \phi_\beta^*(j)\, \phi_\beta(j)\, d\tau_i\, d\tau_j$$

$$G(\alpha|\beta) = \iint \phi_\alpha^*(i)\, \phi_\beta(i) \frac{1}{r_{ij}} \phi_\beta^*(j)\, \phi_\alpha(j)\, d\tau_i\, d\tau_j \qquad \text{(A.1)}$$

$$I(\alpha) = \int \phi_\alpha^*(i) \left[-\tfrac{1}{2}\nabla_i^2 - \frac{Z}{r_i} \right] \phi_\alpha(i)\, d\tau_i$$

$$L(\alpha) = \int \phi_\alpha^*(i) \frac{1}{r_{ui}} \phi_\alpha(i)\, d\tau_i$$

The two electron integrals, F and G are the familiar coulomb and exchange types respectively. The integral I represents the kinetic energy of an electron described by orbital ϕ_α plus its potential energy in the field of the heavy nucleus of the XH_n system with charge Z. The only two centre integral requiring evaluation is L, which gives the potential energy of interaction between an electron in ϕ_α and a proton.

Considering the two electron integrals first, the $\frac{1}{r_{ij}}$ appearing in them may be expanded in spherical harmonics and the usual angular integration performed. This leaves integrals over radial co-ordinate. Consider a G integral. After performing the angular integration, their remains an integral of the type:

$$G_K(\alpha|\beta) = \iint R(\alpha|r_i)\, R(\beta|r_i) \left\{ r_i, r_j \right\}^K R(\alpha|r_j)\, R(\beta|r_j)\, dr_i\, dr_j \qquad (A.2)$$

In which

$$R(\alpha|r) = r^{l_1} e^{-\alpha r} P_{l_1}(r)$$

$$R(\beta|r) = r^{l_2} e^{-\alpha r} P_{l_2}(r)$$

where

$$P_{l_1}(r) = a_0 + a_1 r + a_2 r^2 + \cdots + a_s r^s \qquad (A.3)$$

$$P_{l_2}(r) = b_0 + b_1 r + b_2 r^2 + \cdots + b_t r^t$$

Also

$$\left\{ r_i, r_j \right\}^K = \frac{r_i^{K+2}}{r_j^{K-1}} \qquad (r_i < r_j)$$

$$= \frac{r_j^{K+2}}{r_i^{K-1}} \qquad (r_i > r_j)$$

So

$$R(\alpha|r_i)\, R(\beta|r_i) = r_i^{(l_1+l_2)}\, e^{-(\alpha+\beta) r_i} \sum_{m=0}^{s+t} E_m r_i^m$$

in which

$$E_m = \sum_{\mu=0}^{m} a_\mu b_{m-\mu}$$

and s and t are the degrees of polynomials P_{l_1} and P_{l_2} respectively.

Consider now the integral over r_i in (A.2).

$$G_k(\alpha|\beta) = \int_0^\infty \int_0^{r_j} R(\alpha|r_i)\, R(\beta|r_i) \left(\frac{r_i^{k+2}}{r_j^{k-1}} \right) R(\alpha|r_j)\, R(\beta|r_j)\, dr_i\, dr_j$$

$$+ \int_0^\infty \int_{r_j}^\infty R(\alpha|r_i)\, R(\beta|r_i) \left(\frac{r_j^{k+2}}{r_i^{k-1}} \right) R(\alpha|r_j)\, R(\beta|r_j)\, dr_i\, dr_j \qquad \text{(A.4)}$$

Consider the integral over r_i in the first part of (A.4), i.e.

$$\int_0^{r_j} R(\alpha|r_i)\, R(\beta|r_i)\, r_i^{k+2}\, dr_i$$

$$= \sum_{m=0}^{s+t} E_m \int_0^{r_j} r_i^{m+k+2+l_1+l_2}\, e^{-(\alpha+\beta) r_i}\, dr_i \qquad \text{(A.5)}$$

Let $R = 1_1 + 1_2 + k + 2$

A typical integral in (A.5) is

$$\int_0^{r_j} r_i^{R+m} e^{-(\alpha+\beta) r_i} dr_i$$

$$= -\sum_{p=0}^{R+m} \frac{r_j^p (R+m)!\, e^{-(\alpha+\beta) r_j}}{p!\, (\alpha+\beta)^{R+m-p+1}} + \frac{(R+m)!}{(\alpha+\beta)^{R+m+1}} \qquad \text{(A.6)}$$

So, integrating over r_j for the first term in (A.4):

$$\int_0^\infty \left(\sum_{m'=0}^{s+t} E_{m'} r_j^{m'} \right) r_j^{(l_1+l_2)} \frac{e^{-(\alpha+\beta) r_j}}{r_j^{k-1}} \sum_{m=0}^{s+t} E_m \left\{ \frac{(R+m)!}{(\alpha+\beta)^{R+m+1}} - \sum_{p=0}^{R+m} \frac{r_j^p (R+m)!\, e^{-(\alpha+\beta) r_j}}{p!\, (\alpha+\beta)^{R+m-p+1}} \right\} d$$

Writing $S = 1_1 + 1_2 - k + 1$, the integral over r_j is:

$$\int_0^\infty \sum_{m'=0}^{s+t} \sum_{m=0}^{s+t} \left\{ \frac{(R+m)!\, r_j^{S+m'} e^{-(\alpha+\beta) r_j}}{(\alpha+\beta)^{R+m+1}} - \sum_{p=0}^{R+m} \frac{(R+m)!\, r_j^{S+p+m'} e^{-2(\alpha+\beta) r_j}}{p!\, (\alpha+\beta)^{R+m-p+1}} \right\} dr_j$$

$$= \sum_{m'=0}^{s+t} \sum_{m=0}^{s+t} E_m E_{m'} \left\{ \frac{(R+m)!\, (S+m')!}{(\alpha+\beta)^{R+m+1} (\alpha+\beta)^{S+m'+1}} - \sum_{p=0}^{R+m} \frac{(S+p+m')\, (R+m)!}{p!\, (\alpha+\beta)^{R+m-p+1} \left[2(\alpha+\beta)\right]^{S+p+m'+1}} \right\}$$

(A.7)

Consider the integral over r_i in the second term of (A.4), i.e.

$$\int_{r_j}^{\infty} \frac{r_i^{l_1+l_2} e^{-(\alpha+\beta) r_i}}{r_i^{k-1}} \sum_{m=0}^{s+t} E_m r_i^{m} \, dr_i \tag{A.8}$$

$$= \sum_{m=0}^{s+t} E_m \int_{r_j}^{\infty} r_i^{s+m} e^{-(\alpha+\beta) r_i} \, dr_i$$

$$= \sum_{m=0}^{s+t} E_m \sum_{q=0}^{s+m} \frac{(s+m)! \, r_j^{q} \, e^{-(\alpha+\beta) r_j}}{q! \, (\alpha+\beta)^{s+m-q+1}} \tag{A.9}$$

Integrating now over r_j:

$$\sum_{m'=0}^{s+t} \sum_{m=0}^{s+t} E_{m'} E_m \int_0^{\infty} \sum_{q=0}^{s+m} \frac{r_j^{s+m'+q} \, (s+m)! \, e^{-2(\alpha+\beta) r_j}}{q! \, (\alpha+\beta)^{s+m-q+1}} \, dr_j$$

$$= \sum_{m'=0}^{s+t} \sum_{m=0}^{s+t} E_{m'} E_m \sum_{q=0}^{s+m} \frac{(s+m)! \, (R+m'+q)!}{q! \, (\alpha+\beta)^{s+m-q+1} \left[2(\alpha+\beta)\right]^{R+m'+q+1}}$$

(A.10)

Hence the radial G integral is finally obtained as:

$$G_K(\alpha|\beta) = \sum_{m=0}^{S+t} \sum_{m'=0}^{S+t} E_m E_{m'} \left[\frac{(R+m)!\,(S+m')!}{(\alpha+\beta)^{R+S+m+m'+2}} \right.$$

$$+ (S+m')! \sum_{q=0}^{S+m} \frac{(R+m'+q)!}{q!\,(\alpha+\beta)^{S+m-q+1}\left[2(\alpha+\beta)\right]^{R+m'+q+1}} \qquad \text{(A.11)}$$

$$\left. - (R+m)! \sum_{p=0}^{R+m} \frac{(S+p+m')!}{p!\,(\alpha+\beta)^{R+m+p}\left[2(\alpha+\beta)\right]^{S+p+m'+1}} \right]$$

The F integral may be treated in a similar manner. Thus, the radial coulomb integral to be evaluated is:

$$F_K(\alpha|\beta) = \int_0^{\infty}\int_0^{r_j} R^2(\alpha|r_i) \left(\frac{r_i^{K+2}}{r_j^{K-1}} \right) R^2(\beta|r_j)\, dr_i\, dr_j$$

$$+ \int_0^{\infty}\int_{r_j}^{\infty} R^2(\alpha|r_i) \left(\frac{r_j^{K+2}}{r_i^{K-1}} \right) R^2(\beta|r_j)\, dr_i\, dr_j \qquad \text{(A.12)}$$

Introducing $C_m = \sum_{\mu=0}^{m} a_m a_{m-\mu}$ and considering the first integral over r_i in (A.12) i.e.

$$\int_0^{r_j} r_i^{2l_1} \sum_{m=0}^{2s} C_m r_i^{m+k+2} e^{-2\alpha r_i} dr_i$$

which gives:

$$\sum_{m=0}^{2s} C_m \left\{ \frac{(M+m)!}{(2\alpha)^{M+m+1}} - \sum_{\mu=0}^{M+m} \frac{r_j^{\mu} (M+m)! \, e^{-2\alpha r_j}}{\mu! \, (2\alpha)^{M+m-\mu+1}} \right\}$$

where $M = 2l_1 + k + 2$ (A.13)

Considering now the integral over r_j in the first term in (A.12) i.e.

$$\int_0^{\infty} \sum_{n=0}^{2t} D_n r_j^{N+n} e^{-2\beta r_j} \sum_{m=0}^{2s} C_m \left\{ \frac{(M+m)!}{(2\alpha)^{M+m+1}} - \sum_{\mu=0}^{M+m} \frac{r_j^{\mu} (M+m)! \, e^{-2\alpha r_j}}{\mu! \, (2\alpha)^{M+m-\mu+1}} \right\} dr_j$$

where

$$D_n = \sum_{\nu=0}^{n} b_n b_{n-\nu}$$

$$N = 2l_2 - k + 1$$

Thus the first term in (A.12) gives:

$$\sum_{n=0}^{2t} \sum_{m=0}^{2s} D_n C_m \left\{ \frac{(M+m)!\,(N+n)!}{(2\alpha)^{M+m+1}\,(2\beta)^{N+n+1}} \right.$$

$$\left. - (M+m)! \sum_{p=0}^{M+m} \frac{(N+n+p)!}{(2\alpha)^{M+m-p+1}\, p!\, \left[2(\alpha+\beta)\right]^{N+n+p+1}} \right\}$$

(A.14)

Now consider the second integral in (A.12), i.e.

$$\int_0^\infty \int_{r_j}^\infty R^2(\alpha | r_i) \left(\frac{r_j^{K+2}}{r_i^{K-1}} \right) R^2(\beta | r_j)\, dr_i\, dr_j$$

The integral over r_i gives

$$\sum_{m=0}^{2s} C_m \left\{ \sum_{q=0}^{K+m} \frac{(K+m)!\, r_j^q\, e^{-2\alpha r_j}}{q!\, (2\alpha)^{K+m-q+1}} \right\}$$

where $K = 2l_1 + k - 1$

Performing the integral over r_j produces

$$\sum_{n=0}^{2t} \sum_{m=0}^{2s} C_m D_n (K+m)! \sum_{q=0}^{K+m} \frac{(L+n+q)!}{\left[2(\alpha+\beta)\right]^{L+n+q+1} (2\alpha)^{K+m-q+1}\, q!}$$

where $L = 2l_2 + k + 2$

So, finally, the radial F integral obtained is

$$F_K(\alpha|\beta) = \sum_{n=0}^{2s} \sum_{m=0}^{2s} D_n C_m \left[\frac{(M+m)!\,(N+n)!}{(2\alpha)^{M+m+1}\,(2\beta)^{N+n+1}} \right.$$

$$+ (K+m)! \sum_{q=0}^{K+m} \frac{(L+n+q)!}{[2(\alpha+\beta)]^{L+n+q+1}\,(2\alpha)^{K+m-q+1}\,q!}$$

$$\left. - (M+m)! \sum_{p=0}^{M+m} \frac{(N+n+p)!}{(2\alpha)^{M+m-p+1}\,p!\,[2(\alpha+\beta)]^{M+n+p+1}} \right] \qquad (A.15)$$

Consider now the L-type integral species:

$$L_K(\alpha) = \int R^2(\alpha|r_i)\left\{r_i, R\right\}^K dr_i \qquad (A.16)$$

where

$$\left\{r_i, R\right\}^K = \frac{r_i^{K+2}}{R^{K+1}} \qquad (r_i < R)$$

$$= \frac{R^K}{r_i^{K-1}} \qquad (r_i > R)$$

For an X-H bond length distance R.

Thus

$$L_K(\alpha) = \int_0^\infty \sum_{m=0}^{2s} r_i^{2l_1} e^{-2\alpha r_i} C_m r_i^m \left\{ r_i, R \right\}^K dr_i$$

$$= \sum_{m=0}^{2s} C_m \left\{ \int_0^R \frac{r_i^{2l_1+m+k+2}}{R^{k+1}} e^{-2\alpha r_i} dr_i + R^k \int_R^\infty r_i^{2l_1-k+m+1} e^{-2\alpha r_i} dr_i \right\}$$

Hence, introducing

$$M = 2l_1 + k + 2$$

$$K = 2l_1 - k + 1$$

$$L_K(\alpha) = \sum_{m=0}^{2s} C_m \left[\frac{1}{R^{k+1}} \left\{ \frac{(M+m)!}{(2\alpha)^{M+m+1}} - \sum_{p=0}^{M+m} \frac{R^p (M+m)! e^{-2\alpha R}}{p! (2\alpha)^{M+m-p+1}} \right\} \right.$$

$$\left. + R^K \sum_{q=0}^{K+m} \frac{(K+m)! R^q e^{-2\alpha R}}{q! (2\alpha)^{K-q+m+1}} \right] \qquad (A.17)$$

The final integral type to consider is the I type, i.e.

$$I(\alpha) = \int \psi_\alpha^* \, h \, \psi_\alpha \, d\tau \tag{A.18}$$

where

$$h = -\frac{1}{2}\nabla^2 - \frac{Z}{r}$$

$$\psi_\alpha = r^l e^{-\alpha r} \sum_{m=0}^{s} a_m r^m S_{lm}(\theta,\phi)$$

Hence

$$I(\alpha) = \sum_{m'=0}^{s} \sum_{m=0}^{s} I_{m'm}(\alpha)$$

Operating with h leaves the result

$$I_{m'm}(\alpha) = \int_{r=0}^{\infty} a_{m'} a_m \left\{ -\frac{\alpha^2}{2} r^{2l+m+m'+2} e^{-2\alpha r} \right.$$

$$+ r^{2l+m+m'+1} e^{-2\alpha r} \left[\alpha(l+m+1) - Z \right]$$

$$\left. + r^{2l+m+m'} e^{-2\alpha r} \left[(l+m) - \frac{(l+m)(l+m-1)}{2} + \frac{l(l+1)}{2} \right] \right\} dr$$

So introducing $\Omega = 2l + m + m'$ and performing the radial integral gives:

$$I(\alpha) = \sum_{m=0}^{2l} \sum_{m'=0}^{2l} \frac{a_{m'} a_m \, \Omega!}{2\,(2\alpha)^{\Omega+1}} \left\{ -\frac{(\Omega+1)(\Omega+2)}{4} \right.$$

$$\left. -(\Omega+1)(l+m+1) - \frac{Z(\Omega+1)}{\alpha} + \left[l(l+1) - (l+m)(l+m-3) \right] \right\}$$

(A.19)

REFERENCES

1 R. Gaspar, Acta Phys. Hung. 7, 151 (1957); ibid 7, 447 (1957); 7, 208 (1958); 10, 149 (1959); J. Chem. Phys. 36, 740 (1962)

2 D.M. Bishop, J.R. Hoyland and R.G. Parr, Mol. Phys. 6, 467 (1963)

3 K.E. Banyard and N.H. March, J. Chem. Phys. 26, 1416 (1957)

4 K.E. Banyard and N.H. March, Acta Cryst. 9, 385 (1956)

5 K.E. Banyard and R.B. Hake, J. Chem. Phys. 41, 3221 (1964); ibid 43, 2684 (1965); 44, 3523 (1966)

6 R.B. Hake and K.E. Banyard, J. Chem. Phys. 45, 3199 (1966); ibid 43, 657 (1965)

7 K.E. Banyard and A. Sutton, J. Chem. Phys. 46, 2143 (1966); Mol. Phys. 12, 377 (1967)

8 R.B. Hake, Ph.D., Thesis University of Leicester, 1965.

9 V. Fock and M.J. Petrashen, Phys. Z. Sowjet 6, 368 (1934)

10 E.L. Albasiny and J.R.A. Cooper, Proc. Phys. Soc., 88, 315 (1966); ibid 85, 1133 (1965)

11 I. Waller and D.R. Hartree, Proc. Roy. Soc. (London) A124, 119 (1929)

12 J.H. Van Vleck, Theory of Electric and Magnetic Susceptibilities (Oxford University Press, London, 1932)

13 J.R. Eshbach and M.W.P. Straudberg, Phys. Rev. 85, 24 (1952)

14 D. Steele, E.K. Lippincott and J.T. Vanderslice, Rev. Mod. Phys. 34, 239 (1962)

15 C.W.F.T. Pistorius, J. Chem. Phys. 27, 965 (1957)

16 R. Moccia, J. Chem. Phys. 37, 910 (1962); ibid 40, 2164 (1964); 40, 2176 (1964); 40, 2186 (1964)

17 T.F. Moran and L. Friedman, J. Chem. Phys. 40, 860 (1964)

18 J.R. Platt, J. Chem. Phys. 18, 932 (1950)

19 S. Peyerimhoff, J. Chem. Phys. 43, 998 (1965)

20 R.P. Feynman, Phys. Rev. 56, 340 (1939)

21 H. Hellmann, Einfuhrung in die Quantenchemie (1937)

22 A.J. Freeman, Acta Cryst. 12, 271 (1959); Phys. Rev. 113, 169 (1959); Acta Cryst. 13, 618 (1960)

23 J.A. Ibers, Acta Cryst. 11, 178 (1958); Ibid 11, 447 (1958)

24 C.C.J. Roothaan, J. Chem. Phys. 23, 69 (1951)

25 V. Fock, Zeits. f. Physik 61, 126 (1930)

26 C. Møller and M.S. Plesset, Phys. Rev. 46, 618 (1934)

27 L. Brillouin, Act. Sci. et Ind., Nos. 71, 159, 160 (1933-34)

28 P. Jennings and E.B. Wilson Jr., J. Chem. Phys. 45, 1847 (1966); 47, 2130 (1967); J. Goodisman and W.A. Klemperer, J. Chem. Phys. 38, 721 (1963)

29 R.A. Bellinger, Mol. Phys. 2, 139 (1959)

30 A.M. Karo and L.C. Allen, J. Chem. Phys. 31, 968 (1959)

31 R.K. Nesbet, J. Chem. Phys. 36, 1518 (1962)

32 M.C. Harrison, J. Chem. Phys. 41, 499 (1964)

33 J.W. Moskowitz et. al., Quantum Theory of Atoms, Molecules and Solid State, Academic Press Inc., New York (1966)

35 P.E. Cade and W.M. Huo, J. Chem. Phys. 47, 614 (1967)

36 A.F. Saturno and R.G. Parr, J. Chem. Phys. 33, 22 (1960)

37 M. Krauss, J. Chem. Phys. 38, 564 (1963)

38 J. Sinai, J. Chem. Phys. 39, 1575 (1963); ibid 40, 3596 (1964)

39 B.J. Woznick, J. Chem. Phys. 40, 2860 (1963)

40 J.R. Hoyland, J. Chem. Phys. 47, 3556 (1967)

41 C. Sonnenschein, SSMTG Quart. Rept. MIT (1962)

42 R.S. Mullikan, J. Chem. Phys. 36, 3248 (1961)

43 C. Hollister and O. Sinanoglu, J. Am. Chem. Soc. 88, 13 (1966)

44 G.P. Arrighini et. al., J. Chem. Phys. 49, 2224 (1968)

45 S.L. Altmann et. al., Proc. Cam. Phys. Soc. 53, 343 (1957); Phil. Trans. Roy. Soc. A255, 199 (1963)

46 E. Wigner, Group Theory and its Application to the Quantum Mechanics of Atomic Spectra A.P. 1959

47 N.F. Ramsey, Molecular Beams, O.U.P., N.Y.(1956); Phys. Rev. 149, 14 (1966)

48 A.D. Buckingham, Quart. Rev. Chem. Soc. Lond., 13, 183 (1959)

49 S. Kielich, Physica 31, 444 (1965)

50 D.E. Stogryn and A.P. Stogryn, Mol. Phys. 11, 371 (1966)

51 G. Thomer, Phys. Zeit. 38, 48 (1937)

52 A.H. Stroud and D. Secrest, Gaussian Quadrature Formulas, Prentice-Hall

53 R. Weiss, Phys. Rev. 131, 659 (1963)

54 R.M. Pitzer, J. Chem. Phys. 46, 4871 (1967)

55 P. Ehrlich, Zeit. Anorg. U. Allgem. Chem. 249, 219 (1942)

56 R.S. Mullikan, J. Chem. Phys. 23, 1833 (1955); ibid 23, 1841 (1955)

57 A.D. McLean and M. Yoshamine, J. Chem. Phys. 47, 3256 (1967)

58 J.R. Hoyland et. al., J. Chem. Phys. 40, 3216 (1964)

59 R.F.W. Bader et. al., J. Chem. Phys. 47, 3387 (1967); J. Am. Chem. Soc., 87, 3063 (1965); J. Chem. Phys. 87, 3063 (1965)

MOLECULAR PHYSICS, 1967, VOL. 12, NO. 4, 377–380

The electronic structure of AlH_4^-

by A. SUTTON and K. E. BANYARD
Department of Physics, University of Leicester, Leicester, England

(*Received* 19 *December* 1966)

The electronic structure of AlH_4^- has been studied by using a determinantal wave function constructed from a minimal basis set of one-centre atomic orbitals of analytical form. Besides the determination of the molecular energy and bond length, values were also found for the 'breathing' force constant, the coherent x-ray scattering factor and the purely diamagnetic contribution to the molar magnetic susceptibility. The results of the present treatment for AlH_4^- were compared with the recent calculations of Albasiny and Cooper who used a one-centre Hartree–Fock approach within a spherical and a non-spherical approximation. In the light of the relative labour involved in each treatment, the comparison of physical properties proved to be quite favourable.

1. INTRODUCTION

Several hydride molecules of the argon-like series have been studied recently [1] by means of the united-atom (UA) approximation. The method employs the non-relativistic molecular hamiltonian, within the Born–Oppenheimer approximation, but makes the approximation that all the molecular orbitals are centred on the heaviest nucleus. Each molecular orbital is approximated by using one atomic orbital of analytical form, hence, the treatment involves the use of a minimal basis set of wave functions. The orbital exponents are then varied in order to minimize the total molecular energy in accordance with the variation principle. Considering the simplicity and comparative ease of application of this treatment, the resulting physical properties for the hydride molecules compared favourably with experiment [2]. In this paper the results of a similar calculation are presented for the molecular-ion AlH_4^-.

At the commencement of this work, no other electronic structure calculation had been reported for AlH_4^-. However, as this article was in preparation, Albasiny and Cooper [3] presented numerical one-centre Hartree–Fock wave functions for AlH_4^- and PH_4^+ for several values of the bond lengths using both a spherical and a non-spherical approximation. For each molecular-ion, the associated physical properties were also reported. Reference will be made to these SCF results, where appropriate, in the following discussion.

2. CALCULATION AND RESULTS

The united-atom model has been discussed in detail elsewhere [1]. As before, the total wave function of determinantal form is constructed from one-centre orthonormal wave functions of the same general type as those used by Fock and Petrashen [4] and other workers [1, 5]. Since we assume tetrahedral symmetry for the nuclear framework of AlH_4^-, the p_x, p_y and p_z orbitals, within a

particular shell, will have a common variational parameter and therefore, in this instance, the electron density will possess spherical symmetry. As in the treatment for some of the rare-gas hydride ions [6], all orbital exponents were regarded as variational parameters and were optimized by means of the energy minimization procedure†. The bond length R was also included in the calculations as an additional unknown parameter. The total energy E obtained for the ground state of AlH_4^- was $-242{\cdot}0270$‡ which corresponds to a theoretical value of the bond length of 3·132 A.U. By means of further energy minimization calculations for fixed values of R in the region of the theoretical bond length, the 'breathing' force constant k for AlH_4^- was found [1 *b*] to be 7·58§. An experimental value for k is 7·57 [8].

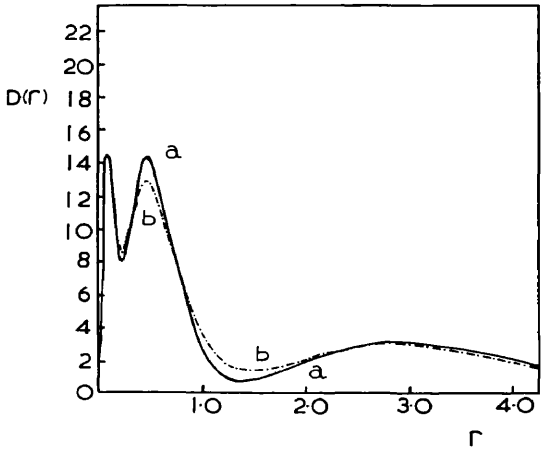

Figure 1. The radial density distribution of electrons for AlH_4^-. Curve (*a*) is determined from the UA treatment. Curve (*b*) was obtained by Albasiny and Cooper from the Hartree–Fock scheme within a non-spherical approximation.

The radial density distribution of electrons $D(r)$ obtained from the UA results associated with the theoretical bond length is shown in curve (*a*) of figure 1; for comparison, curve (*b*) shows the corresponding electron density determined by Albasiny and Cooper [3] from the non-spherical one-centre SCF wave functions at the theoretical R value. For a highly symmetric system such as AlH_4^-, the radial density distribution will determine, to within graphical accuracy, the shape of the coherent x-ray scattering curve. Hence, the electron densities shown in curves (*a*) and (*b*) of figure 1 give rise [1 *b*], respectively, to the x-ray scattering factors shown in curves (*a*) and (*b*) of figure 2. No estimates of the experimental results are available for comparison. The radial density was also used, as before [1 *b*], to determine the purely diamagnetic contribution χ_r‖ to the total molar

† The authors would like to thank Dr. R. B. Hake for the use of several of his computer routines.

‡ Unless stated otherwise, all physical quantities given here are quoted in terms of atomic units, see [7].

§ The units for force constants used throughout this work are 10^5 dyn/cm.

‖ Values of χ_r, expressed with respect to the heavy nucleus as the origin, are given in units of 10^{-6} electromagnetic units per mole.

magnetic susceptibility χ. The UA density for AlH_4^- gave a value for χ_r of $-79{\cdot}81$. This result lies between the two SCF values for χ_r obtained by Albasiny and Cooper. For AlH_4^-, a theoretical value for the temperature independent paramagnetic contribution $\chi_{h.f.}$ to the molar susceptibility is not known by us. This 'high frequency' contribution to χ, which vanishes for the case of atoms as a result of their spherically symmetrical nuclear field, is extremely difficult to calculate since it requires a knowledge of all excited electronic states. An experimentally based value for $\chi_{h.f.}$ for AlH_4^- is also not known and, although it is possible to estimate [9] a value for $\chi_{h.f.}$, the general lack of experimental data for this molecular-ion makes it difficult to suggest a most probable value for $\chi(AlH_4^-)$ as was done earlier for the PH_4^+ ion [1 *b*].

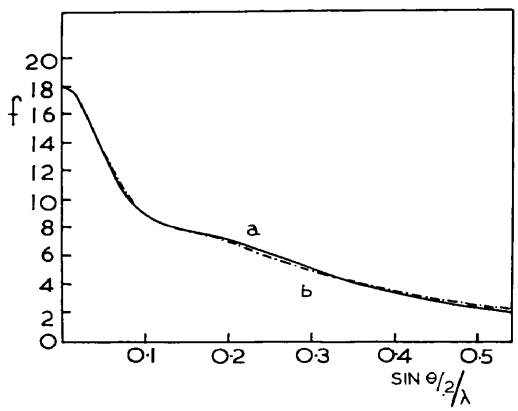

Figure 2. The coherent x-ray scattering factor for AlH_4^-. Curves (*a*) and (*b*) are determined, respectively, from the radial densities given by the present treatment and the Hartree–Fock approach within the non-spherical approximation.

For convenience, the results mentioned above are summarized in the table. Included in the table are the values of the physical properties for AlH_4^- determined by Albasiny and Cooper from the one-centre numerical SCF treatment within the spherical and non-spherical approximation.

Method	Energy (A.U.)	Bond length (A.U.)	Force constant† k	χ_r‡
UA § approach	−242·0270	3·132	7·58	−79·8
A/C § spherical	−243·222	3·137	6·85	−88·3
A/C § non-spherical	−243·734	2·965	9·96	−76·5

† The units for force constants used throughout this work are 10^5 dyn/cm.

‡ Values of χ_r, expressed with respect to the heavy nucleus as the origin, are given in units of 10^{-6} electromagnetic units per mole.

§ UA, united-atom; A/C, Albasiny and Cooper.

Comparison of results for AlH_4^-.

3. Discussion

As anticipated, the table reveals that the present molecular energy for AlH_4^- is higher than that obtained from either of the one-centre SCF approximations. However, if the UA value is expressed as a percentage of the best SCF energy obtained by Albasiny and Cooper, it is found that the present result is in keeping with the corresponding energy ratios obtained for PH_4^+ and SiH_4 [10]. The value for R obtained from the present UA approach is seen to be marginally better than the result derived from the spherical SCF treatment, however, the improvement is not as great as was observed for corresponding comparisons for the molecular systems PH_4^+ and SiH_4. As was observed for both PH_4^+ and SiH_4, the value for R predicted by the non-spherical SCF approximation is expected to be the most reliable result since, as discussed recently [6], the presence of angular terms in the density will affect the overall force which acts on each proton.

The value of the 'breathing' force constant obtained here for AlH_4^- is in excellent agreement with experiment. However, because the UA treatment normally provides k values for XH_n molecules which are somewhat too large when compared with experiment, the excellence of the present result is thought to be rather fortuitous.

On the whole, the results obtained for AlH_4^- by means of the present treatment are found to be quite satisfactory when compared with similar quantities derived from the more elaborate SCF calculations.

The authors would like to thank Dr. R. B. Hake for the use of certain of his computer routines. One of us (A. S.) also expresses appreciation for the award of a maintenance grant from the Science Research Council.

References

[1] (*a*) Gáspár, R., Tamássy-Lentei, I., and Kruglyak, Y., 1962, *J. chem. Phys.*, **36,** 740. (*b*) Banyard, K. E., and Hake, R. B., 1964, *J. chem. Phys.*, **41,** 3221; 1965, *Ibid.*, **43,** 2684; 1966, *Ibid.*, **44,** 3523.
[2] Hake, R. B., and Banyard, K. E., 1966, *J. chem. Phys.* **45,** 3199.
[3] Albasiny, E. L., and Cooper, J. R. A., 1966, *Proc. phys. Soc.*, **88,** 315.
[4] Fock, V., and Petrashen, M. J., 1934, *Phys. Z. SowjetUn.*, **6,** 368.
[5] Bernal, M. J. M., 1953, *Proc. phys. Soc.* A, **66,** 514. Banyard, K. E., and March, N. H., 1956, *Acta crystallogr.*, **9,** 385.
[6] Banyard, K. E., and Sutton, A., 1967, *J. chem. Phys.* (in the press).
[7] Shull, H., and Hall, G. G., 1959, *Nature, Lond.*, **184,** 1559.
[8] Pistorius, C. W. F. T., 1957, *J. chem. Phys.*, **27,** 965.
[9] Carter, C., 1956, *Proc. R. Soc.* A, **235,** 321. Eshbach, J. R., and Strandberg, M. W. P., 1952, *Phys. Rev.*, **85,** 24.
[10] Albasiny, E. L., and Cooper, J. R. A., 1965, *Proc. phys. Soc.*, **85,** 1133.

Reprinted from THE JOURNAL OF CHEMICAL PHYSICS, Vol. 46, No. 6, 2143–2146, 15 March 1967
Printed in U. S. A.

One-Center Study of the Rare-Gas Hydride Ions NeH^+ and ArH^+

K. E. BANYARD AND A. SUTTON
Department of Physics, University of Leicester, Leicester, England

(Received 11 October 1966)

The ground states of the rare-gas hydride ions NeH^+ and ArH^+ have been studied by means of the united-atom (UA) treatment. Values are reported for the energy, theoretical bond length, force constant, and the diamagnetic part of the molar magnetic susceptibility. However, the present work is primarily intended as a test of the UA approach and, as such, it was useful to compare the results with those obtained by the same treatment for HF and HCl. Also, it proved to be most instructive to analyze the forces which act on the protons within each molecular ion.

As anticipated, the UA treatment of NeH^+ and ArH^+ met with meager success. Nevertheless, the analysis provided considerable understanding as to why a similar study, applied to neon- and argonlike molecules, yields fairly reasonable values for the above molecular properties when compared with experiment.

INTRODUCTION

THE one-center approximation has been used extensively for hydride molecules of the neon- and argonlike series.[1] Included within such an approximation are the simple united-atom calculations,[2] the one-center expansion treatment of Moccia,[3] and also the numerical Hartree–Fock calculations of Albasiny and Cooper.[4] In a recent series of articles,[5] it was found that although the united-atom (UA) method was not as energetically favorable as the more elaborate one-center treatments, it did provide good values for the theoretical bond length, especially for the argonlike molecules. Also, tolerable values were obtained for the purely diamagnetic part of the total molar susceptibility and, when one considers the simplicity of the UA model, the calculated values of the "breathing" force constants were not too disappointing when compared with corresponding experimental quantities. Therefore, in an effort to explore the workings of the UA treatment, particularly its success at predicting bond lengths, it was decided to take the method to its limit by applying it to the study of the rare-gas hydride ions NeH^+ and ArH^+.

Rare-gas hydride ions were observed originally in mass spectrometers and, since they possess only a short lifetime, a knowledge of accurate wavefunctions and the associated molecular properties would be of considerable interest. In this context the two-center calculations on HeH^+ and NeH^+ carried out by Peyerimhoff[6] are particularly noteworthy. Although we report physical properties which result from our calculations on NeH^+ and ArH^+, the present work is primarily intended as a test of the UA model and, as such, we find it useful to compare the reliability of the present results with corresponding calculations[2,7] carried out on HF and HCl. Finally, it proved instructive to analyze the forces which act on the protons within NeH^+ and ArH^+.

CALCULATIONS

The details of the united-atom treatment applied to neon- and argonlike molecules have been discussed fully elsewhere.[2] As in the previous calculations, the total molecular wavefunction for the ground state of each molecular ion was expressed as a single Slater determinantal function constructed from orthonormal one-electron orbitals of the type used by Fock and Petrashen.[8] The origin of the coordinate system is taken to be the heavy atom and the proton is positioned on the z axis; hence, from symmetry considerations, the p_x and p_y orbitals within the same shell will have a common variational parameter. Within this symmetry restriction, the total molecular energy was then minimized with respect to all orbital parameters. It is noted that in our previous UA calculations,[2b] the $1s$ and $2s$ orbital exponents for the heavy atom were not varied but were preselected to have the neutral atom values.

Unfortunately, no experimental values of the bond length R for NeH^+ and ArH^+ were known by us, hence, R was included in each calculation as an additional variational parameter. The resulting energy E and

[1] See, for example, the work of R. A. Buckingham, H. S. W. Massey, and S. R. Tibbs, Proc. Roy. Soc. (London) **A178**, 119 (1941); M. J. M. Bernal, Proc. Phys. Soc. (London) **A66**, 514 (1953); C. Carter, Proc. Roy. Soc. (London) **A235**, 321 (1956); A. F. Saturno and R. G. Parr, J. Chem. Phys. **33**, 22 (1960); D. M. Bishop, Theoret. Chim. Acta **1**, 410 (1963); see also Refs. 2, 3, and 4.

[2] (a) R. Gaspar, I. Tamassy-Lentei, and Y. Kruglyak, J. Chem. Phys. **36**, 740 (1962); (b) K. E. Banyard and R. B. Hake, *ibid.* **41**, 3221 (1964); **43**, 2684 (1965); **44**, 3523 (1966).

[3] R. Moccia, J. Chem. Phys. **40**, 2164, 2176, and 2186 (1964).

[4] E. L. Albasiny and J. R. A. Cooper, Mol. Phys. **4**, 353 (1961); Proc. Phys. Soc. (London) **82**, 289 (1963); **85**, 1133 (1965); **88**, 315 (1966).

[5] R. B. Hake and K. E. Banyard, J. Chem. Phys. **43**, 657 (1965); **45**, 3199 (1966).

[6] S. Peyerimhoff, J. Chem. Phys. **43**, 998 (1965).

[7] R. B. Hake, "A Theoretical Study of Some Molecular Systems," Ph.D. thesis, University of Leicester, 1965.

[8] V. Fock and M. J. Petrashen, Physik. Z. Sowjetunion **6**, 368 (1934).

TABLE I. Comparison of results obtained for NeH^+ and ArH^+.

Method	NeH^+				ArH^+			
	E (a.u.)	$R_{theoret}$ (a.u.)	k[d]	χ_r[e]	E (a.u.)	$R_{theoret}$ (a.u.)	k[d]	χ_r[e]
United atom[a]	−127.5703	2.33	0.17	−5.58	−524.5752	3.11	0.18	−16.84
Two-center Hartree–Fock–Roothaan[b]	−128.6284	1.83	5.29	...	...	...	...	...
Modified Platt electrostatic model[c]	...	1.53	5.52	...	...	2.15	5.53	...

[a] Present treatment.
[b] The results of Peyerimhoff; see Ref. 6.
[c] The results of Moran and Friedman; see Ref. 13.
[d] See Ref. 11.
[e] See Ref. 10.

theoretical bond length $R_{theoret}$[9] for each molecular ion are reported in Table I. The electron densities associated with the above results were used to calculate the purely diamagnetic contribution χ_r[10] to the molar magnetic susceptibility χ; see Table I. For completeness, the radial densities were also used to calculate the coherent x-ray scattering factor, however, for each system, the result was graphically indistinguishable from the corresponding curve derived from analogous wavefunctions for the appropriate rare-gas atom.

For each molecular ion, the optimization of all orbital exponents was repeated for several fixed R values in the region of the theoretical bond length and hence, as before,[2b] a "breathing" force constant k was determined.[11] The results are presented in Table I.

It is helpful in the discussion that follows if we have some knowledge of the forces which act on the protons within each system. For a diatomic hydride, the resultant force in the positive z direction which acts on the proton due to the effect of the heavy nucleus and the electronic charge cloud is given by

$$F_H = \frac{Z}{R^2} - \int \frac{\rho(r,\theta,\phi)\cos\alpha}{S^2}\, d\tau, \qquad (1)$$

where Z is the charge on the heavy nucleus, R is the internuclear distance, and $\rho(r, \theta, \phi)$ is the electron density. The volume element $d\tau$, which is situated at (r, θ, ϕ) with respect to the heavy nucleus as the origin, is located at a distance S from the proton such that α is the angle between the z axis and the direction of S. The electron density for a diatomic system can be written, in general, as

$$\rho(r,\theta,\phi) = \sum_{n=0}^{\infty} \rho_{n0}(r)\,\Theta_{n0}(\theta)\,\Phi_0(\phi). \qquad (2)$$

However, in the UA treatment, with its limited angular dependence, we find that

$$\rho(r,\theta,\phi) = \rho_{00}(r)\,\Theta_{00}(\theta)\,\Phi_0(\phi) + \rho_{20}(r)\,\Theta_{20}(\theta)\,\Phi_0(\phi). \qquad (3)$$

Substituting Eq. (3) into Eq. (1), we obtain after some manipulation

$$F_H = \frac{Z}{R^2} - \frac{2(\pi)^{1/2}}{R^2}\int_0^R \rho_{00}(r)\,r^2 dr - 6\left(\frac{\pi}{5}\right)^{1/2}\frac{1}{R^4} \times \int_0^R \rho_{20}(r)\,r^4 dr + 4\left(\frac{\pi}{5}\right)^{1/2} R \int_R^{\infty} \frac{\rho_{20}(r)}{r}\, dr. \qquad (4)$$

The terms which occur in Eq. (4) can easily be understood by the application of simple electrostatic theory; in particular, the second term represents a screening of the first or nuclear term from the proton. This screening effect arises from that part of the electronic charge cloud located within a sphere of radius R which is centered on the heavy nucleus. The remaining integrals in Eq. (4) are obviously dependent on the angular term which occurs in the UA density. The curves (a) and (b) of Fig. 1 are obtained from Eq. (4) and show, respectively, the total force which acts on the proton in NeH^+ and ArH^+ for various values of R. For each system, the electron density was derived from optimized orbital exponents for the appropriate value of R.

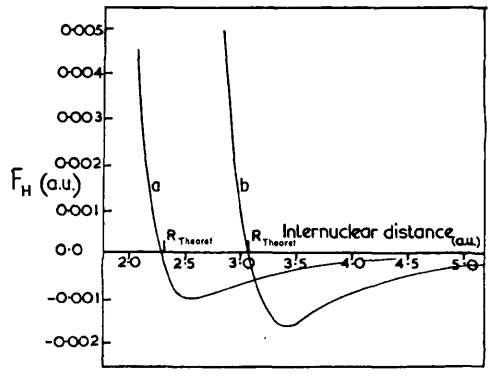

FIG. 1. The force on the proton within NeH^+ and ArH^+ for different internuclear distances R. Curve a is for NeH^+ and Curve b is for ArH^+.

[9] Unless stated otherwise, all physical quantities given in this article are quoted in terms of atomic units [see H. Shull and G. G. Hall, Nature **184**, 1559 (1959)].

[10] All values of χ and χ_r (which is expressed here with respect to the heavy nucleus as the origin of the coordinate system) are given in units of 10^{-6} emu/mole.

[11] The units for force constants used throughout this work are 10^5 dyn/cm.

DISCUSSION OF RESULTS

Due to the difficulty of carrying out experimental observations on rare-gas hydride ions, it is not possible to compare the physical properties listed in Table I with experiment. However, a comparison with other theoretical work is possible. For NeH^+, we have the results provided by Peyerimhoff[6] who carried out an extensive two-center LCAO MO SCF calculation after the manner of Roothaan.[12] Also, a comparison of theoretical bond lengths and force constants for each system is possible by reference to the analysis of Moran and Friedman.[13] These workers applied a modification of the Platt electrostatic model[14] to the study of several diatomic hydride ions. The appropriate results obtained from the above calculations are summarized in Table I.

For NeH^+, it is seen that the physical properties predicted by the extension of Platt's model, used by Moran and Friedman, agree reasonably well with the results obtained from the basic calculation of Peyerimhoff. The energy for NeH^+ given by the two-center calculation is observed to be about one atomic unit lower than the value given by the UA treatment. Such an energy difference is also observed for HF between the UA calculation[2,7] and the elaborate one-center treatment of Moccia.[3] The values for R_{theoret} and k given by the UA treatment of NeH^+ are, respectively, larger and significantly smaller than the corresponding quantities derived by the previous workers. If we consider the results of Peyerimhoff to be close to future experimental observations, then the trend of the present results is different from that found in previous applications of the UA model to both neon- and argonlike hydride systems.[2,7] For those molecules it was found that, in general, the values obtained for R_{theoret} were in quite good agreement with experiment and also the results for the "breathing" force constant were, in each case, larger than the corresponding experimental data.

Similar conclusions are expected to hold for ArH^+. The UA model provides a theoretical bond length which is larger than that obtained by Moran and Friedman and the present force constant, which is of the same order of magnitude as that obtained for NeH^+, would again appear to be suspiciously small. Since the UA treatment of NeH^+ and ArH^+ appears to provide theoretical bond lengths which are much too large, the values for χ_r reported in Table I will also be too large.

It would be helpful if we could understand why the values for R_{theoret} and k predicted here for the rare-gas hydride ions do not follow the general trend found when the UA treatment was applied to other neon- and argonlike hydride systems. In this connection, the study of the forces which act on the proton within each system is of particular interest.[15] It is seen from Fig. 1 that in both cases, the total force acting on the H nucleus is close to zero at the theoretical value for R.[16] Similar results were found for the UA treatment of the corresponding diatomic hydride molecules HF and HCl. Such a result gives some measure of the sensitivity of the computer program which minimizes the total molecular energy.[17] For NeH^+ and ArH^+, the force on the proton tends to zero as $R\rightarrow\infty$. This is because the heavy nucleus is completely screened by the $\rho_{00}(r)$ term in the electron density while the force on the proton due to the angular terms in the density is zero at $R=\infty$. Hence, it follows that, if the electron density for these systems contained only a $\rho_{00}(r)$ term, the theoretical value for R would, ideally, have to be infinite in order to give a zero force acting on the proton. On the other hand, if a similar situation occurred for HF and HCl, a balance between the first two terms of Eq. (4) is possible at values for R which would be in fairly reasonable agreement with experiment. Such a central-field study of XH_n systems[18] possesses similar features to the Platt electrostatic model.[14] Therefore, for rare-gas hydride ions, in contrast with systems such as HF and HCl, a realistic prediction of the bond length depends markedly on the angular terms within the electron density. Hence, in the UA model, the $\rho_{20}(r)$ contribution to the density plays a major role in providing a finite value for R_{theoret}. On the other hand, the two-center treatment of Peyerimhoff for NeH^+ should contain many well-described angular terms when the density is expanded in spherical harmonics about the heavy nucleus, consequently, this treatment should predict a bond length which may be in close agreement with experiment.

We have seen that the limited angular dependence which arises when the electron density is obtained from a UA treatment results in bond lengths for NeH^+ and ArH^+ which are too large. Such a situation also gives rise to a "breathing" force constant k which is much too small. The present treatment gives an electron density for each system which is small and slowly varying in the region of the proton.[19] Therefore, it is not surprising that the molecular energy is also a slowly varying function of R, and hence k, which is

[12] C. C. J. Roothaan, Rev. Mod. Phys. **23**, 69 (1951).
[13] T. F. Moran and L. Friedman, J. Chem. Phys. **40**, 860 (1964).
[14] J. R. Platt, J. Chem. Phys. **18**, 932 (1950).

[15] For an accurate wavefunction the resultant force on each nucleus within a diatomic system should be zero at the theoretical bond length. However, within the UA treatment, the heavy nucleus will experience no resultant force arising from the electron density, hence, the force acting on this nucleus will always be Z/R^2, due entirely to the proton.

[16] The force on the proton at the theoretical bond length is -0.0002 a.u. for NeH^+ and zero, to within four decimal places, for ArH^+.

[17] The authors would like to express their sincere thanks to R. B. Hake for the use of several of his computer routines.

[18] See, for example, K. E. Banyard, and N. H. March, Acta Cryst. **9**, 385 (1956).

[19] At R_{theoret} the proton is only just penetrating the electron charge cloud for both NeH^+ and ArH^+. The number of electrons contained within the sphere of radius R_{theoret}, centered on the heavy nucleus, is 9.98 for NeH^+ and 17.96 for ArH^+.

given by the second differential of E with respect to R and evaluated at R_{theoret}, will obviously be small.

From the above discussion we have seen that the UA treatment of NeH^+ and ArH^+ has not proved to be very successful. However, the analysis presented above has helped considerably in the understanding of the reason for this failure, further, it has also helped to explain why the UA treatment is capable, on the other hand, of providing reasonable values for the physical properties for HF and HCl. The arguments presented here can also be used to show why a similar study, when applied to the remaining neon- and argon-like molecules, does provide acceptable values for R_{theoret} and k when compared with experiment.

ACKNOWLEDGMENTS

The authors wish to offer appreciation to Dr. R. B. Hake for helpful comments concerning the use and interpretation of certain of his computer routines. Thanks are also due to Mrs. A. Wyatt for the careful preparation of the diagram. One of us (A.S.) wishes to acknowledge with gratitude the award of a maintenance grant from the Science Research Council.